2010-07-12

The Common Pond Snail Lymnaea stagnalis: Extracellular Fluid Recovery in Adults and Calcification and Lead Sensitivity During Embryonic Development

Sue C. Ebanks
University of Miami, sac2004@yahoo.com

UNIVERSITY OF MIAMI

THE COMMON POND SNAIL *LYMNAEA STAGNALIS*: EXTRACELLULAR FLUID RECOVERY IN ADULTS AND CALCIFICATION AND LEAD SENSITIVITY DURING EMBRYONIC DEVELOPMENT

By

Sue C. Ebanks

A DISSERTATION

Submitted to the Faculty
of the University of Miami
in partial fulfillment of the requirements for
the degree of Doctor of Philosophy

Coral Gables, Florida

June 2010

UNIVERSITY OF MIAMI

A dissertation submitted in partial fulfillment of
the requirements for the degree of
Doctor of Philosophy

THE COMMON POND SNAIL *LYMNAEA STAGNALIS*: EXTRACELLULAR FLUID RECOVERY IN ADULTS AND CALCIFICATION AND LEAD SENSITIVITY DURING EMBRYONIC DEVELOPMENT

Sue C. Ebanks

Approved:

_____ Martin Grosell, Ph.D. Professor of Marine Biology	_____ Terri A. Scandura, Ph.D. Dean of the Graduate School
_____ Lynne Fieber, Ph.D. Professor of Marine Biology	_____ Christopher Langdon, Ph.D. Professor of Marine Biology
_____ David Letson, Ph.D. Professor of Economics	_____ Christopher M. Wood, Ph.D. Professor of Biology McMaster University

EBANKS, SUE C. (Ph.D., Marine Biology and Fisheries)

The Common Pond Snail *Lymnaea stagnalis*: Extracellular Fluid Recovery in Adults and Calcification and Lead Sensitivity During Embryonic Development (June 2010)

Abstract of a dissertation at the University of Miami.

Dissertation supervised by Professor Martin Grosell.
No. of pages in text. (141)

Freshwater organisms are known to maintain hyperosmotic internal conditions despite outward diffusive loss of ions. The freshwater common pond snail *Lymnaea stagnalis* faces this challenge while additionally attaining the necessary ions for calcification. These are the first documented assessments of the time and mode of recovery for ions lost due to full-body withdrawal in adults of this species. Additionally, this document reports on the physiological and developmental onset of embryonic calcification and the commencement of active acquisition of shell-forming ions from the surrounding environment. The effect of water chemistry and lead (Pb) exposure on embryonic growth, development, and calcium (Ca^{2+}) acquisition was also tested. Pharmacological and water chemistry manipulations were used to determine mechanisms for embryonic Ca^{2+} and HCO_3^-/CO_3^{2-} acquisition and the sensitivity of those pathways. Lastly, *L. stagnalis*, was shown to have a lowest effective concentration of <1.5 µg Pb l^{-1} using net Ca^{2+} uptake, growth, and developmental endpoints in laboratory and natural waters. This is the lowest effective concentration observed for any organism to date. One of the most insightful findings reported here is the interconnectedness of the

pathways for acquisition of Na^+ and Ca^{2+} through endogenous production of H^+ and HCO_3^- via carbonic anhydrase-catalyzed hydration of metabolic CO_2. The combination of high demand for Ca^{2+} throughout early life stages and periodic acute demands for Na^+ recovery following extracellular fluid loss apparently causes *L. stagnalis* to be highly sensitive to changes in water chemistry, including [Pb] in the embryos, and possibly pH. The findings reported here warn of the need to establish freshwater environmental indicators and consider raising awareness of the threat of freshwater acidification, which may be greater than that of ocean acidification.

ACKNOWLEDGMENTS

I only have space to thank a few.
Left unfettered, I could fill this whole book through and through.

To my committee, also Kevin Brix and Dr. Andrew Esbaugh, as well as lab mates past and present:
Thank you for your help over the course of these projects.

My sincere thanks to Michael O'Donnell and his research group for their hospitality during my visit to McMaster for the collaborative project on the egg masses.

I also thank Drs. Michael Schmale and Lynne Fieber for the use of their cameras & microscopes and Charles Farmer, M.S. for the DOC analysis of the natural waters.

To my RSMAS family:
Each of you has filled a special niche in my life and I hope to share many more memories with you.

To my parents,
Oscar & Rebecca Chaplin and Atol & Esther Ebanks
Thank you for all of your sacrifices to help me to realize this goal.

To my dear husband,
Dwight
I am indeed blessed to have you as my support through this process and in life.
I would not trade you for the world.

To my superkid,
Junpei
Thank you for your energy and encouragement!
A mother could not ask for a better son.

This research was funded in part by the following:

NOAA Educational Partnership Program, Environmental Cooperative Science Center and the RSMAS MSGSO Student Travel Fund.

TABLE OF CONTENTS

Page

LIST OF FIGURES

Chapter 2

Chapter 3

Chapter 4

Chapter 5

LIST OF TABLES

Chapter 2

Chapter 3

Chapter 5

Chapter 1:

Introduction

Freshwater and coastal systems are often the first water bodies affected by anthropogenic inputs due to their close proximity to developed areas. Aquatic organisms are especially challenged in freshwater habitats to maintain hyperosmotic internal conditions compared to the relatively ion-poor ambient environment. The common pond snail *Lymnaea stagnalis* combats these osmotic challenges and thrives in these conditions despite continuous diffusive loss of essential ions and other solutes to the surrounding environment. This calciphile is nearly exclusively reliant upon aquatic calcium sources and thus preferentially inhabits hard water conditions of >20 mg Ca l^{-1} in contrast to some other lymnaeid species such as *L. palustris*, which is more tolerant of softer water (<20 mg Ca l^{-1}; Boycott 1936, van der Borght and Puymbroeck 1966). *L. palustris* meets a significant portion of its calcium requirements through dietary intake.

Predator avoidance responses in aquatic snails including *Lymnaea* are dependent upon the type of predator and include emergence from the water and reinforcement of shell (Alexander and Covich 1991, McCarthy and Fisher 2000, Rundle and Brönmark 2001). However, *L. stagnalis* can also retract its soft tissue into the shell to evade predation (Arshavsky *et al.* 1994) at the expense of significant solute losses to the environment. Schlichter (1981) found that pulmonate snails, such as the common pond snail *Lymnaea stagnalis*, either emerge from the water to escape predation or complete full-body withdrawal into their shell by ejecting up to 60% of total hemolymph volume through the pneumostome. The solute loss associated with full-body withdrawal is a

greater sacrifice for freshwater snails relative to marine species due to the greatly reduced environmental ion availability.

The primary objective of the first set of experiments in this dissertation (chapter 2, Ebanks and Grosell 2008) was to assess the severity of the consequence of extracellular fluid (ECF) release in *L. stagnalis* by determining the magnitude of electrolyte loss associated with full-body withdrawal. The time required for full recovery was also determined. Sodium, the major cation present in the extracellular fluid, is acquired from aquatic sources via active carrier-mediated uptake (Greenaway 1970) as is the case for other freshwater organisms (Krogh 1939, Krogh 1946). Active Na^+ uptake could be dependent upon anions available in the water (de With 1980, de With *et al.* 1987), namely Cl^- (Kirschner 2004) or possibility HCO_3^- via a Na^+: HCO_3^--dependent carrier system (Perry *et al.* 2003a, 2003b). Additionally, Na^+ transport may be reliant upon availability of endogenously produced H^+ ions (Kirschner 2004), which are produced in part through the hydration of CO_2, and would therefore be dependent upon carbonic anhydrase (CA). Thus two final objectives of chapter two were to determine whether Na^+ uptake under recovery conditions was Cl^-- or HCO_3^--dependent and conduct a pharmacological assessment of transport mechanisms involved in Na^+ recovery.

Another cation that is of obvious importance to the aragonite-producing *L. stagnalis* (Kniprath 1972) is calcium (Ca^{2+}). The experiments for chapters three (Ebanks *et al.* 2010a) and four (Ebanks *et al.* 2010b) were designed to determine the requirements, rates, mechanisms, and conditions of Ca^{2+} and HCO_3^- acquisition. Additionally, the effect of water chemistry, specifically ambient [Ca^{2+}] and [HCO_3^-] on uptake of these necessary ions for shell formation was studied during late-stage embryonic development.

Lymnaea stagnalis produces embryos that complete direct development within a sessile, gelatinous, semi-transparent egg mass, hatching within eight to ten days post-oviposition at 22°C. At this temperature, metamorphosis and the onset of shell formation occur at approximately day five in *L. palustris* (Morrill 1982) and *L. stagnalis* (pers. obs.). To complete shell-formation, *Lymnaea* must either be provided with the necessary Ca^{2+} and carbonate forms for calcification through maternal stores or acquire the ions from the surrounding environment.

In the calcification process, two HCO_3^- equivalents are consumed for each Ca^{2+} equivalent.

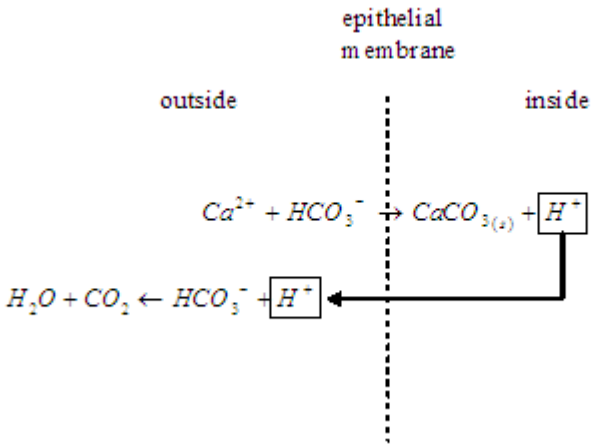

The two sources of bicarbonate for shell formation are uptake from the water (diagram above) and through the hydration of metabolic CO_2 (diagram below), most of which is from a reaction catalyzed by CA.

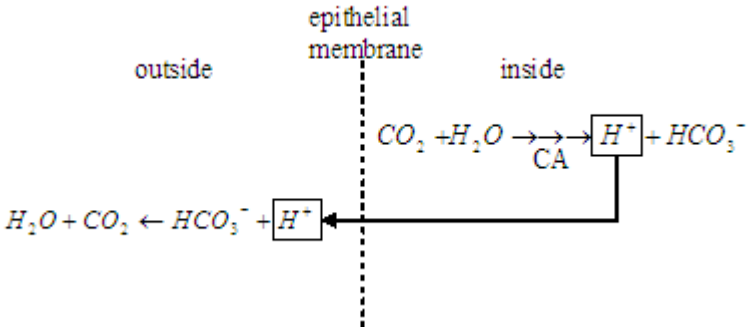

For either means of HCO_3^-/CO_3^{2-} acquisition, uptake from the water or endogenous production, total NH_4^+/NH_3 affects total acid-base exchange between the snail and the environment. As NH_3 is excreted, it reacts with H^+ in the water. With increased H^+ availability due calcification and the hydration of CO_2, ammonia is converted to NH_4^+. This process effectively reduces the $[NH_3]_{aquatic}$ and $[H^+]_{aquatic}$, which facilitates increased H^+ excretion from the animal/tissue. Calcification occurs throughout the life cycle of *L. stagnalis* but the point at which active uptake begins and the mode of acquisition for substrate during the embryonic stages are not well known. The high demand for calcium in this species relative to the environmental availability of the ion makes an assessment of the uptake pathways an interesting study, particularly during the earliest stages of development. Thus, the major objective for the second set of experiments (chapter three, Ebanks *et al.* 2010a) was to determine whether *L. stagnalis* embryos are provided with sufficient maternal stores of shell-forming ions to complete embryonic development or rely upon uptake from the environment. Subsequently, using water chemistry manipulations and pharmacological inhibitors, the pathways of acquisition for shell-forming ions were assessed and a model was proposed (chapter four, Ebanks *et al.* 2010b).

Lastly, laboratory testing of two lymnaeid species, *L. palustris* (Borgmann *et al.* 1978) and *L. stagnalis* (Grosell *et al.* 2006), has demonstrated that the two species, and to a greater extent *L. stagnalis*, are the most sensitive organisms studied to date for chronic exposures to lead (Pb). Adults of *Lymnaea palustris* exhibit significant mortality at 19 µg Pb l^{-1} (Borgmann *et al.* 1978) and new *L. stagnalis* hatchlings are negatively impacted in growth with a lowest effect concentration of 16 µg Pb l^{-1} and a 20% effective concentration of <4 µg Pb l^{-1} (Grosell *et al.* 2006). Lead is one of the most potent inhibitors of voltage-sensitive calcium channels in both invertebrates and vertebrates (Audesirk 1993). In rainbow trout *Oncorhynchus mykiss*, Pb competes with Ca^{2+} for entry on voltage-independent Ca^{2+} channels in branchial tissues (Rogers and Wood 2004). Lead exposure (1-250 µmol l^{-1} $PbCl_2$) in a pulmonate freshwater snail, the bloodfluke planorb *Biomphalaria glabrata* is accompanied by reduced growth and significant mortality with no significant effect on reproduction (Allah *et al.* 2003). Another factor that was necessary for consideration was the role that water chemistry plays in the degree to which Pb has a toxic effect on physiological systems. In general, there is an inverse relationship between ambient water hardness, specifically [Ca^{2+}] and the toxicity of Pb ([USEPA] 2009, Grosell *et al.* 2006). However, recent studies indicate the need for broader inclusion of water chemistry variables in the establishment of water quality criteria for Pb (Grosell *et al.* 2006, Mager *et al.* 2008, Mager *et al.* 2010a, Mager *et al.* 2010b). The concentrations of Ca^{2+}, HCO_3^-, and DOC have been shown to ameliorate the toxic effects of Pb in other freshwater species (Mager *et al.* 2010a, Mager *et al.* 2010b). Thus the overall objectives of the final series of experiments were to determine whether chronic Pb exposure has a toxic effect on Ca^{2+} uptake, shell formation, development, and hatching in embryos of *L. stagnalis*. Additionally, natural waters with a range of water

chemistry characteristics were used to determine whether Ca^{2+}, HCO_3^-, and DOC have a cumulative ameliorating effect on Pb toxicity in *L. stagnalis* embryos.

Chapter 2:

Fluid and Osmolyte Recovery in the Common Pond Snail *Lymnaea stagnalis* Following Full-Body Withdrawal

2.1. Background

Predatory avoidance in aquatic snails is facilitated by surfacing and emergence from the water in snails that have relatively fragile shells, and by hiding or possibly burial in the case of snails with shells of greater crush resistance (Alexander and Covich 1991, McCarthy and Fisher 2000, Rundle and Brönmark 2001). The response is also highly dependent on the type of predator- i.e. shell-invading leeches and flatworms (Brönmark and Malmqvist 1986, Townsend and McCarthy 1980) versus shell-crushing sunfish or crayfish (Alexander and Covich 1991, Brown 1991). Additionally, and central to the present study, snails can perform graded withdrawal of soft tissue into their shells corresponding to the intensity of the predatory attack (Arshavsky *et al.* 1994). Pulmonate snails, such as the common pond snail *Lymnaea stagnalis*, exhibit emergence behavior to escape predation but when the predatory threat is eminent, *L. stagnalis* can also complete full-body withdrawal by ejecting up to 60% of its total hemolymph volume (Schlichter 1981), which averages 0.45 ml g^{-1} snail bodyweight (van Aardt 1968). The extra-cellular fluid (ECF) enters the pulmonate cavity via the haemal pore and is then ejected into the environment through the pneumostome. Because this response can be achieved experimentally by stimulating the foot of the snail, and because the released fluids can be easily collected, the response provides a means by which internal conditions of the snail can be determined without sacrifice or puncture of the integument. While the withdrawal response offers protection against predation, it is also potentially associated with reduced

fitness. One possible cost of this escape response is that the snail becomes temporarily immobilized on the bottom during the initial recovery phase (pers. obs.) and is likely more subjected to benthic predators such as crayfish during that time. A presumably sub-lethal effect is the energetic expense associated with the needed recovery of fluids and osmolytes lost with the release of ECF.

Freshwater snails exhibiting the whole-body retraction and associated fluid loss have a physiological challenge associated with the escape response that may be of greater significance than for marine snails. Marine snails conform to ambient ion concentrations, thus the challenge of recovering ions lost due to retraction is minimal and mostly occurs in parallel with fluid recovery (Krogh 1946). However, freshwater species are osmoregulators, maintaining hyperosmotic conditions relative to the ambient waters. Thus, although both freshwater and seawater species lose fluids to complete full-body withdrawal, solute recovery of this magnitude (presumably as high as 60%), which requires active transport by freshwater species such as *L. stagnalis*, is likely of significant energetic cost for evading predation.

In an attempt to evaluate the severity of the consequence of ECF release, the primary goals of this investigation were to determine (1) the magnitude of electrolyte loss associated with the full-body withdrawal, (2) whether *L. stagnalis* recovers solutes to initial levels following ECF release, and (3) the time required to such full recovery. These goals were pursued by completion of a time course study of hemolymph sampling (bleeding) to determine the time to recovery following the initial bleed in naïve, cultured snails.

Findings of relatively rapid recovery of ECF volume and osmotic pressure prompted investigations into the nature of this remarkable homeostatic response. Because Na^+ is the major cationic osmotic component of the ECF in these organisms (Schlichter 1981), understanding the mechanism(s) for its recovery following ECF release is essential. It has long been recognized that *L. stagnalis* like other freshwater organisms (Krogh 1939, Krogh 1946) obtains Na^+ from the surrounding freshwater media by active carrier-mediated uptake (Greenaway 1970), but the mechanism remains to be characterized. Consequently, the next objective was to (4) determine the Na^+ transport kinetics under basal (un-bled) and early recovery (bled) conditions. This was done to evaluate whether the accelerated uptake under fluid recovery conditions was due to altered transport kinetics of the Na^+ uptake pathways utilized to maintain homeostasis under basal conditions.

In all freshwater organisms examined to date, the process of Na^+ uptake is mediated at least in part by an electro-chemical gradient generated by the basolateral electrogenic Na^+/K^+-ATPase (Marshall and Grosell 2006), which is responsible for low intracellular Na^+ concentrations and polarization of the cell membrane. Apical entry of Na^+ appears to be linked to H^+ extrusion either via direct Na^+/H^+ exchange as first proposed by Krogh (1939) or to H^+ extrusion via the vacuolar H^+-ATPase (Bury and Wood 1999, Fenwick *et al.* 1999, Grosell and Wood 2002, Lin and Randall 1991). In the latter case, electrogenic H^+ extrusion further polarizes the apical membrane to facilitate Na^+ entry via a putative Na^+ channel, which so far has not been identified.

Results revealed greatly amplified Na^+ uptake in *L. stagnalis*, which can lose 30% or more of hemolymph Na^+ content in the response associated with whole-body

withdrawal (Schlichter 1981). One possible characteristic of pathways involved in Na^+ recovery could be dependency on availability of extra-cellular anions (de With 1980, de With *et al.* 1987). Uptake of Na^+ in many freshwater organisms requires Cl^- (Kirschner 2004) and the possibility of HCO_3^--dependent Na^+ uptake via a Na^+: HCO_3^--dependent carrier system exists (Perry *et al.* 2003a, 2003b). The observed stimulated Na^+ uptake associated with recovery from ECF release was attributed to both increased transport capacity and affinity. Because apical Na^+ channels or Na^+/H^+ exchange proteins likely would be the primary means by which Na^+ enters the cell, sensitivity of Na^+ uptake to amiloride was evaluated to provide insight into the mechanism(s) of enhanced Na^+ uptake following ECF loss. Furthermore, microtubule-dependent relocation of transport proteins from the cytoplasm to the apical membrane (Tresguerres *et al.* 2006) could also contribute to the rapid activation of the Na^+ uptake mechanism. Additionally, the enhanced transport may rely on availability of H^+ ions (Kirschner 2004), which are produced by the hydration of CO_2, and would therefore be dependent upon carbonic anhydrase (CA). Therefore, the two final objectives were to (5) determine whether the amplified Na^+ uptake was Cl^-- or HCO_3^--dependent and (6) conduct a pharmacological assessment of transport mechanisms involved in Na^+ recovery.

2.2. Materials and methods

Experimental snails

Common pond snails *Lymnaea stagnalis* were cultured from a stock originally procured from Dr. Naweed Syed, University of Calgary, Canada. Cultures were reared in flow-through tanks supplied with dechlorinated, aerated Miami-Dade County, USA tap

water (Table 2.1) and were offered a continuous diet of Romaine lettuce, carrot, and sweet potato. Snails reproduced readily under these conditions.

Table 2.1. Water chemistry for dechlorinated Miami-Dade county tap water, which supplied flow-through system for snail cultures. All concentrations are in mmol l^{-1} except DOC, which is reported in µmol l^{-1} of carbon. Bicarbonate concentration and $[CO_3^-]$ were calculated from measured pH and the mean total $[CO_2]$. Values are adopted from Grosell *et al.* (2007).

Characteristic	Value
$[Na^+]$	1.1
$[K^+]$	0.04
$[Ca^{2+}]$	0.31
$[Mg^{2+}]$	0.12
$[Cl^-]$	1.03
$[SO_4^{2-}]$	0.11
$[HCO_3^-]$	0.68
$[CO_3^-]$	0.01
[DOC]	199.1
Total CO_2	0.71
pH	7.69

Hemolymph sampling & time course for solute recovery

To determine the time necessary for the snails to recover solutes following loss of ECF, the foot of the snail was stimulated using a pipette tip to cause full retraction of the soft tissue into the shell and consequently ECF release. This procedure will subsequently be referred to as bleeding. The released fluid obtained from the bleeding procedure was retained for later analysis. A total of 134 snails were weighed, bled, and reweighed. A

second stimulation was performed on subsets of the 134 snails at 2 h (N = 8), 4 h (N = 8), 6 h (N = 8), 8 h (N = 8), 10 h (N = 8), 12 h (N = 8), 16 h (N = 8), 18 h (N = 8), 24 h (N = 8), 48 h (N = 8), 72 h (N = 8), 1 wk (168 h, N = 10), 2 wk (336 h, N = 10), 5 wk (N = 10), and 10 wk (N = 9) following the initial bleeding.

Na^+ transport kinetics: Radioisotope flux experiments

To determine whether rapid recovery of Na^+ post-bleeding was associated with stimulated Na^+ uptake capacity and/or enhanced affinity of the Na^+ transport system, Na^+ transport kinetics were determined pre- and post-bleeding in individual snails. Sodium-free artificial tap water (ATW) with ion concentrations (except for Na^+ and Cl^-) similar to water from Miami-Dade County (Table 2.1) was used for these experiments and contained nominal concentrations of 100 μmol l^{-1} $MgSO_4$, 400 μmol l^{-1} $CaSO_4$, and 100 μmol l^{-1} $KHCO_3$. For uptake kinetics measurements, NaCl was added to achieve a range of nominal [Na^+]: 100, 250, 500, 1000, 2000 μmol l^{-1}. Individual snails with wet weights between 0.5 - 1 g were randomly selected, weighed, and placed in individual chambers containing 15 ml of the appropriate media (N = 10 snails each in individual chambers for each concentration). Equal amounts of radio-labeled ^{22}Na (2 μCi) were then added to each chamber and within 10 min chamber media was mixed and 5 ml of the water (initial) was removed for later analysis of ^{22}Na activity and [Na^+]. Snails were then allowed to flux for 1-3 h and all calculations were normalized for flux time. Each snail was then removed from its flux chamber, given a quick rinse in artificial ^{22}Na-free tap water having the same Na^+ concentration as the flux media, bled, rinsed again, and allowed to recover in individual chambers with dechlorinated tap water (ca. 1 μmol Na^+ l^-

^{1}) for approximately 1h. The flux process was then repeated with each snail being allowed to take up ^{22}Na from the same [Na^+] as was used in the initial flux in the un-bled condition but in fresh chambers and solutions including ^{22}Na isotope. For example a snail initially fluxed in 500 μmol Na^+ l^{-1} in the un-bled condition was subsequently allowed to flux under the bled condition with fresh media containing 500 μmol Na^+ l^{-1}.

Assessment of anion-dependency in amplified Na^+ uptake post-bleeding

To determine whether Na^+ uptake under solute recovery conditions was dependent on anion availability in the ambient water, two flux experiments were completed testing Cl^-- and HCO_3^--dependency. In the Cl^- dependency experiment, [Cl^-] was varied while maintaining nominal concentrations of Mg^{2+}, Ca^{2+}, K^+, and HCO_3^- as described above and maintaining 500 μmol Na^+ l^{-1}. Control media contained 500 μmol Na^+ l^{-1} as NaCl (500 μmol l^{-1} nominal [Cl^-], N = 10) and two treatment media contained 500 μmol Na^+ l^{-1} as sodium gluconate (0 μmol l^{-1} nominal [Cl^-], N = 10) or as Na_2SO_4 (0 μmol l^{-1} nominal [Cl^-], N = 10), respectively. To test HCO_3^--dependency of enhanced uptake post-bleed, control media contained 500 μmol Na^+ l^{-1} as sodium bicarbonate (500 μmol l^{-1} nominal [HCO_3^-], N = 10) and three treatment media contained 500 μmol Na^+ l^{-1} as NaCl (100 μmol l^{-1} nominal [HCO_3^-], N = 10), sodium gluconate (0 μmol l^{-1} nominal [HCO_3^-], N = 10), and Na_2SO_4 (0 μmol l^{-1} nominal [HCO_3^-], N = 10), respectively. Concentrations of ambient Mg^{2+}, Ca^{2+}, and K^+ were maintained at nominal concentrations listed in the initial kinetics experiment. The same flux procedures described above were completed on pre-weighed snails 1 - 1.5 g wet weight and each chamber contained 20 ml of media for all controls and treatments. Snails were then bled,

given a 1-h recovery in appropriate 500 μmol Na^+ l^{-1} media, and were allowed to flux again for 2 h after ^{22}Na was added. Initial and final water samples for both sets of fluxes were analyzed for ^{22}Na activity and [Na^+] as described below. Additionally, "Cl^--free" conditions were verified as described below.

Pharmacological assessment of mechanisms contributing to amplified Na^+ uptake post-bleeding

An affinity shift observed in bled relative to un-bled condition in Na^+ kinetics experiments indicated the possible use of two distinct transport pathways by which the snails take up Na^+, one under basal conditions and a second during recovery following fluid loss. These two transport pathways were expected to possibly display different pharmacological characteristics. Amiloride (N-amidino-3,5-diamino-6-chloropyrazinecarboxamide hydrochloride: hydrate, Sigma-Aldrich), was utilized in this experiment at concentrations that bracketed the effective range of the drug for both the Na^+ channel and the Na^+/H^+ exchanger. Amiloride inhibits Na^+ transport by blocking Na^+ channels at lower concentrations and other forms of Na^+ transport (including Na^+/H^+ exchangers) at higher concentrations (Kleyman and Cragoe 1988, Masereel *et al.* 2003). For these experiments 30 un-bled and 30 bled snails with pre-bleed weights of 1 - 1.5 g were placed in individual chambers containing 20 ml of ATW (500 μmol l^{-1} nominal [Na^+] as NaCl) and either dimethyl sulfoxide ($(CH_3)_2SO$, DMSO, vehicle control, N = 10), 10^{-5} mol l^{-1} amiloride (N = 10), or 10^{-4} mol l^{-1} amiloride (N = 10) dissolved in DMSO. Snails were then allowed to recover for approximately 60 min prior to addition of $^{22}Na^+$ and commencement of 2 h-flux as described above. This was the only

experiment in which separate snails were used for the bled and un-bled conditions. Thus amiloride could be tested under both basal and recovery conditions to evaluate whether different mechanisms were being utilized to maintain Na^+ homeostasis compared to recovery following fluid loss.

To assess whether the rapid activation of Na^+ uptake was mediated by cellular trafficking or recruitment of transport proteins in vesicular compartments to the apical membrane, colchicine was employed. Colchicine is a microtubule disruptor that provides for a rudimentary assessment of possible transporter relocation from cytoplasmic compartments to the epithelial membrane. Un-bled snails were subjected to flux measurements employing the same procedure described above for 2 h in 20 ml of ATW containing ^{22}Na (2 μCi) and 500 μmol l^{-1} Na^+ as NaCl. Following the initial flux, snails were bled and allowed to recover for 1 h in ^{22}Na-free ATW with 500 μmol l^{-1} Na^+ as NaCl that was either drug-free (control), had DMSO (vehicle control), or that had 10^{-4} mol l^{-1} colchicine ($C_{22}H_{25}NO_6$, Sigma-Aldrich) dissolved in DMSO after which a second ^{22}Na flux was performed in the same recovery chambers. Thus, fluxes were completed on the same group of snails (10 controls and 10 per treatment) first in the un-bled, then in the bled condition.

Regardless of the mechanism of Na^+ transport employed by freshwater organisms, cellular substrate in the form of H^+ appears to be important for Na^+ uptake. To test the possibility that an increase in cellular substrate availability through increased cellular hydration of CO_2 to form HCO_3^- and H^+ was involved in the rapidly activated Na^+ transport, a lipophilic carbonic anhydrase inhibitor was employed. An experiment with control (ATW), DMSO (vehicle control), and 10^{-4} mol l^{-1} 6-ethoxy-2-

benzothiazolesulfonamide ($C_9H_{10}N_2O_3S_2$, ethoxzolamide (ETOX), Sigma-Aldrich) dissolved in DMSO was performed as described above for the colchicine experiments. This experiment was completed for a total of 10 control, 10 DMSO control, and 10 ETOX-treated snails.

Analytical techniques and calculations for Na^+ kinetics experiments

All hemolymph samples were analyzed for pH, total CO_2, osmotic pressure, [Na^+], [Cl^-], [Ca^{2+}], and protein concentration. In addition, samples from selected time points were analyzed for [Cu], the central metal in gastropod respiratory proteins (Sminia 1977). Within 1 h after collection, samples were analyzed for pH (Radiometer Analytical MeterLab PHM201, Cedex, France) and total CO_2 (Corning Carbon Dioxide Analyzer 965, Essex, England), which were later used to determine partial pressure of CO_2 (P_{CO_2}) using the Henderson-Hasselbalch equation and pK_I and pK_{II} values of 6.135 and 9.61, respectively as obtained from Truchot (1976) alignment nomograms. Osmotic pressure was measured by vapor pressure osmometry (Wescor Vapro 5520, Logan, Utah, USA), while cation concentrations were determined via flame atomic absorption spectrophotometry (Varian SpectrAA220, Mulgrave, Victoria, Australia), and [Cl^-] was determined by a colorimetric reaction based on the method of Zall *et al.* (1956). Samples of the test solutions of NaCl, sodium gluconate, Na_2SO_4, and initial and final flux waters for six randomly selected snails (three un-bled and three bled) from each treatment were analyzed for [Cl^-] and [SO_4^{2-}] using anion chromatography (DIONEX DX 120 PeakNet 6, Sunnyvale, California, USA) to verify "Cl^--free" conditions. Total protein concentration in each hemolymph sample was determined by the Bradford protein assay

using bovine serum albumin standards (Bradford 1976). The [Cu] was determined using graphite furnace atomizer, atomic absorption spectrophotometry (Varian SpectrAA220 with a SpectrAA GTA110, Mulgrave, Victoria, Australia).

The initial and final water samples from flux experiments were analyzed for ^{22}Na activity (Packard Cobra II Auto-Gamma, Meriden, Connecticut, USA) with a window of 15-2000 keV and [Na^+] was measured by flame atomic absorption spectrophotometry. Unidirectional Na^+ influx was calculated from the mean specific activity of the initial and final water samples, the snail mass, and the total flux time as described previously (Grosell *et al.* 2000). Net flux values were obtained from the change in total [Na^+] during the flux period, snail mass, and elapsed flux time while efflux was determined as the difference between net flux and influx.

Statistical analyses

Time course data were analyzed using one-way repeated measures ANOVA comparing initial hemolymph characteristics to those at later time points with statistically significant differences among means being evaluated by Student's t-test using multi-sample Bonferroni correction. Uptake kinetic constants were determined assuming Michaelis-Menten kinetics and using the non-linear regression function in SigmaPlot for Windows version 8.00.

$$J = \frac{J_{max} \times [Na^+]}{k_m + [Na^+]}$$

Kinetic constants from snails in the bled and un-bled condition were subsequently compared using Student's t-test. For the anion-dependency and pharmacological analyses, Student's t-tests were used to determine the significance of drug effects and

ambient anion (Cl^- and/or HCO_3^-) availability on Na^+ uptake rates in bled and un-bled conditions. All analyses were completed using SigmaStat for Windows version 3.00 and comparisons were considered significantly different at $P < 0.05$.

2.3. Results

Solute recovery in extra-cellular fluid

All snails exhibited significant losses of extra-cellular fluid (ECF) volume, major ions, and other solutes following the initial bleeding event. Of the 134 snails sampled at the initial time point, seven escaped or died over the course of the experiment. Data from the initial sampling of these snails were not included in the analyses.

The significant loss of nearly 30% of ECF evident from fluid volumes obtained at the second bleeding was regained in 8 h as indicated by the increase in body weight (fig. 2.1A), but fluid composition did not completely return to initial conditions during the first two weeks of the time course. Despite substantial fluid loss, osmotic pressure was generally 9 - 10% lower for the first 18 - 24 h, but rarely significantly so (fig. 2.1B). Sodium and Cl^- were the major ionic constituents of the initial osmotic pressure value of 109.8 mosmol kg^{-1}. Sodium took 24 - 48 h to recover to initial values from a 29% loss (fig. 2.1C); and Cl^- also recovered from a significant loss of 39% in the same timeframe, though with greater variability (fig. 2.1D). Calcium contributed much less to osmotic pressure and showed no significant change in concentration over the experimental period (fig. 2.1E); and though total CO_2 concentration (mainly HCO_3^-) was much greater than that of Ca^{2+}, it also did not vary significantly during the time course (fig. 2.1F). Additionally, snail ECF had brief periods of significant alkalosis and increases in P_{CO2}

(table 2.2). The significant loss of Cu (fig. 2.2A) and total proteins (fig. 2.2B) did not recover over the two week sampling period and subsequent experiments revealed recovery by five weeks after the initial fluid loss. Surprisingly, plasma protein concentration exceeded initial values at ten weeks.

Na^+ transport kinetics

Sodium uptake rates increased with increasing ambient [Na^+] in a hyperbolic pattern characteristic of Michaelis-Menten kinetics in snails under both bled and un-bled conditions (fig. 2.3); however, snails in the bled condition had significantly greater capacity (3.1-fold) and affinity (3-fold) for Na^+ relative to un-bled condition. In both cases, the affinity value (apparent k_m) was well below the [Na^+] in which the snails were reared (approx 1 mmol l^{-1}, fig. 2.3). Flux values recorded at 2 mmol l^{-1} Na^+ did not conform to the saturation kinetics observed at flux concentrations below the rearing concentration of 1 mmol l^{-1}. Therefore, values recorded for snails in the bled and un-bled condition that were fluxed at nominal [Na^+] of 2 mmol l^{-1} were excluded from the regression analysis but are included in fig. 2.3.

Figure 2.1. Fluid volume released during bleeding (A), osmotic pressure (B), and concentrations of main electrolytes (C-F; Na^+, Cl^-, Ca^{2+}, and total CO_2) in hemolymph from *L. stagnalis* taken from all individuals at the initial time point (open circles) and again from subsets of eight at one time point 2 - 72 h (closed circles) following initial sampling. Asterisks indicate values significantly different from initial time point. Values are presented as mean ± S.E.M.

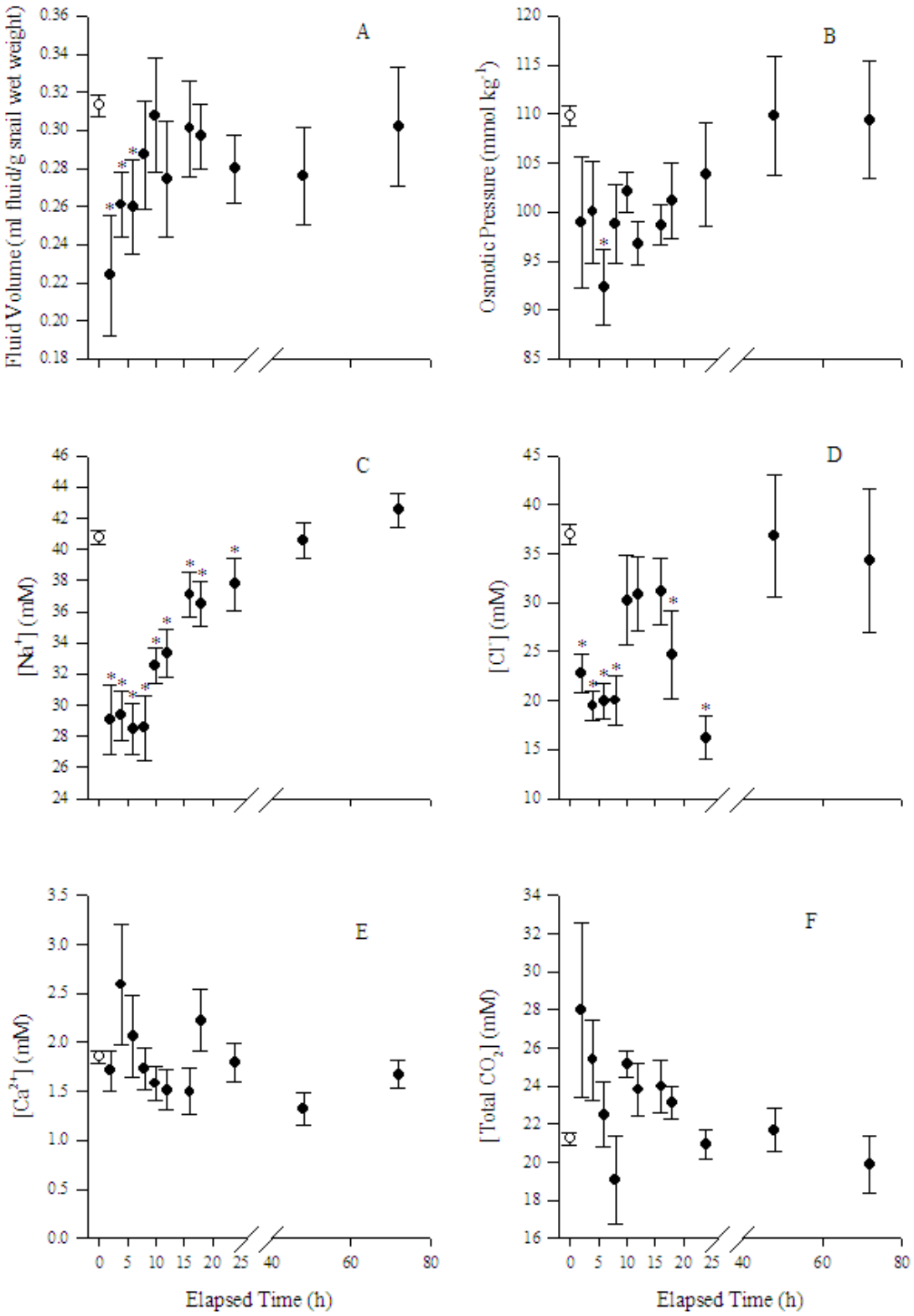
A
Fluid Volume (ml fluid/g snail wet weight)
0.36
0.34
0.32
0.30
0.28
0.26
0.24
0.22
0.20
0.18
B
Osmotic Pressure (mmol kg-1)
120
115
110
105
100
95
90
85
C
[Na+] (mM)
46
44
42
40
38
36
34
32
30
28
26
24
D
[Cl-] (mM)
45
40
35
30
25
20
15
10
E
[Ca2+] (mM)
3.5
3.0
2.5
2.0
1.5
1.0
0.5
0.0
0 5 10 15 20 25 40 60 80
Elapsed Time (h)
F
[Total CO2] (mM)
34
32
30
28
26
24
22
20
18
16
0 5 10 15 20 25 40 60 80
Elapsed Time (h)

Table 2.2. Mean pH and P_{CO2} for extra-cellular fluid samples taken from snails at initial time point and sub-sets of the initial group re-sampled at time intervals listed. Asterisks indicate time points for which data were significantly different from time 0 mean. Smaller sample sizes at 2 h and 4 h was due to insufficient fluid volumes to complete all analyses at these time points. Values are presented as mean ± S.E.M.

Time Point (N) *H*	pH	pCO_2 *torr*
0 (118)	8.34 ± 0.01	2.89 ± 0.10
2 (3)	8.37 ± 0.09	2.02 ± 0.64
4 (3)	8.32 ± 0.05	2.85 ± 0.06
6 (8)	8.45 ± 0.05*	2.46 ± 0.36
8 (8)	8.33 ± 0.04	2.56 ±0.35
10 (8)	8.43 ± 0.04*	2.73 ± 0.19
12 (8)	8.35 ± 0.02	3.11 ± 0.24
16 (8)	8.40 ± 0.05	3.10 ± 0.64
18 (7)	8.27 ± 0.03	3.68 ± 0.24*
24 (8)	8.31 ± 0.03	3.00 ± 0.27
48 (8)	8.34 ± 0.02	2.85 ± 0.17
72 (7)	8.43 ± 0.09*	2.19 ± 0.33
168 (10)	8.24 ± 0.02	3.10 ± 0.21
336 (10)	8.23 ± 0.04	2.91 ± 0.28
5 wk (10)	8.21 ± 0.04	2.71 ± 0.23
10 wk (8)	8.02 ± 0.06*	4.47 ± 0.75*

Figure 2.2. A) Copper and B) total protein concentrations in hemolymph of *L. stagnalis* as a function of time. Individuals were bled at time 0 (open bars; N = 54 for Cu, N = 53 for proteins) and sub-groups (closed bars) were bled again at 6 h (N = 8 for Cu and N = 6 for proteins), 12 h (N = 7 for Cu and N = 8 for proteins), 1 wk (N = 10 for Cu and total proteins), 2 wk (N = 10 for Cu and total proteins), 5 wk (N = 10 for Cu and total proteins), and 10 wk (N = 9 for Cu and total proteins). Asterisks indicate values significantly different from initial time point values. Values are presented as mean ± S.E.M.

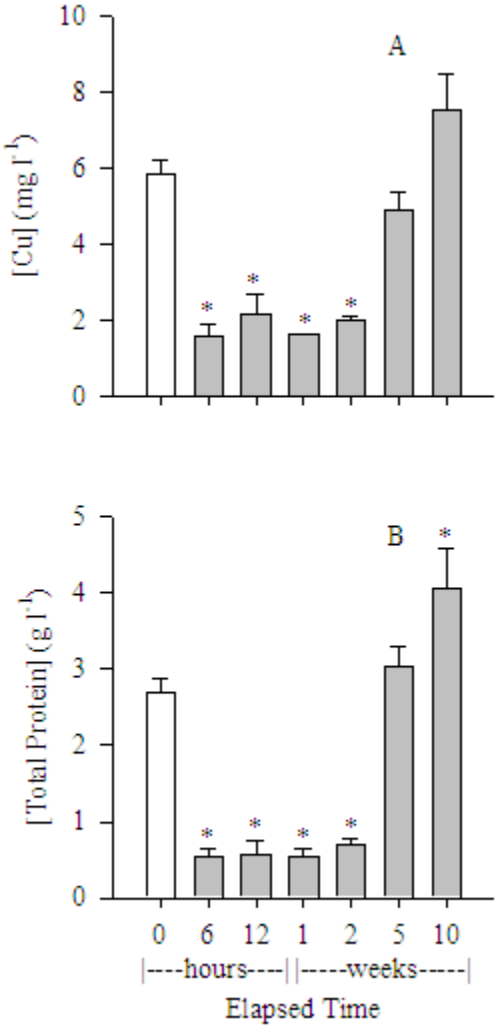

Figure 2.3. Sodium uptake rates (nmol g^{-1} h^{-1}) as a function of ambient Na^+ ion concentration in the pond snail *L. stagnalis*. Values are for bled (closed circles) and un-bled (open circles) snails. Regression lines are Michaelis-Menten curves (SigmaPlot 8.0 for Windows). N = 10 for each data point. Values are presented as mean ± S.E.M.

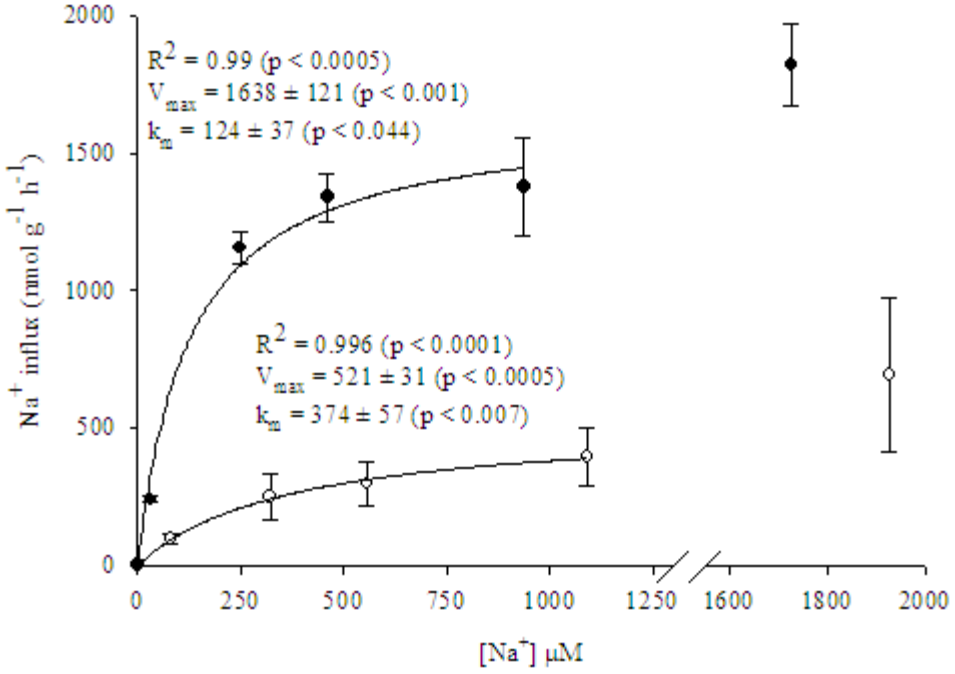

In addition to increased uptake rates with respect to ambient [Na^+] and whether snails were fluid-depleted, bled snails also exhibited a general increase in unidirectional Na^+ efflux relative to when they were under un-bled conditions. Nevertheless, there was consistently less net Na^+ loss and generally a net gain of Na^+ (table 2.3) with few exceptions. Although snails fluxed at 100 µmol l^{-1} Na^+ conformed to the aforementioned general trend, they still experienced a net loss of Na^+ under bled conditions, albeit less loss than under pre-bleed conditions.

Table 2.3. Sodium efflux and net flux in pond snail *Lymnaea stagnalis* under un-bled and bled condition with varying ambient [Na^+]. Asterisk indicates concentration at which snails were reared and to which all statistical comparisons of Na^+ effects were made (1000 µmol l^{-1}). Values for un-bled compared to bled condition within treatment concentration were significantly different except 100 µmol l^{-1} Na^+ concentration. [a]Significantly lower efflux rate compared to respective condition in 1000 µmol l^{-1} treatment. [b]Significantly lower net flux rate than bled snails in 1000 µmol l^{-1} treatment. Values are presented as mean ± S.E.M.

Nominal [Na^+] (µmol l^{-1})	Condition, N	Efflux (nmol g^{-1} h^{-1})	Net Flux (nmol g^{-1} h^{-1})
100	Un-bled, 10	-226 ± 14[a]	-131 ± 19
	Bled, 10	-277 ± 9[a]	-39 ± 9[b]
250	Un-bled, 9	-361 ± 57	-111 ± 33
	Bled, 10	-932 ± 57	223 ± 34
500	Un-bled, 10	-446 ± 57	-150 ± 35
	Bled, 10	-1045 ± 91	293 ± 38
1000*	Un-bled, 9	-456 ± 99	-61 ± 23
	Bled, 9	-1163 ± 151	212 ± 71
2000	Un-bled, 8	-735 ± 256	-41 ± 38
	Bled, 10	-1518 ± 107	303 ± 53

Assessment of anion dependency in Na^+ transport

The changes in transport kinetics equated to a general 4- to 5-fold increase in Na^+ uptake rate for bled snails in 500 µmol l^{-1} Na^+. This increase was neither Cl^-- (fig. 2.4) nor HCO_3^--dependent (fig. 2.5). When 500 µmol l^{-1} Na^+ was made available to the snails in Cl^--free media (sodium gluconate and sodium sulfate) versus the NaCl control, there was no significant difference in Na^+ uptake rates for either the bled or un-bled condition.

Figure 2.4. Data from assessment of Cl^- dependency in Na^+ uptake by un-bled and bled *L. stagnalis* as tested under control (NaCl) and treatment (sodium gluconate or sodium sulfate) conditions. Each treatment media contained 500 µmol l^{-1} of Na^+. Differences between un-bled and bled conditions within treatments were significantly different. There were no significant differences among Na-treatment groups in un-bled or bled conditions. N = 10 snails in all cases. Values are presented as mean ± S.E.M.

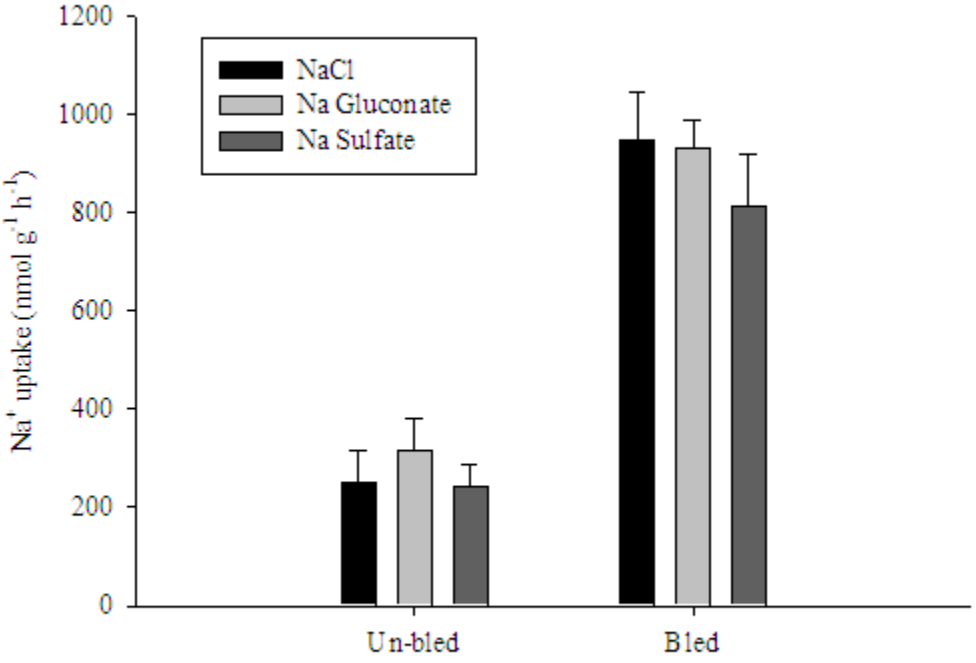

Figure 2.5. Assessment of HCO_3^- dependency in Na^+ uptake by bled and un-bled *L. stagnalis* as tested under control (sodium bicarbonate) and treatment (NaCl, sodium gluconate, or sodium sulfate) conditions. Each treatment media contained 500 µmol l^{-1} of Na^+. Differences between un-bled and bled conditions within treatments were significantly different. There were no significant differences among Na-treatment groups in un-bled or bled conditions. N = 10 in all cases except control (NaCl, N = 8) and sodium gluconate treatment (N = 9). Values are presented as mean ± S.E.M.

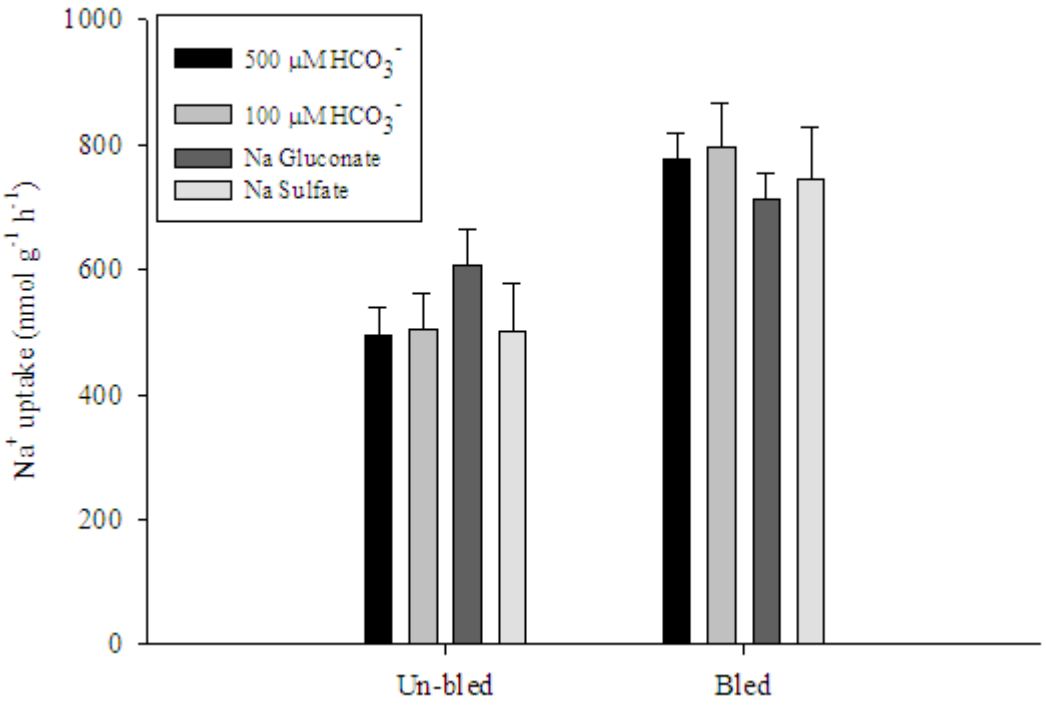

However, there was significantly greater unidirectional efflux of Na^+ in un-bled snails in 500 µmol l^{-1} Cl^- media relative to those in 0 µmol l^{-1} nominal [Cl^-], which resulted in significant net Na^+ loss relative to NaCl control (table 2.4). There was no apparent correlation in snails under recovery conditions between Cl^- availability and unidirectional Na^+ efflux or net flux. The Cl^- concentration in the NaCl stock solution was 490.3 µmol l^{-1}, in the sodium gluconate stock it was 10.1 µmol l^{-1} Cl^-, and in the sodium sulfate stock it was below detection limit (~2 µmol l^{-1}). The mean [Cl^-] in snail flux chambers with ^{22}Na isotope were 534.1 ± 27.88 S.E.M. (maximum 698.3 µmol l^{-1}), 41.1 ± 5.01 S.E.M. (maximum 72.9 µmol l^{-1}), and 60.4 ± 16.96 S.E.M. (maximum 177.1 µmol l^{-1}) for NaCl, sodium gluconate, and sodium sulfate, respectively. Bicarbonate availability did not affect Na^+ uptake in snails in the bled or un-bled condition provided with 500 µmol l^{-1} Na^+ and 0, 100, or 500 µmol l^{-1} HCO_3^- (fig. 2.5). Un-bled snails had significantly greater unidirectional efflux rates compared to rates when they were in the bled condition (table 2.5). However, there was still a net gain of Na^+ across all HCO_3^--treatments and ECF-level conditions.

Table 2.4. Assessment of Cl^- dependency of Na^+ efflux and net flux. Values for un-bled compared to bled condition within treatment concentration were significantly different. [a]Significantly greater unidirectional efflux than un-bled snails in 500 µmol l^{-1} Na^+. [b]Significantly greater net Na loss relative to un-bled snails in 500 µmol l^{-1} Na^+. Values are presented as mean ± S.E.M.

Na Compound (Nominal [Cl⁻])	Condition, N	Efflux (nmol g^{-1} h^{-1})	Net Flux (nmol g^{-1} h^{-1})
NaCl	Un-bled, 9	-232 ± 28	19 ± 54
500 µM	Bled, 10	-362 ± 38	587 ± 124
Na gluconate	Un-bled, 10	-457 ± 32[a]	-141 ± 59[b]
0 µM	Bled, 10	-267 ± 17	665 ± 55
Na sulfate	Un-bled, 10	-595 ± 35[a]	-354 ± 64[b]
0 µM	Bled, 10	-326 ± 29	487 ± 89

Table 2.5. Assessment of HCO_3^- dependency of Na^+ efflux and net flux. Values for un-bled compared to bled condition within treatment concentration were significantly different except unidirectional efflux within the 100 µmol l^{-1} [Na^+]. Values are presented as mean ± S.E.M.

Na Compound (Nominal [HCO_3^-])	Condition, N	Efflux (nmol g^{-1} h^{-1})	Net Flux (nmol g^{-1} h^{-1})
$NaHCO_3^-$	Un-bled, 9	-426 ± 60	69 ± 83
500 µmol l^{-1}	Bled, 9	-200 ± 46	574 ± 80
NaCl	Un-bled, 7	-240 ± 17	263 ± 58
100 µmol l^{-1}	Bled, 9	-223 ± 43	571 ± 62
Na gluconate	Un-bled, 10	-468 ± 31	137 ± 48
0 µmol l^{-1}	Bled, 9	-168 ± 21	545 ± 30
Na sulfate	Un-bled, 9	-443 ± 63	57 ± 76
0 µmol l^{-1}	Bled, 10	-194 ± 62	551 ± 108

Pharmacological assessment of Na^+ uptake

Of the three drugs tested, only amiloride and ethoxzolamide treatments elicited significant reductions of post-bleed Na^+ uptake. Bled snails treated with amiloride exhibited a concentration-dependent suppression of the amplified Na^+ uptake, which was significant at the 100 μmol l^{-1} amiloride concentration, compared to DMSO-control snails (fig. 2.6). The significantly lower uptake at 100 μmol l^{-1} amiloride translated to significantly lower net uptake in the 100 μmol l^{-1} amiloride-treated snails (table 2.6). Sodium uptake in un-bled control snails did not exhibit amiloride sensitivity and there was no significant effect of DMSO on Na^+ uptake in un-bled (fig. 2.6) or bled snails (fig. 2.6, 2.7). DMSO-carrier control treated snails had slightly higher Na^+ uptake (fig. 2.6) and significantly greater net Na^+ uptake (table 2.6) than bled control snails.

There was a significant decrease in unidirectional Na^+ uptake (fig. 2.7) and consequently net uptake (table 2.7) observed for bled snails treated with the CA-inhibitor ethoxzolamide relative to DMSO controls. The system responsible for the amplified Na^+ uptake observed in bled snails displayed no apparent sensitivity to colchicine for unidirectional influx, efflux, and net flux (fig. 2.7 and table 2.7).

Figure 2.6. Effect of dimethyl sulfoxide (DMSO) and amiloride on un-bled (closed circles) and bled (gray bars) snails. N = 10 for each concentration/treatment. Both un-bled and bled snails were exposed to DMSO or amiloride. Asterisk indicates value significantly less than DMSO control value. Differences between un-bled and bled conditions within treatments were significantly different. There was no significant difference between flux rates in regular control relative to rates in the DMSO carrier control media (data not shown). Values are presented as mean ± S.E.M.

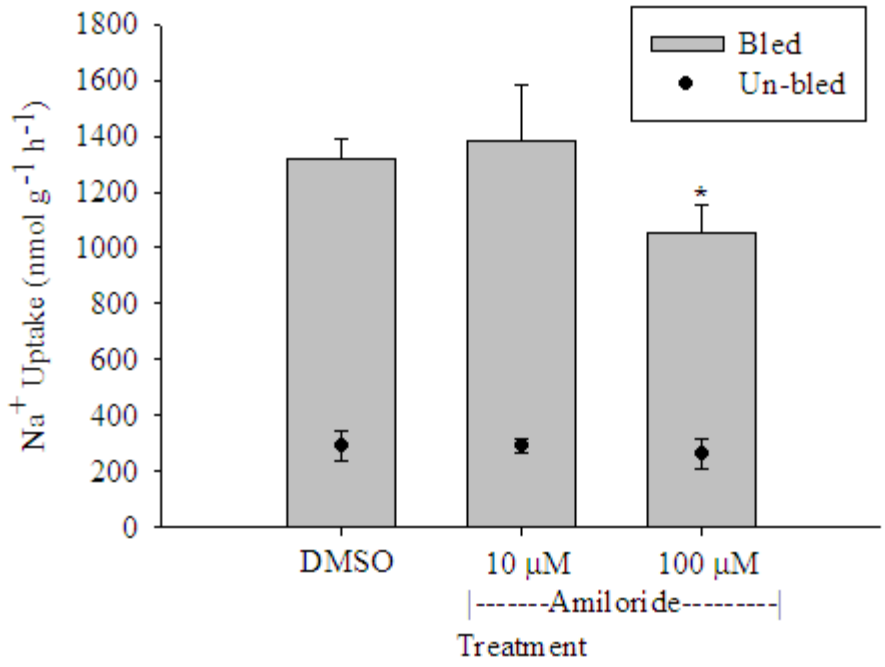

Figure 2.7. Sodium uptake in bled (gray bars) DMSO-treated (N = 10), colchicine-treated (N = 9), and ethoxzolamide-treated (N = 10) snails. Snails represented in this figure were not treated with any drugs when under basal conditions (line indicates mean ± S.E.M., N = 29). Asterisk indicates value significantly lower than DMSO control value. There was no significant difference between flux rates under control conditions relative to rates in the DMSO carrier control media (data not shown). Values are presented as mean ± S.E.M.

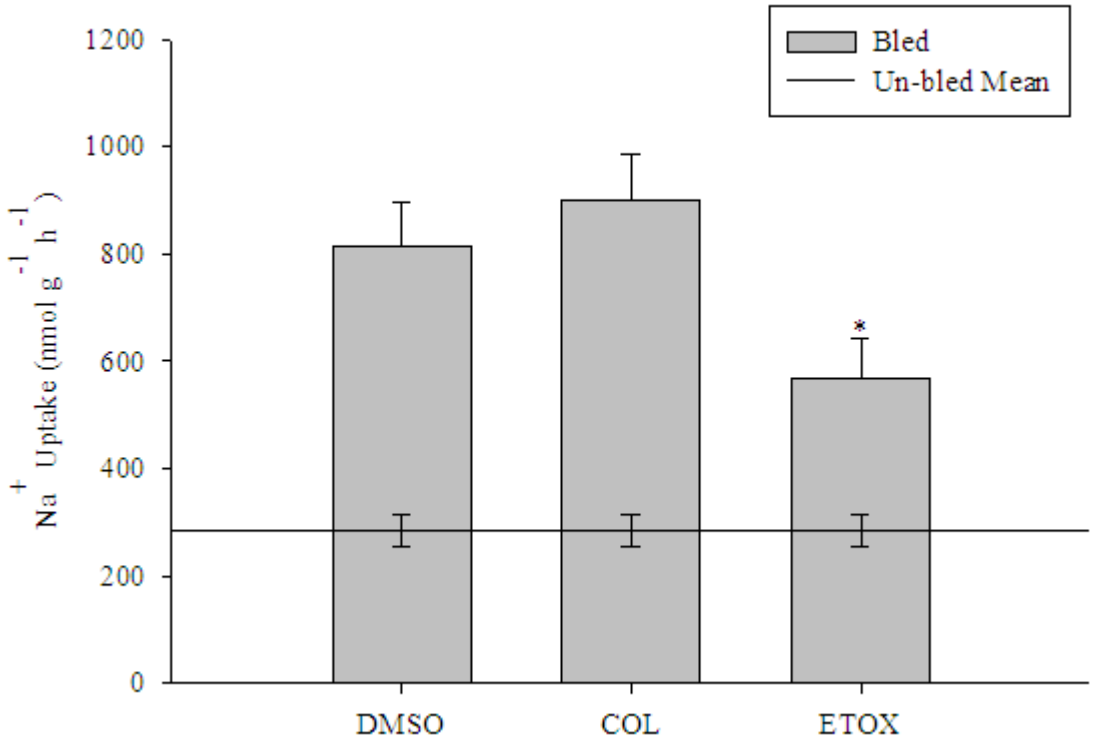

Table 2.6. Effect of a Na^+ transport inhibitor amiloride on Na^+ efflux and net flux. [a]Significantly less unidirectional efflux relative to un-bled snails in DMSO. For all other within treatment efflux comparisons, un-bled and bled condition values were not significantly different. [b]Significantly greater net uptake relative to bled control. Net flux values for un-bled compared to bled condition within treatments were significantly different. Values are presented as mean ± S.E.M.

Drug	Condition, N	Efflux ($nmol\ g^{-1}\ h^{-1}$)	Net Flux ($nmol\ g^{-1}\ h^{-1}$)
Control	Un-bled, 9	-617 ± 54	-389 ± 49
	Bled, 8	-587 ± 214	685 ± 86
DMSO control	Un-bled, 10	-559 ± 65	-269 ± 56
	Bled, 10	-154 ± 26[a]	1162 ± 68[b]
Amiloride 1 $\mu mol\ l^{-1}$	Un-bled, 10	-648 ± 69	-358 ± 64
	Bled, 10	-408 ± 281	976 ± 126
Amiloride 10 $\mu mol\ l^{-1}$	Un-bled, 9	-421± 47	-157 ± 65
	Bled, 9	-64 ± 127	988 ± 104[b]

Table 2.7. Effect of colchicine and ethoxzolamide on unidirectional Na^+ efflux and net flux in snails under bled condition. DMSO carrier control values were not significantly different from regular control values (data not shown). [a]Net flux in ethoxzolamide treatment significantly less than snails in DMSO vehicle control. Values are presented as mean ± S.E.M.

Drug	Condition, N	Efflux ($nmol\ g^{-1}\ h^{-1}$)	Net Flux ($nmol\ g^{-1}\ h^{-1}$)
DMSO control	Bled, 10	-254 ± 55	559 ± 74
Colchicine	Bled, 9	-280 ± 64	620 ± 120
Ethoxzolamide	Bled, 10	-208 ± 36	360 ± 44[a]

2.4. Conclusions and implications

The naïve *L. stagnalis* utilized in the time course experiment exhibited a remarkable ability to recover significant losses of extra-cellular fluid (ECF) volume, major, and some minor ions in a relatively short period of time despite its hypoosmotic environment. The major osmolytes recovered from a 30% loss in 1-2 d. Initial concentrations of the major ions, Na^+ and Cl^-, in pallial fluid of *L. stagnalis* were 40.73 ± 0.445 and 37.04 ± 1.027 mmol l^{-1}, respectively and were slightly lower than those previously reported in hemolymph, which were approximately 49 mmol l^{-1} Na^+ (Burton 1968, de With and van der Schors 1982) and approximately 44 mM Cl^- (de With and van der Schors 1982) from the same species. Based on Schlichter (1981), the expectation was for higher ion concentrations in pallial fluid relative to hemolymph literature values.

With respect to other ions measured, there were no significant changes in [Ca^{2+}] or total CO_2 (mostly HCO_3^-) though pH and P_{CO2} data indicated possible respiratory acidosis and partial compensation. Additionally, significant losses of protein and Cu, a component of the respiratory pigment hemocyanin, did not recover until 5 wk after the initial fluid loss. Therefore, it was clear that though these snails recover quickly for the major osmotic constituents, the delayed recovery for some potentially important components such as Cu and plasma proteins indicate that repeat sampling may influence hemolymph chemistry significantly.

L. stagnalis exhibited saturation kinetics in Na^+ uptake in relation to ambient sodium concentrations, and displayed amplified Na^+ uptake in the bled condition similar to that previously documented. Greenaway (1970) reported uptake rates of 132 nmol g^{-1} h^{-1} for un-bled snails acclimated to artificial tap water containing 350 µmol l^{-1} [Na^+].

Additionally, Na^+ uptake was 363 ± 0.27 nmol g^{-1} h^{-1} in snails bled in a similar manner to that used in our study but acclimated to 350 µmol l^{-1} [Na^+] and maintained in a 280 µmol l^{-1} Na^+ solution for a 1 h ^{22}Na flux. Unidirectional influx rates of 249 ± 86 nmol g^{-1} h^{-1} and 1155 ± 57 nmol g^{-1} h^{-1} were measured for ambient [Na^+] of 321 µmol l^{-1} [Na^+] and 248 µmol l^{-1} [Na^+] for snails under un-bled and bled conditions, respectively. Though the absolute flux values are different between the present and the earlier studies, the approximately 3-fold increase in the Greenaway (1970) study was not remarkably different from the 4-fold increase in our study. One point for consideration is that in the Greenaway (1970) study, different snails were utilized for the un-bled and bled snail experiments but flux values presented in our study are for the same snails in the un-bled and bled conditions. Furthermore, the net flux rates observed in snails fluxed in 100 µmol l^{-1} nominal [Na^+] indicated continued net loss of sodium even under post-bled conditions, which suggested a possible lower threshold of 100-250 µmol l^{-1} [Na^+] below which the snails may be unable to recover from a bleeding event.

Four- to five-fold increases in sodium uptake rates of post-bleed snails used in the present study relative to basal conditions provide indications to the mode of relatively fast recovery observed in the time course. Utilizing the pre-bleed snail bodyweight and pallial fluid [Na^+], total body hemolymph volume was calculated as determined using the 0.45 ml hemolymph per gram snail bodyweight value reported by van Aardt (1968). Also, initial whole-body [Na^+] was estimated to be approximately 33 µmol Na^+. Over a 48 hour period, *L. stagnalis* recovered the estimated 13 µmol of Na^+ lost due to the initial bleeding event. When compared to the 18 µmol of Na^+ that could be recovered at the observed net flux rates of 212 nmol Na^+ g^{-1} h^{-1}, clearly these recovery pathways can

account for the quantity of Na^+ recovered to return to basal concentrations in 48 h post-bleed.

Because the post-bled uptake rate increase was attributed to significant increases of both capacity and affinity of the system, it was necessary to consider increased activity of transporters already active under basal conditions and the likely activation (translation, trafficking, or recruitment) of dormant and perhaps distinct transporters. However, the first step was to consider whether the system was dependent on availability of anions in ambient media. Environmental Cl^- may facilitate Na^+ uptake through exchange of excess cytoplasmic HCO_3^- to maintain favorable conditions for continued H^+ production via CA-mediated CO_2 hydrolysis to be used in two known pathways for Na^+ uptake. This could be via electroneutral apical Na^+/H^+ exchange and/or the epithelial Na^+ channel, which functions in conjunction with an apical H^+ pump. To determine whether either of these systems was utilized to maintain Na^+ homeostasis or for recovery, both pathways were assessed under basal and recovery conditions. Previous studies have determined that Na^+ uptake can occur in the absence of ambient Cl^- availability (Kirschner 2004, Krogh 1938, Krogh 1939), although the rate may be reduced relative to conditions that provide Cl^- (de With *et al.* 1987). Thus it was not surprising to find a lack of dependency on Cl^-. We also evaluated whether this system was dependent on environmental availability of HCO_3^- to allow uptake via Na^+:HCO_3^- co-transport. After finding no significant dependency of the system on ambient anion availability, we attempted to characterize possible transporters involved in the Na^+ uptake under recovery and control conditions.

Pharmacological assessment of possible Na^+ transport proteins facilitating the increased Na^+ uptake rates in bled *L. stagnalis* revealed that the amplified uptake is at

least partially attributed to an amiloride-sensitive pathway (i.e. Na^+ channels and possibly Na^+/H^+ exchange) and may be limited by availability of cellular substrate in the form of H^+ but is unlikely due to microtubule-dependent relocation of transport proteins. Amiloride significantly reduced the recovery-phase Na^+ uptake at the 100 μmol l^{-1} concentration but did not completely inhibit influx. The significant reduction of Na^+ uptake by ETOX indicated likely dependence of the uptake pathway on cellular substrate in the form of H^+ from CA-catalyzed hydration of CO_2. However, the lack of effect on Na^+ uptake with exposure to colchicine following bleeding indicated that the amplified uptake observed in bled animals was not likely due to relocation of cytoplasmic transport proteins from the cytoplasm to the apical membrane.

Though ECF chemistry is not completely restored to naïve, pre-bleed conditions, the noteworthy ability of this species to mobilize compensatory mechanisms on time scales of less than 3 h after significant fluid loss, is worthy of further study. Additionally, *L. stagnalis* recover significant losses in volume first; then and possibly more importantly they recover major solutes from hypoosmotic media in a matter of hours following fluid recovery. Finally, the ethoxzolamide sensitivity and the modest amiloride sensitivity of the system responsible for the Na^+ recovery indicates that the recovery process is at least partially dependent upon cellular substrate in the form of protons and possibly occur via a Na^+/H^+ anti-porter.

Implications of findings

The consequences of the prolonged periods of reduced protein and Cu concentrations in the ECF are unknown but if we assume hemocyanin (and with that Cu)

is one of the proteins lost with the ECF, impaired O_2 uptake and delivery maybe one consequence. Such respiratory impairment might pose a need for more frequent surfacing for these facultative air-breathing snails following ECF loss, which could render them more susceptible to predation.

Furthermore, the energetic cost of the greatly increased Na^+ (and Cl^-) uptake following a substantial loss of ECF might be significant to these snails and is clearly worthy of investigation. As a final point of interest, these studies were performed on snails cultured in captivity for many generations and without threat of predation. Nevertheless, they maintain a remarkable ability to mobilize the necessary pathways and recover major solutes following ECF loss on relatively short time scales. Wild snails frequently exposed to predators/predation or snails challenged by relatively frequent ECF loss events might have an even more pronounced response to ECF loss.

Chapter 3:

Acquisition of Ca^{2+} and HCO_3^-/CO_3^{2-} for Shell Formation in Embryos of the Common Pond Snail *Lymnaea stagnalis*

3.1. Background

The freshwater common pond snail *Lymnaea stagnalis* produces a sessile gelatinous egg capsule (*tunica capsulis*) containing embryos that have a developmental period of approximately ten days at 22°C. The embryos are contained in prolate spheroidal eggs that are embedded in a gelatinous matrix (*tunica interna*). Features of these egg masses have been previously described in great detail (Bayne 1968, Plesch *et al.* 1971, Morrill 1982) and for the purposes here we have conformed to the morphological nomenclature used by Plesch *et al.* (1971). These embryos metamorphose by approximately day five post-oviposition to produce hippo stage, shell-bearing individuals that will be fully-developed snails upon hatching (Morrill 1982). Direct development during the embryonic stage requires that the embryos be provided with sufficient maternally-derived elemental substrate for shell formation and/or have the capacity to acquire the necessary ions from the ion-poor freshwater. Early histological and histochemical studies of the egg masses of various species of *Lymnaea* indicate that the embryo is bathed in perivitelline fluid (Bayne 1968, Plesch *et al.* 1971) that is bound by a double-membrane egg capsule (*membrana interna* and *externa*, fig. 3.1A, Plesch *et al.* 1971). The egg capsules are connected by thin strings embedded in the *tunica interna* (gelatinous matrix) and this complex of up to nearly 100 eggs is bound by a membrane composed mostly of protein and polysaccharides, a double-layered *tunica capsulis*, and

usually a *pallium gelatinosum* that is nearly histochemically neutral but usually contains eosinophils, a type of parasite repellant (Plesch *et al.* 1971). In fact, Bayne (1968) found that proteins are abundant in the egg capsule of this species and in particular in the perivitelline fluids. Polysaccharides are present in all layers of the egg mass with neutral ones abundant in perivitelline fluids; and acid mucopolysaccharides are common in the *tunica capsulis*.

In addition to carbohydrates and proteins (Bayne 1968, Plesch *et al.* 1971, Taylor 1973), snail egg masses have been found to contain maternal stores of shell-forming and other ions all at concentrations exceeding that in surrounding waters (Taylor 1973). Using excised eggs with pre-gastrula embryos, Beadle (1969a) studied *L. stagnalis* and found mean calculated perivitelline fluid volume for *L. stagnalis* to be 0.70 mm^3. In his study, the capsular membrane was found to be more permeable to water than ions. In a series of experiments using excised egg capsules that were exposed to either a large sugar (raffinose), solutes of large molecular weight polyethylene glycols (m.w. 500-600 or 3000), or standard lake water; Beadle (1969a) found that molecules of approximately m.w. 600 could move across the capsular membrane in both directions. Furthermore, an intact gelatinous matrix and outer envelope retarded inward diffusion of raffinose but did not prevent it. Beadle (1969a) also determined that the undifferentiated pre-gastrula embryo could maintain itself in lake water for more than 24 h suggesting that it is capable of actively regulating its salt and water levels. This agrees with later findings by Taylor (1977) who reported that ion uptake and water excretion systems are developed in the earliest cleavage stages in *L. stagnalis* to cope with the problems of osmotic and ionic regulation. Compared to another pulmonate snail examined in the Beadle (1969a) study,

Biomphalaria sudanica, the gelatinous matrix that surrounds the eggs is thicker in the egg mass of *L. stagnalis* and thus provides a greater buffer between the embryo and the ambient environment considering that the egg capsule provides no significant barrier to the diffusion of water and ions (Beadle 1969a).

In a related study, Beadle (1969b) focused on the Na^+ requirements of developing *B. sudanica* and found that active Na^+ uptake occurred during development, increasing embryonic Na^+ content to seven times that of pre-blastula stage levels. Additionally, and pertinent to this study, he found that the embryos developed normally under reduced [Na^+] of 1/7 normal levels (standard lake water: 0.56 meq l^{-1} Na^+), but total ion reduction to 1/10 of normal resulted in the onset of water balance disruption. This suggests that *B. sudanica* can tolerate a wide range of [Na^+] and possibly other cations with no effect on embryonic snail development when varied individually. Lastly, Taylor (1977) determined that the exchangeable Ca^{2+} content of the embryos increases by five orders of magnitude (1.3 pmol to 130 nmol) over the period from the blastula stage through hatching, clearly demonstrating Ca^{2+} absorption from the egg mass and/or the water.

Considering the ion requirements for calcification, and the ability of *L. stagnalis* embryos to complete direct development in freshwater conditions in a relatively short period of time, it was necessary to determine whether embryos are provided with adequate quantities of shell-forming ions via maternal stores or actively extract the necessary inorganic ions from ambient waters. Thus, the objectives of this study were to determine [Ca^{2+}] in the perivitelline fluid and gelatinous matrix encasing the eggs over the course of development to determine whether there are significant fluctuations when comparing pre- and post-metamorphic stages of development. Additionally, fluxes were

measured of shell-forming Ca^{2+} ions on the micro scale and whole egg mass scale to determine whether egg masses of *L. stagnalis* acquire the necessary Ca^{2+} from environmental sources or are provided with them as maternal stores within the egg mass. Based on preliminary findings it became essential to also determine whether HCO_3^- /CO_3^{2-} sources were from exogenous sources or endogenously produced in egg masses containing post-metamorphic embryos as suggested in early respiratory studies on these embryos by Baldwin (1935) and as proposed and modeled by Greenaway (1971a) in adults of this species.

3.2. Materials and methods

Animals

Egg masses of the common pond snail *Lymnaea stagnalis* were collected in 24-hour intervals from mass cultures with the day of collection considered day zero post-oviposition, for age determination. Embryos were incubated at room temperature (20-22°C) in aerated, dechlorinated Miami-Dade County tap water (Grosell *et al.* 2007). Prior to flux experiments, the egg masses were weighed (g), measured (mm), and viability was determined. Egg masses with less than 80% development were excluded from experiments and analyses.

Visual characterization of development

Specimens were examined using a dissecting microscope fitted with a Nikon Coolpix digital camera with Q-Capture software to preserve a time course of images from day zero through hatching and to determine developmental stages under standardized

conditions. Additionally this system was utilized to catalogue developmental differences, particularly ovum/shell length among embryos raised in control (Miami-Dade County tap water), nominally Ca^{2+}-free (measured 3 µmol l^{-1} Ca^{2+}), and nominally HCO_3^--free (measured 7.5 µmol l^{-1} HCO_3^-) media (table 3.1).

Table 3.1. Nominal chemical concentrations for artificial waters. Values for Miami-Dade County tap water from Grosell *et al.* 2007.

Miami-Dade tap water (µmol l^{-1})	Ca^{2+}-free media (µmol l^{-1})	HCO_3^--free media (µmol l^{-1})
1100 Na^+	650 $NaHCO_3$	1000 NaCl
1030 Cl^-	500 NaCl	120 $MgSO_4 \cdot 7H_2O$
680 HCO_3^-	50 $KHCO_3$	40 KCl
310 Ca^{2+}	120 $MgSO_4 \cdot 7H_2O$	310 $C_{12}H_{22}CaO_{14}$
40 K^+		
120 Mg^{2+}		
110 SO_4^{2-}		

Voltage and Ca^{2+}-selective microelectrodes

Microelectrodes, used for recordings of voltage across the *tunica capsulis* or the *membrana interna and externa*, were pulled from filamented 1.5 mm diameter borosilicate capillary glass (WPI, Sarasota, FL). The microelectrodes were filled with 3 mol l^{-1} KCl and had tip resistances of approximately 30 MΩ. Ca^{2+}-selective microelectrodes used to measure Ca^{2+} concentration in the *tunica interna* and perivitelline fluid were pulled from unfilamented 1.5 mm borosilicate capillary glass (A-M systems, Carlsborg, WA), silanized by exposure to the vapors of dimethyldichlorosilane at 200 °C and stored over silac gel until use. Microelectrodes were backfilled with 100 mmol l^{-1} $CaCl_2$ and tip-filled with a 300 – 500 µm column of Ca^{2+} ionophore I, cocktail A (Fluka, Buchs, Switzerland). Microelectrodes were mounted on micromanipulators (Marzhauser MM33, Fine Science Tools, North

Vancouver, BC) and observed through a dissecting microscope (Wild-Leitz, Heidelberg, Germany).

For measurement of Ca^{2+} concentration in the *tunica interna* of day 2 egg masses, it was necessary to cut two slits, each approximately 300 µm long, in the *tunica capsulis* using the tip of a 25 gauge syringe needle. This incision was necessary because the outer integument of the *tunica capsulis* was too rigid to pierce with the microelectrode without compromising the electrode. The outer integument became increasingly fluidic over the course of development, making the pre-incision necessary only for day 2 measurements. For older egg masses it was feasible to advance the microelectrodes directly across the *tunica capsulis* and into the *tunica interna*. A voltage electrode was then inserted through one slit and advanced 1 - 2 mm into the *tunica interna* and the Ca^{2+}-selective microelectrode was inserted through the second slit. The voltage detected by the voltage microelectrode was subtracted from that detected by the Ca^{2+}-selective microelectrode, yielding a signal proportional to Ca^{2+} concentration. Voltage and Ca^{2+}-selective microelectrodes were connected through a high impedance (> 10^{14} Ω) electrometer (pH/ion Amp, A-M systems, Carlsborg, WA) to a PC-based data acquisitions and analysis system (PowerLab 4/25, AD Instruments, Colorado Springs, CO) running CHART software (AD Instruments).

Calcium concentration ($[Ca^{2+}]_{med}$) in the bathing medium (i.e. artificial Miami Dade water) was calculated as:

$$[Ca^{2+}]_{med} = [Ca^{2+}]_{cal} \cdot 10^{(\Delta V/S)}$$

where $[Ca^{2+}]_{cal}$ is the calcium concentration in a calibration solution (0.1, 1 or 10 mmol l^{-1} Ca^{2+}), ΔV is the voltage difference recorded from the calcium electrode between the

medium and the same calibration solution, and S is the slope of the microelectrode for a 10-fold change in calcium concentration. Although ion-selective microelectrodes measure ion activity and not concentration, data can be expressed in terms of concentrations if it is assumed that the ion activity coefficient is the same in calibration and experimental solutions. Expression of data in units of concentrations aids comparison of Ca^{2+} microelectrode data with techniques such as atomic absorption spectrophotometry, which measures Ca^{2+} concentration. Concentrations can be converted to activities by multiplying by the activity coefficient (0.81 for Miami Dade County tap water). It is important to point out that activity measurements may underestimate calcium concentrations in the *tunica interna* and the perivitelline fluid. This is because polyvalent anions will lower the activity coefficient, relative to the surrounding water, and because some Ca^{2+} is likely bound to macromolecules and not readily diffusible, as demonstrated by Taylor (1973).

Calcium concentration ($[Ca^{2+}]_{ti}$) in the *tunica interna* (i.e. gelatinous matrix) was then calculated as:

$$[Ca^{2+}]_{ti} = [Ca^{2+}]_{med} \cdot 10^{(\Delta V / S)}$$

where ΔV is the voltage difference recorded from the calcium electrode between the matrix and the bathing medium.

For measurement of net electrochemical potential, no slits were made in the *tunica capsulis* and voltage and Ca^{2+}-selective microelectrodes were advanced through the *tunica capsulis* and both voltage and Ca^{2+}-selective microelectrodes were referenced to a bath electrode constructed from a 1.5 mm glass capillary filled with 3 mol l^{-1} KCl in 3% agar and connected through a Ag/AgCl half-cell to the ground input of the amplifier.

This procedure sometimes caused the ionophore column to be pushed back from the tip of the Ca^{2+}-selective microelectrode, requiring replacement of the Ca^{2+}-selective microelectrode. The net electrochemical potential ($\Delta\mu^{tc}_{Ca}/F$) in mV for Ca^{2+} across the *tunica capsulis* was calculated as:

$$\Delta\mu^{tc}_{Ca}/F = RT/F \ln([Ca^{2+}]_{ti}/[Ca^{2+}]_{med}) + zV_{tc}$$

$$= 58 \log([Ca^{2+}]_{ti}/[Ca^{2+}]_{med}) + zV_{tc}$$

where R is the gas constant, T is the temperature (degrees Kelvin), z is the valence, and V_{tc} is the voltage difference across the *tunica capsulis*. A positive value indicates that the concentration of Ca^{2+} in the *tunica interna* is above that expected on the basis of electrochemical equilibrium, and that passive efflux across the *tunica capsulis* and into the bathing medium is therefore favored.

For measurements of calcium concentration in the perivitelline fluid and for calculations of net electrochemical potential across the *membrana interna and externa*, voltage- and Ca^{2+}-selective microelectrodes were advanced through the membranes and into the perivitelline fluid. The calcium concentration in the perivitelline fluid ($[Ca^{2+}]_{PVF}$) was calculated as

$$[Ca^{2+}]_{PVF} = [Ca^{2+}]_{med} \cdot 10^{(\Delta V/S)}$$

The net electrochemical potential across the *membrana interna* and *externa* ($\Delta\mu^{mi\&me}_{Ca}/F$) was calculated as:

$$\Delta\mu^{mi\&me}_{Ca}/F = 58 \log([Ca^{2+}]_{PVF}/[Ca^{2+}]_{med}) + zV_{mi\&me}$$

where $V_{mi\&me}$ is the voltage difference between the perivitelline fluid and the bathing medium for isolated eggs (i.e. across the *membrana interna and externa* together). Dividing $\Delta\mu$ by the Faraday converts the units to mV (Dawson and Liu 2008). A positive

value indicates that the concentration of Ca^{2+} in the perivitelline fluid is above that expected on the basis of electrochemical equilibrium, and that passive efflux across the *membrana interna and externa* and into the bathing medium is therefore favored.

Time course of Ca^{2+}, titratable alkalinity, and ammonia fluxes: Whole egg masses

To evaluate whether the embryos were developing fully from maternal stores or were extracting necessary Ca^{2+} and HCO_3^-/CO_3^{2-} from the water over the course of development, eight egg masses were selected from mass cultures, scored, and placed in individual flux chambers that contained 20 ml of Miami-Dade tap water. Daily 10 ml initial stock and final water samples were collected for each egg mass. Daily net Ca^{2+} flux was determined using the difference in $[Ca^{2+}]$ between the initial and final waters following the 24-h flux as measured by flame atomic absorption spectrophotometry (Varian SpectrAA220, Mulgrave, Victoria, Australia), mass of egg mass (g), and elapsed time (h). Daily net titratable alkalinity flux was calculated from the change in titratable alkalinity from the initial and final flux media samples as determined via double endpoint titration, mass of egg mass (g), and elapsed time (h). The double endpoint titration, rather than a standard titration method, was used to determine titratable alkalinity because the double endpoint titration method is insensitive to non-bicarbonate/carbonate buffering in the media. This technique has been suggested (Hills 1973) and since modified (Wilson *et al.* 1996) and used successfully for this type of titratable alkalinity determination (Wilson *et al.* 1996, Grosell *et al.* 1999). In experiments with low volume:biomass ratios the potential for release of organic material with buffer capacity exists which could lead to erroneous conclusions based on single endpoint titrations. For the double endpoint

titration procedure, which avoids this problem, a 5 ml flux media sample with 5 ml of pH electrode-stabilization media (450 mmol l^{-1} NaCl) were gassed with N_2 for 30 min after which starting pH was noted. Using a Gilmont micro-burette syringe filled with 0.02 N HCl, the sample was titrated down to pH 3.8 and 15 min was allowed for CO_2 degassing. Sample pH was then returned to the original pH value using a second Gilmont micro-burette syringe filled with 0.02 N NaOH while continuously gassed. Using the difference in the amount of acid and base necessary to titrate to 3.800 and the start pH, HCO_3^-/CO_3^{2-} titratable alkalinity equivalents were determined. To evaluate whether the changes in titratable alkalinity were attributable to ammonia flux, we determined ammonia excretion rates over the course of development by calculating total ammonia concentration in initial and final water samples from the 24-h flux. Total ammonia was assessed using a modified colorimetric ammonia assay (Verdouw *et al.* 1978) in which ammonia was reacted with salicylate and hypochlorite to form a blue indophenol in a sodium nitroprusside-catalyzed reaction. The assay was measured on a micro-plate reader (Molecular Devices ThermoMax, Sunnyvale, California, U.S.A.) at 640 nm. Final values for Ca^{2+} and titratable alkalinity net flux as well as total ammonia excretion were presented as μmol g^{-1} h^{-1}.

Time course of Ca^{2+} fluxes: Microscale measurements using the scanning ion electrode technique

Transport of Ca^{2+} into or out of egg masses produces gradients in $[Ca^{2+}]$ in the unstirred layer adjacent to the surface of the tissue. These gradients can be calculated from the voltages recorded by a Ca^{2+}-selective microelectrode moved between two points

within the unstirred layer. Calcium flux can then be calculated from the concentration gradients using Fick's law, as described below. Measurement of fluxes in this way is the basis of the scanning ion electrode technique (SIET), which allows fluxes to be repeatedly measured in near real-time at sites along the length of an egg mass. Extensive descriptions of the use of SIET are reported in Rheault and O'Donnell (2001, 2004) and Donini and O'Donnell (2005).

SIET measurements were made using hardware from Applicable Electronics (Forestdale, MA, USA) and automated scanning electrode technique (ASET) software (version 2.0) from Science Wares Inc. (East Falmouth, MA, USA). Egg masses were placed in 35 mm diameter petri dishes filled with 5 ml of artificial Miami-Dade water. Reference electrodes were made from 10 cm lengths of 1.5 mm borosilicate glass capillaries that were bent at a 45° angle, 1-2 cm from the end, to facilitate placement in the sample dish. Capillaries were filled with boiling 3 mol l^{-1} KCl in 3% agar and connected to the ground input of the Applicable Electronics amplifier through an Ag/AgCl half cell.

Ca^{2+}-selective microelectrodes for use with SIET were calibrated in 0.1, 1, and 10 mmol l^{-1} Ca^{2+}. All scans were performed in artificial Miami-Dade County water with a Ca^{2+} concentration of 310 µmol l^{-1}. The Ca^{2+}-selective microelectrode was initially placed 5-10 µm from the surface of the egg mass. The microelectrode was then moved a further 50 µm away, perpendicular to the egg mass surface. The "wait" and "sample" periods at each limit of the 50 µm excursion distance were 4.5 and 0.5 s, respectively. Voltage differences across this excursion distance were measured three times at each of the five to eighteen sites along each egg mass and scans of the same sites were repeated

four or more times over a 1-h period. Voltage differences were corrected for electrode drift measured at a reference site 10-20 mm away from the egg mass. Voltage differences (ΔV) were converted to the corresponding [Ca^{2+}] difference by the following equation (Donini and O'Donnell 2005):

$$\Delta C = C_B \times 10^{(\Delta V/S)} - C_B$$

where ΔC is the [Ca^{2+}] difference between the two limits of the excursion distance (µmol cm^{-3}), C_B is the background [Ca^{2+}] in the bathing medium , ΔV is the voltage difference (mV); and S is the slope of the electrode between 0.1 and 1 mmol l^{-1} Ca^{2+}. Concentration differences were used to determine the Ca^{2+} flux using Fick's law of diffusion:

$$J_{Ca} = D_{Ca}(\Delta C/\Delta X)$$

where J_{Ca} is the net flux in µmol cm^{-2} s^{-1}, D_{Ca} is the diffusion coefficient of Ca^{2+} (1.19×10^{-5} cm^2 s^{-1}), ΔC is the Ca^{2+} concentration difference (µmol cm^{-3}) and ΔX is the excursion distance between the two points (cm).

Ca^{2+} and HCO_3^-/CO_3^{2-} kinetics

For Ca^{2+} uptake kinetics experiments, day seven egg masses were incubated for 24 h in 20 ml of media with nominal ion concentrations approximating that of Miami-Dade County tap water except for Ca^{2+}, which was adjusted to nominal concentrations of 10, 20, 60, 90, 100, 200, 600, or 900 µmol l^{-1} Ca^{2+} using $CaCl_2$ (Sigma-Aldrich). Egg masses were dip-rinsed in appropriate flux media prior to the start of the flux. For determination of fluxes, 10 ml of initial media stock and 10 ml of final media from flux chambers were collected for each treatment. Calcium and titratable alkalinity net flux

were determined for each [Ca^{2+}] as described above in the time course section and presented as µmol g^{-1} h^{-1}.

For HCO_3^- kinetics experiments, [Ca^{2+}] was maintained at 310 µmol l^{-1} and [HCO_3^-] was adjusted to either 200, 400, 800, or 1200 µmol l^{-1} HCO_3^- with choline bicarbonate (Sigma-Aldrich, [2-hydroxyethyl] trimethylammonium, $C_5H_{14}NO{\cdot}HCO_3$). Both Ca^{2+} net flux and titratable alkalinity net flux were determined for each [HCO_3^-]. Ammonia fluxes were not included here due to the nearly undetectable concentrations measured during the time course experiments. Egg masses and flux procedures were handled in the same manner as described above for time course and Ca^{2+} kinetics experiments.

Fluxes in HCO_3^-/CO_3^{2-}-free HEPES-buffered media

Day seven egg masses were scored and dip-rinsed then placed in individual chambers with 20 ml of flux media that contained either 680 µmol l^{-1} HCO_3^-, which is comparable to Miami-Dade County tap water, or HCO_3^-/CO_3^{2-}-free HEPES-buffered media (1.5 mmol l^{-1} each HEPES-free H^+ and HEPES-Na^+ salt; Sigma-Aldrich) with all other ions maintained at concentrations comparable to Miami-Dade County tap water. This concentration of HEPES provided for adequate buffering under bicarbonate-free conditions while still allowing for measurements of changes in apparent titratable alkalinity (Grosell and Taylor 2007). Egg masses were incubated for 24 h. Then 15 ml of the initial and final media samples were taken and analyzed for [Ca^{2+}], titratable alkalinity, and total ammonia. Net Ca^{2+} flux was determined as described above. Net titratable alkalinity flux was calculated from results of single endpoint titrations on initial

and final media samples as outlined in Grosell and Taylor (2007). In the absence of HCO_3^-/CO_3^{2-}, changes in apparent titratable alkalinity would be a result of H^+ excretion and its effects (i.e. NH_4^+ trapping). Therefore, it was not necessary to complete double-endpoint titrations as in the HCO_3^-/CO_3^{2-}-buffered solutions. For the single-endpoint procedure, aliquots of 10 ml were collected and gassed continuously in 50 ml Falcon tubes with N_2 for 30 min prior to and during the titration to insure the absence of CO_2. pH was noted following the initial 30 min gassing and then the 10 ml sample was titrated using a Gilmont micro-burette syringe filled with 0.02 N HCl down to pH 7.0 noting the pH and amount of 0.02 N HCl added at the final pH and for no less than three points along the titration curve. Linearity was conserved down to pH 7.0 but was lost below that value thus $[H^+]$ values below pH 7.0 were not used in the H^+ excretion calculation. Initial and final samples were titrated on the same pH electrode and with the same burette. All curves were fit by non-linear regression analysis and only those curves for which $R^2 > 0.95$ were included. The titratable alkalinity net flux (= acid excretion) was calculated using the difference between the H^+ added to reach the known pH of 7.0 for both the initial and final flux media, the mass of the egg mass (g), and the elapsed flux time (h). Total ammonia excretion was determined as described above.

Statistical analyses

Uptake kinetic constants, apparent affinity (k_m), and capacity (V_{max}) were determined assuming Michaelis-Menten saturation kinetics and using the non-linear regression function in SigmaPlot for Windows version 11.00. Comparisons among experimental groups were completed using an ANOVA with pairwise comparisons where

appropriate following the Holm-Sidak method after an evaluation for whether the data sets were normally distributed with the Shapiro-Wilk test. All values are means ± S.E.M. and statements of statistical difference were reserved for $P < 0.05$.

3.3. Results

Developmental observations

Embryos grew from an ovum diameter of 100 µm at day two to a shell length of 800 µm at day ten under control conditions and were enclosed in egg capsules that were approximately 1 x 1.25 mm. Eggs were firmly nested in the *tunica interna* of the egg mass and the entire mass was encased in the *tunica capsulis*, which was approximately 300 - 400 µm thick. The outermost layer, the *pallium gelatinosum*, was approximately 100-200 µm thick. There was no apparent loss in egg viability observed for those egg masses incubated in nominally HCO_3^-/CO_3^{2-}-free artificial Miami-Dade County tap water relative to controls; however, those raised in nominally Ca^{2+}-free media exhibited growth retardation relative to controls in all treated egg masses (e.g. fig. 3.1, 3.2). Control embryos developed to hatching within 10 - 12 d post-oviposition, and metamorphosis to the hippo stage occurred at approximately day five. Reduced aquatic availability of Ca^{2+} resulted in reduced growth rates and longer times to hatch. However, embryos incubated in HCO_3^--free water exhibited faster growth rates relative to controls and Ca^{2+}-free conditions around the time of metamorphosis (day four and day seven, fig. 3.2).

Figure 3.1. Day ten images from a time course of embryonic development of the freshwater common pond snail *L. stagnalis* under control (A; dechlorinated MDTW; 310 µmol l^{-1} Ca^{2+} and 680 µmol l^{-1} HCO_3^-), nominally HCO_3^--free (B; 310 µmol l^{-1} Ca^{2+} and 7.5 µmol l^{-1} HCO_3^-), and nominally Ca^{2+}-free (C; 3 µmol l^{-1} Ca^{2+} and 680 µmol l^{-1} HCO_3^-) conditions. Eggs were placed in the media within 24 hours post-oviposition and maintained for the duration of the development with daily water replacement. Morphological characters are identified in Fig. 3.1A (a: Embryo; b: Perivitelline fluid; c: Egg capsule (*membrana interna* and *membrana externa*); d: *Tunica interna*; e: double-layer outer membrane, *tunica capsulis*; f: *Pallium gelatinosum*).

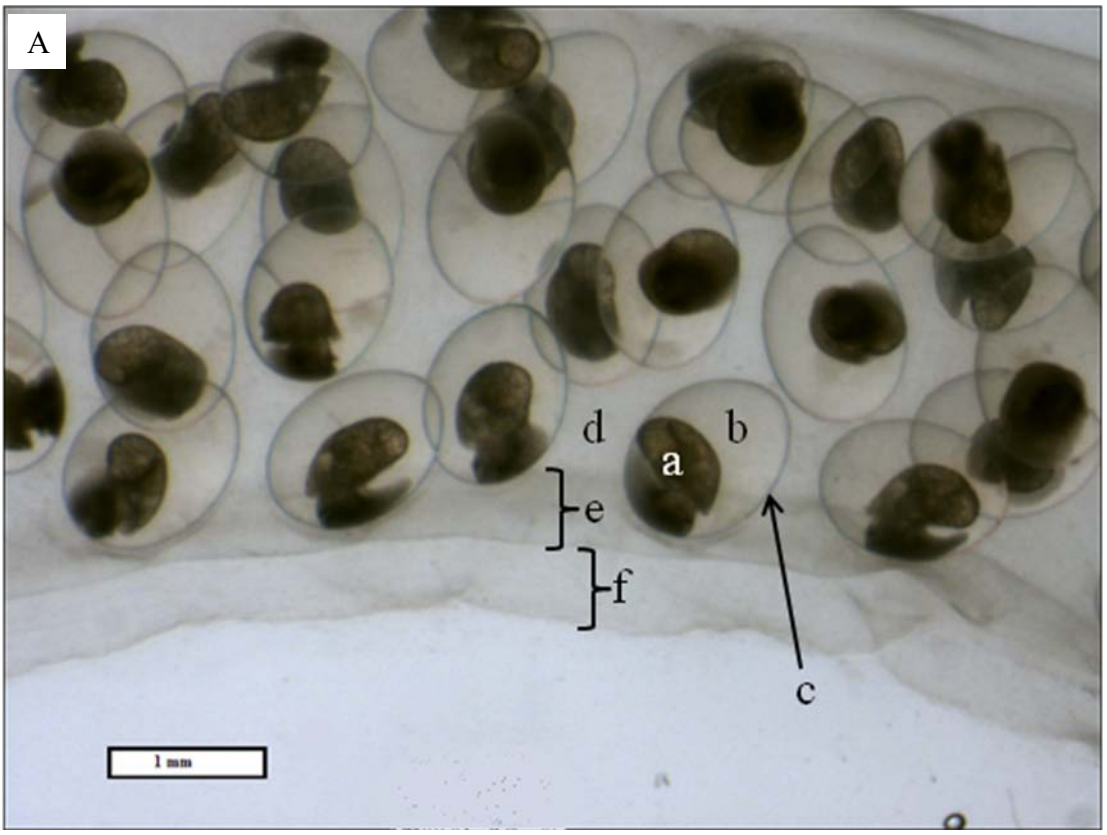

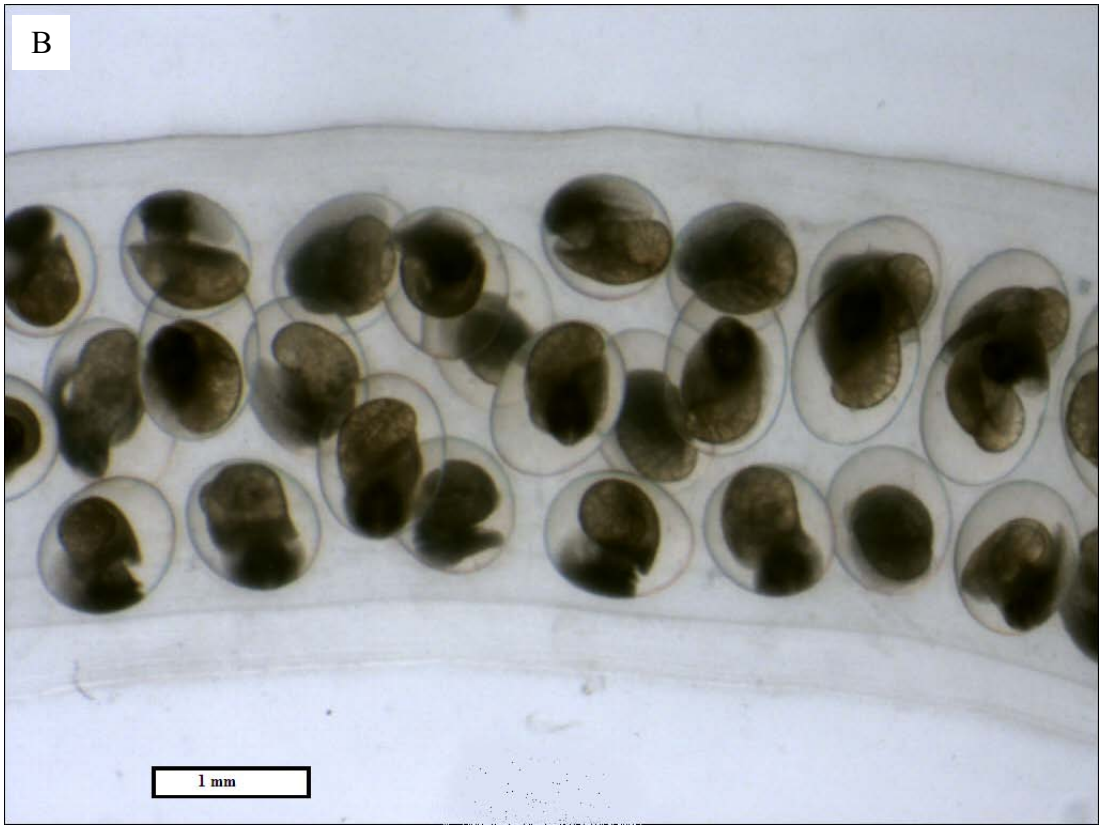
B
1 mm

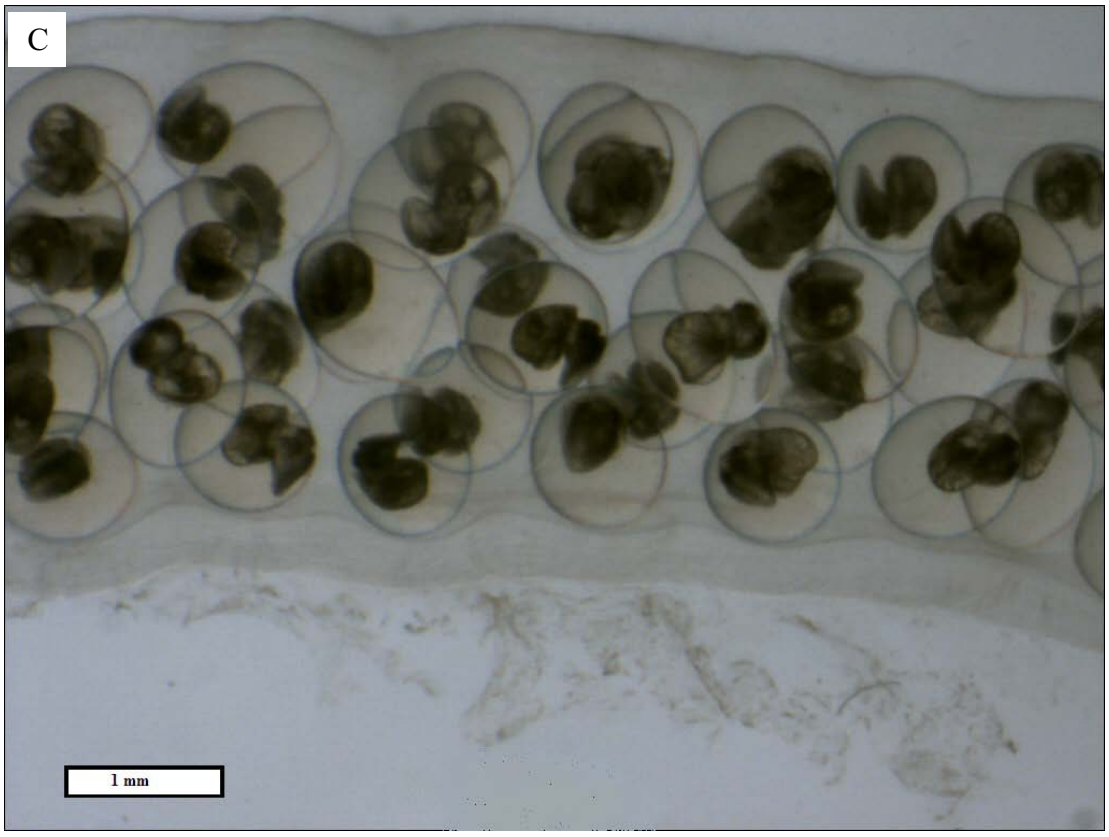
C
1 mm

Figure 3.2. Pre-metamorphic ovum diameter and post-metamorphic shell lengths of embryos of *L. stagnalis* (µm ± S.E.M.) in control (dechlorinated MDTW; 310 µmol l^{-1} Ca^{2+} and 680 µmol l^{-1} HCO_3^-), nominally HCO_3^--free (310 µmol l^{-1} Ca^{2+} and 7.5 µmol l^{-1} HCO_3^-), and nominally Ca^{2+}-free (3 µmol l^{-1} Ca^{2+} and 680 µmol l^{-1} HCO_3^-) media. N = 10 ova or embryos for each measurement. * = significant difference from controls of the same age.

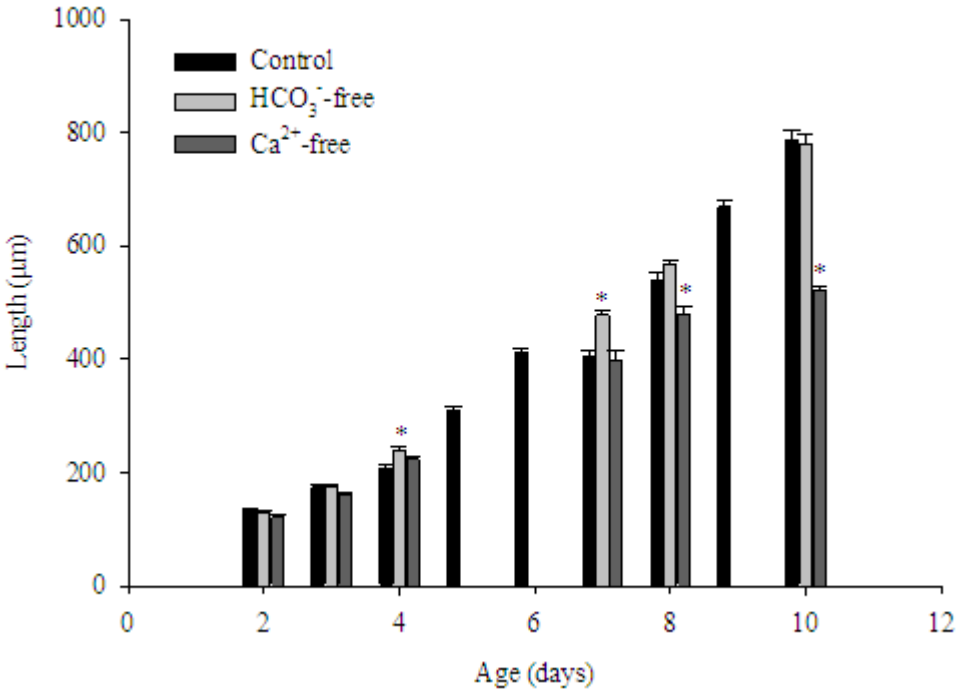

Embryos raised in Ca^{2+}-free water were significantly smaller than controls beginning with day eight and showed no growth after day eight (fig. 3.2). Those incubated in HCO_3^--free media developed to approximately the same size by the end of embryonic development as controls but those in Ca^{2+}-free media developed much less consistently and most individuals in this treatment group did not hatch or reach pre-hatch size within 15-18 days.

Endogenous Ca^{2+} sources

Considering the disparity in developmental rates among varying ambient water conditions it was necessary to evaluate Ca^{2+} availability in the perivitelline fluid bathing the embryos and in the gelatinous matrix (*tunica interna*) that surrounded the eggs. This was accomplished with the use of Ca^{2+}-selective microelectrodes. Calcium concentration in the gelatinous matrix holding eggs of pre-metamorphic embryos was three to four times greater than that of the bathing media (fig. 3.3). Furthermore, $[Ca^{2+}]_{PVF}$ was five to seven times that of the bathing media (fig. 3.4).

The visible onset of shell formation, an indicator of metamorphosis, at approximately day five, was concurrent with significantly decreased $[Ca^{2+}]$ in the *tunica interna* of post-metamorphic egg masses to levels below pre-metamorphic concentrations. Also, perivitelline fluid from post-metamorphic (day seven and nine) eggs had significantly lower $[Ca^{2+}]$ than eggs containing pre-metamorphic embryos (fig. 3.4). Results from the aforementioned experiments indicated a need to consider the likelihood of important interactions between the egg mass and its contents with the surrounding environment, particularly in post-metamorphic stages.

Exogenous Ca^{2+} sources

Using Ca^{2+}-selective and voltage microelectrodes for measurements of $[Ca^{2+}]$ and transmembrane voltage difference, respectively, we were able to quantify the net electrochemical potential ($\Delta\mu_{Ca}/F$) across these barriers in peri- and post-metamorphic stages. Day seven $\Delta\mu_{Ca}/F$ (-19.7 mV) and Δ V (-9.2 ± 0.60 mV) values were negative across *tunica capsulis* membrane. After emergence of the embryos from the egg capsules

on day ten, but prior to their emergence from the egg mass, mean $\Delta\mu_{Ca}/F$ became more negative (-51.0 mV) with no significant change in transmembrane voltage difference (-8.7 ± 1.11 mV, inside negative). For excised eggs, mean $\Delta\mu_{Ca}/F$ across the *membrana interna* and *externa* was more negative on day nine (-26.4 mV) relative to peri-metamorphic values (day five, -3.7 mV); however the voltage difference across these membranes became less negative over the same time period (day five: -21.4 ± 0.92 mV, day nine: -9.1 ± 0.77 mV).

Measurements of 24-h whole egg mass Ca^{2+} net flux with daily water replacement indicated net uptake of Ca^{2+} and titratable alkalinity, but only after metamorphosis and with no significant change in ammonia excretion (fig. 3.5). A time course of near-daily microscale flux measurements indicated a shift from nearly no Ca^{2+} flux during pre-metamorphic stages and a shift to net uptake on day five. Net uptake rates increased and continued through post-metamorphosis within the unstirred boundary layer (fig. 3.6). Calcium uptake rates, which were calculated from the unstirred boundary layer concentration gradients, peaked around day eight to nine. Site-specific measurements of several post-metamorphic egg masses indicated that the uptake was uniform across the surface of the egg mass (data not shown). When exposed to a range of $[Ca^{2+}]$, actively transporting, day seven egg masses exhibited net uptake rates across the range in a significant Michaelis-Menten, saturation-type relationship (fig. 3.7A).

Flux of acid-base equivalents

Titratable alkalinity net flux varied over the range of ambient $[Ca^{2+}]$ in a saturation-like pattern particularly at concentrations ≤170 μmol l^{-1} Ca^{2+}, with saturation

occurring above 170 µmol l^{-1} Ca^{2+} (Fig. 3.7B). The manipulation of ambient water [HCO_3^-] over the nominal range of 200-1200 µmol l^{-1} HCO_3^- resulted in no significant changes in net Ca^{2+} transport (Fig. 3.8A) and no correlation with net titratable alkalinity transport rates (Fig. 3.8B). However, there was a significant effect on Ca^{2+} net flux, titratable alkalinity net flux, and ammonia excretion for egg masses under HCO_3^- -free HEPES-buffered conditions. Net Ca^{2+} uptake was significantly greater under HCO_3^--free, HEPES-buffered conditions relative to controls (Fig. 3.9A) while net titratable alkalinity flux was approximately 1/3 that of the controls (Fig. 3.9B). Lastly, under HCO_3^--free, HEPES-buffered conditions, ammonia excretion rates were significantly greater than control values with rates nearly 2 ½ times that in controls (Fig. 3.9C).

Figure 3.3. Mean concentrations of Ca^{2+} in the *tunica interna* (mmol l^{-1} ± S.E.M.) as measured on days two through ten with Ca^{2+}-selective microelectrodes. Greater than 80% egg viability was observed in all cases. Numbers in parentheses indicates sample size for indicated time point. Developmental stages with the same letter notation are not significantly different. Water [Ca^{2+}] = 0.31 mmol l^{-1}.

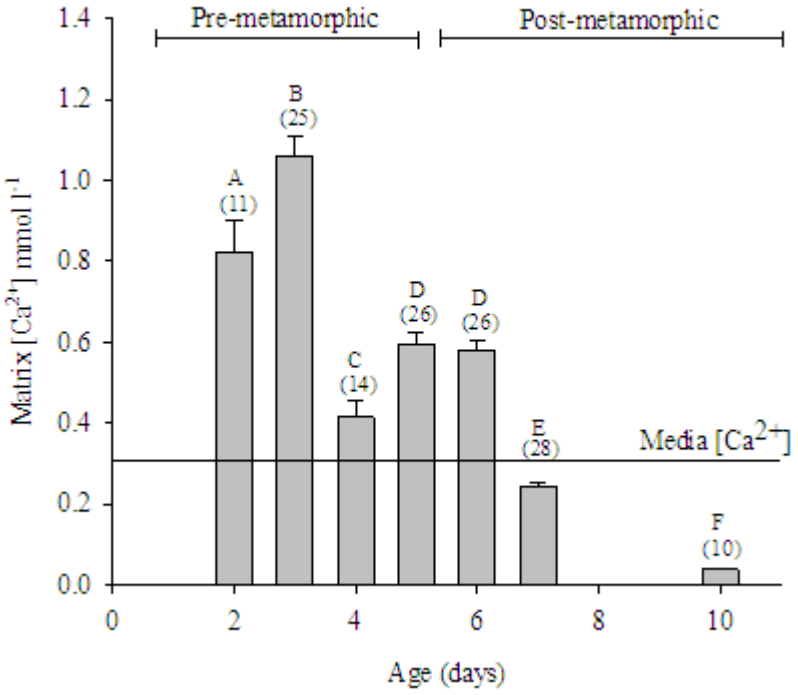

Figure 3.4. Mean concentration of Ca^{2+} in perivitelline fluid (mmol l^{-1} ± S.E.M.) as measured on days two through nine with Ca^{2+}-selective microelectrodes. Numbers in parentheses indicate sample size for indicated time point. Developmental stages with the same letter notation are not significantly different. Water [Ca^{2+}] = 310 µmol l^{-1}.

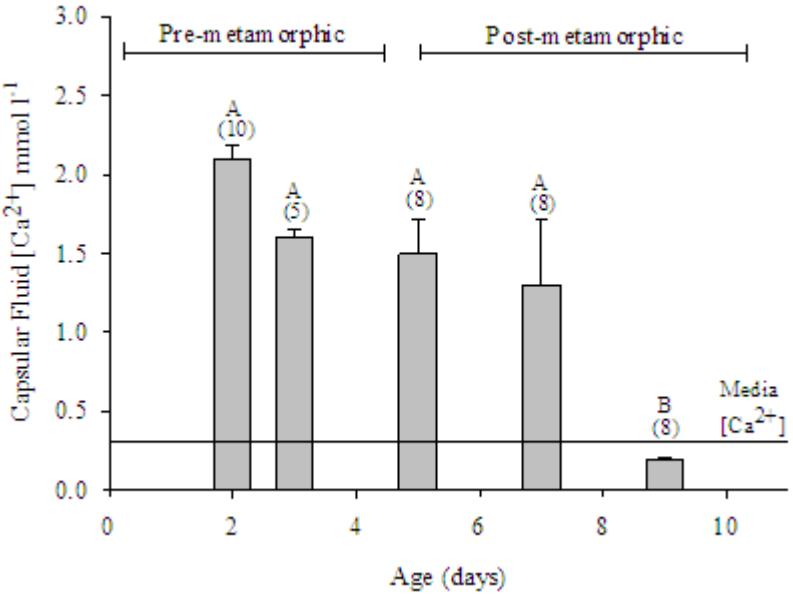

Figure 3.5. Daily net Ca^{2+}, titratable alkalinity (TA), and total ammonia fluxes (µmol g^{-1} h^{-1} ± S.E.M.) for eleven subsequent 24-hr periods for developing egg masses. N = 8 egg masses analyzed for each data point as measured in Miami-Dade County tap water [Ca^{2+}] = 506 ± 3 µmol l^{-1}.

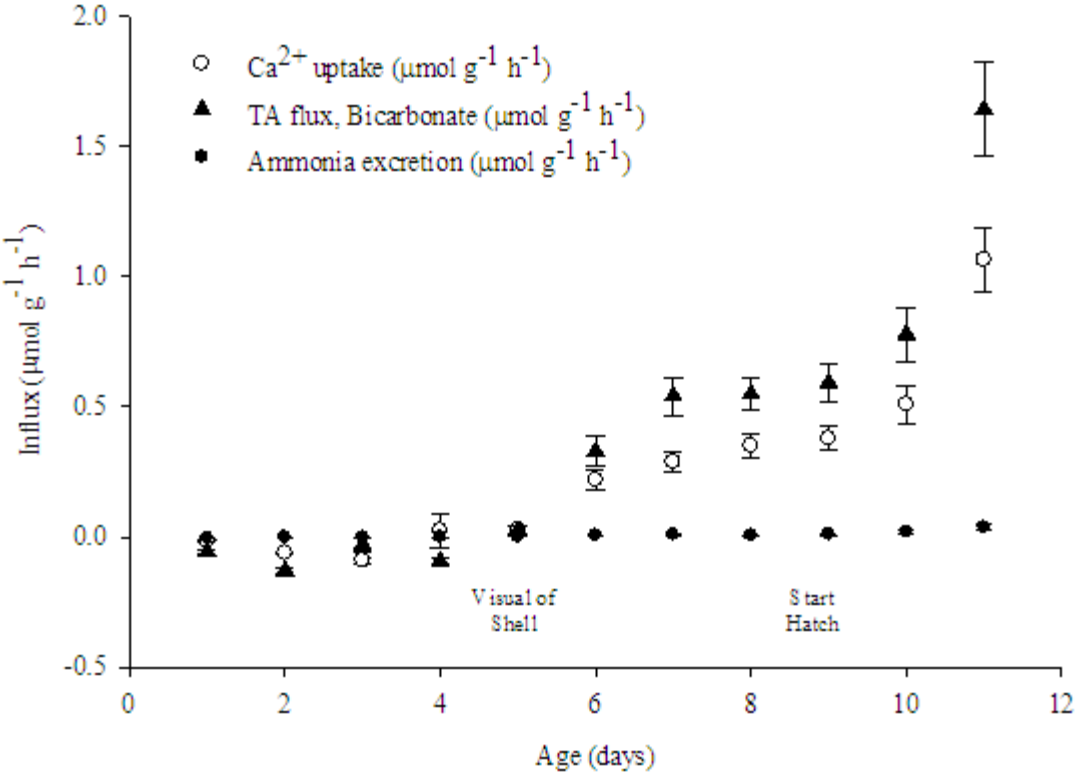

Figure 3.6. SIET measurement of microscale Ca^{2+} flux over development (µmol cm^{-2} h^{-1} ± S.E.M.) for *L. stagnalis* egg masses. Numbers in parentheses indicate sample size for indicated time point. Water [Ca^{2+}] = 310 µmol l^{-1}.

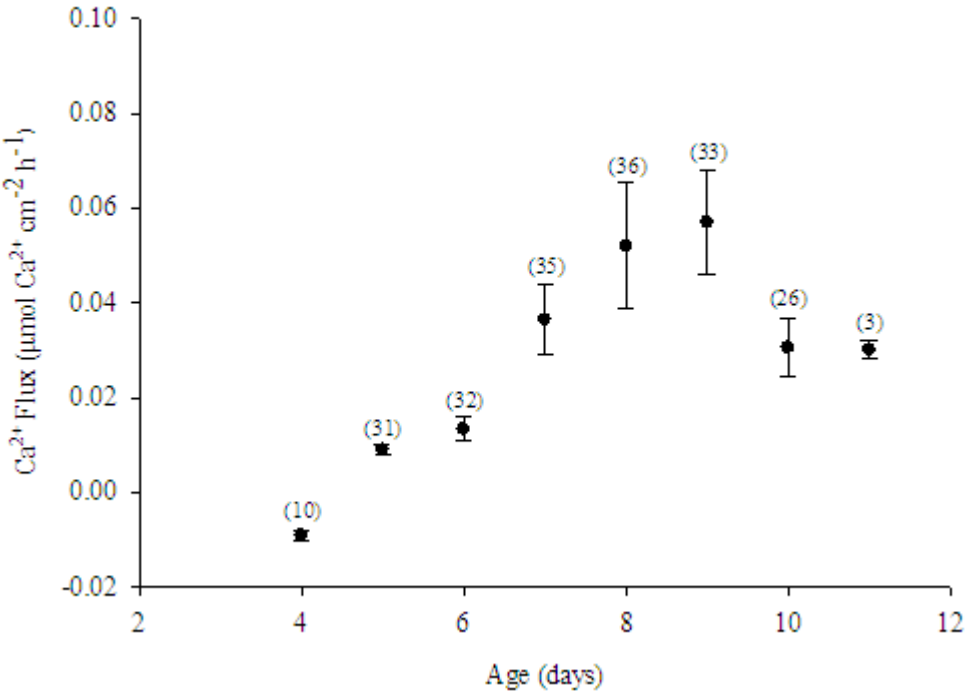

Figure 3.7. Mean net Ca^{2+} (A) and titratable alkalinity (B) fluxes (µmol g^{-1} h^{-1} ± S.E.M.) as a function of ambient [Ca^{2+}] for egg masses of the pond snail *L. stagnalis*. Values are for day seven egg masses that were fluxed for 24 h. Regression line is a Michaelis-Menten curve (Net Ca^{2+}: k_m = 91 ± 41.5 µmol l^{-1} Ca^{2+}, V_{max} = 0.4 ± 0.06 µmol g^{-1} h^{-1}, R^2 = 0.84, $p < 0.002$). There was no significant relationship between [Ca^{2+}] and TA net flux ($P > 0.05$); however the curve is the best fit trace assuming Michaelis-Menten saturation kinetics. Sample size is indicated for respective [Ca^{2+}] above each data point.

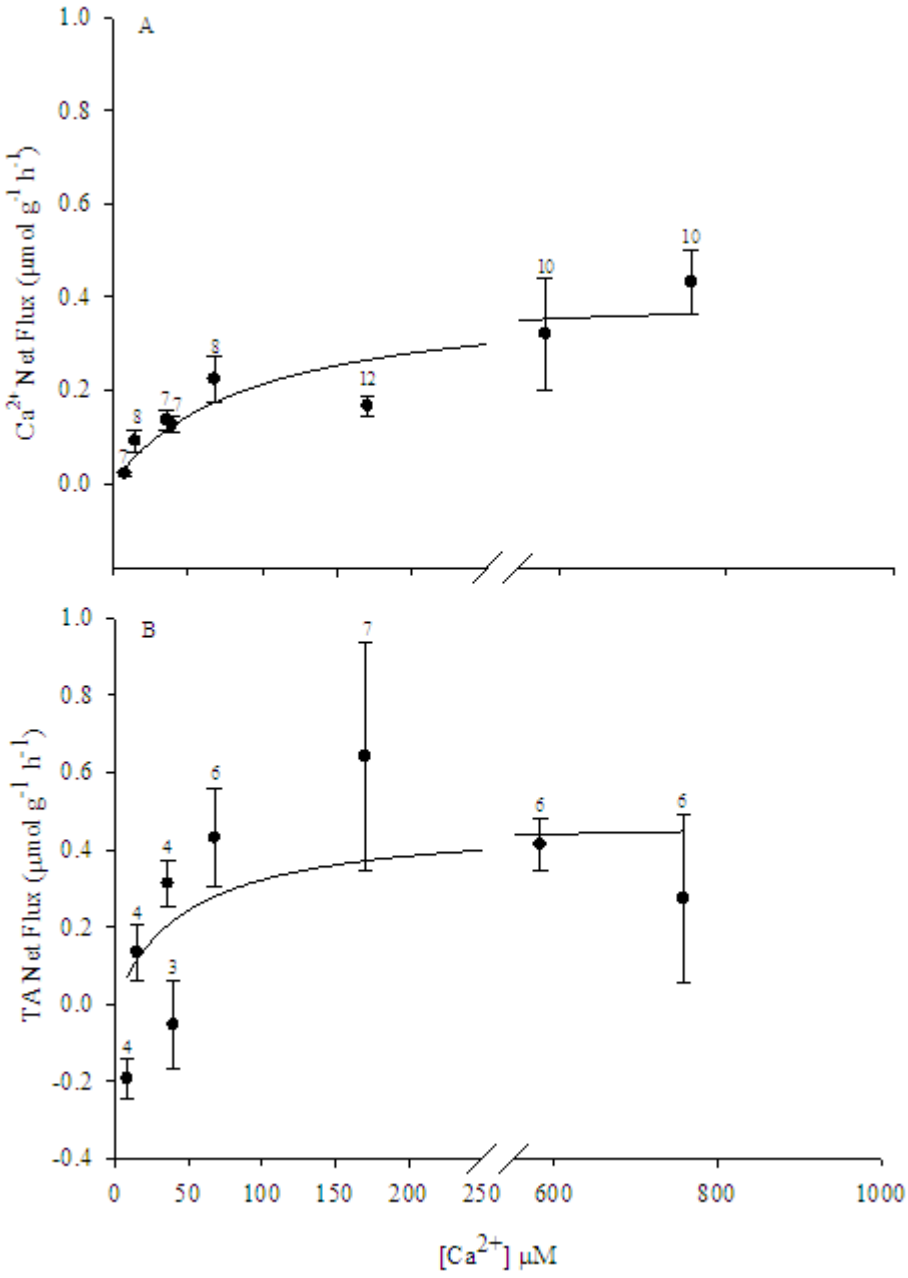

Figure 3.8. Mean net Ca^{2+} (A) and titratable alkalinity (B) fluxes (µmol g^{-1} h^{-1} ± S.E.M.) as a function of ambient [HCO_3^-] for egg masses of the pond snail *L. stagnalis.* Values are for day seven egg masses that were fluxed for 24 h. There was no apparent relationship between Ca^{2+} or TA net flux and [HCO_3^-]. Sample size is indicated for respective [HCO_3^-] above each data point.

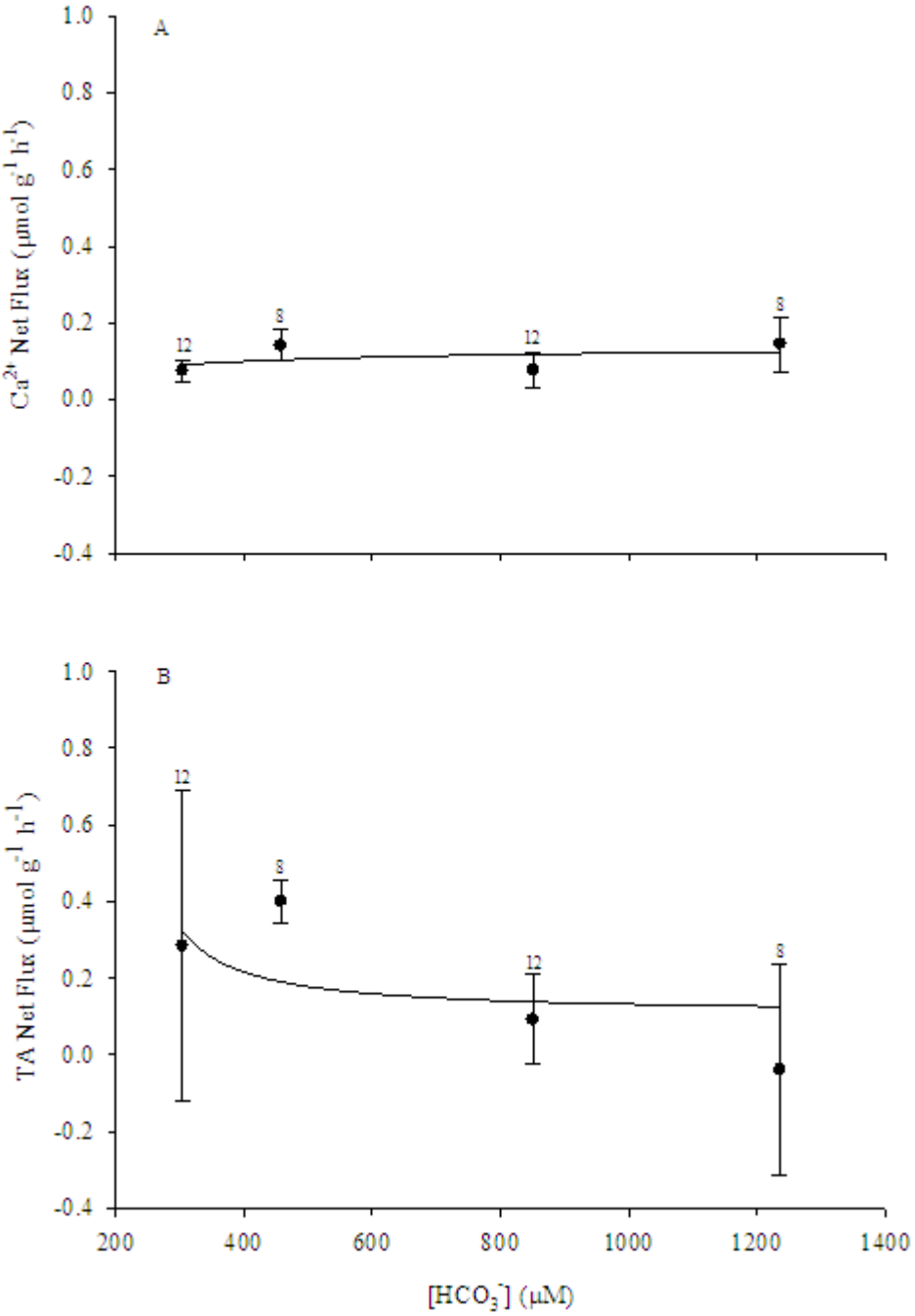

Figure 3.9. Mean net Ca^{2+} uptake (A), titratable alkalinity uptake (B), and ammonia excretion (C) rates (µmol g^{-1} h^{-1} ± S.E.M.) under control (bicarbonate-buffered, 680 µmol l^{-1} HCO_3^-) & nominally HCO_3^--free (HEPES-buffered (BFH), 7.5 µmol l^{-1} HCO_3^-, 3 mmol l^{-1} HEPES) media conditions. Values are for day 7 egg masses that were fluxed for 24 h. N = 8 for controls and N = 7 for treatment. * = significantly different from bicarbonate-buffered ($P < 0.05$).

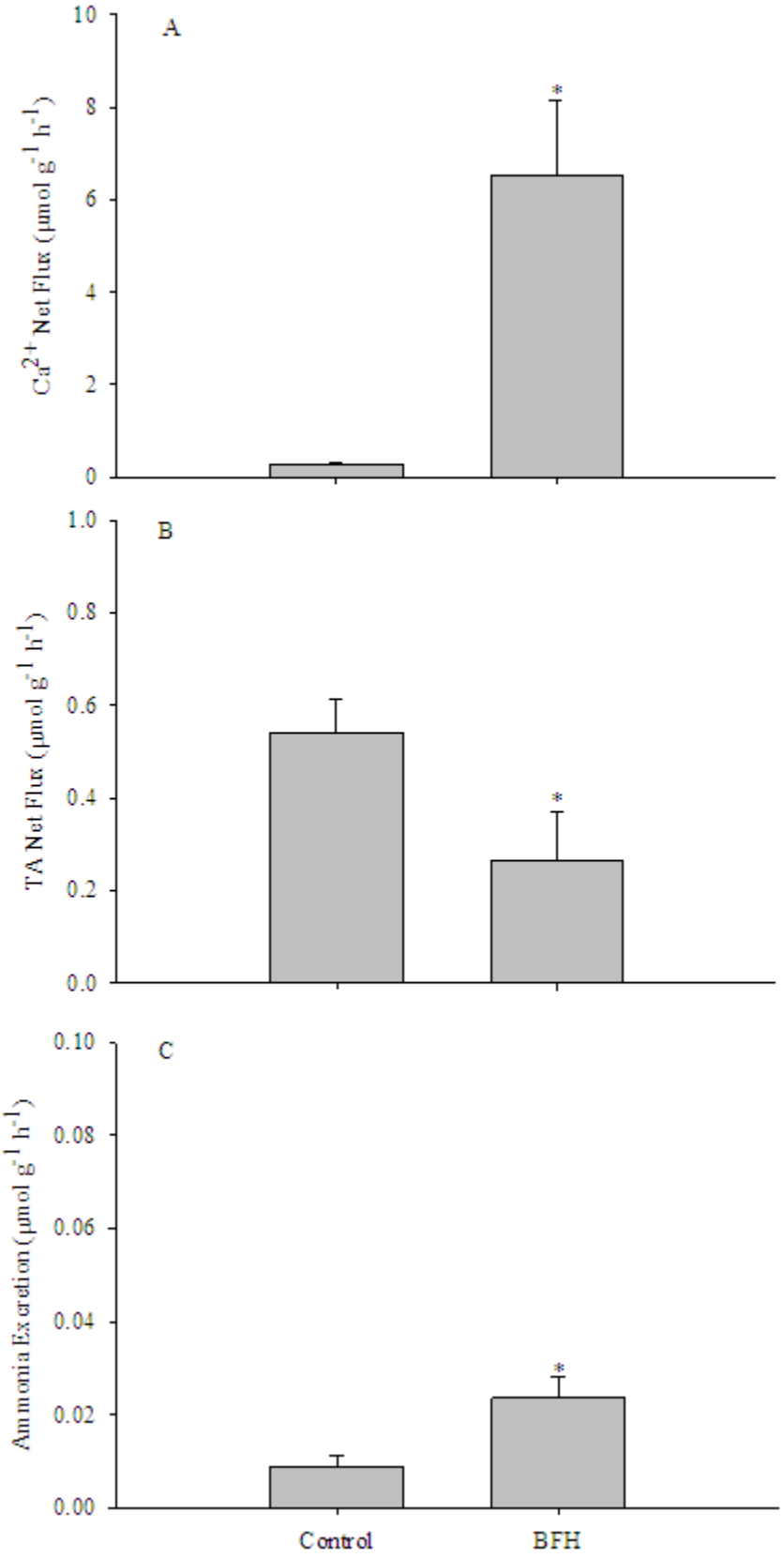
A
B
C
Ca^{2+} Net Flux (μmol g^{-1} h^{-1})
TA Net Flux (μmol g^{-1} h^{-1})
Ammonia Excretion (μmol g^{-1} h^{-1})
0
2
4
6
8
10
0.0
0.2
0.4
0.6
0.8
1.0
0.00
0.02
0.04
0.06
0.08
0.10
*
Control
BFH

3.4. Conclusions and implications

Developing embryos of *L. stagnalis* showed visible dependency on environmental Ca^{2+} sources after depletion of maternal stores in the form of reduced growth rates (figs. 3 and 4), but no apparent dependence on exogenous HCO_3^-/CO_3^{2-} sources (fig. 3.2). We also observed a distinct difference in the structural integrity of the egg mass membrane (i.e. resistant to penetration during early development but more permeable in post-metamorphic stages) and significant differences in the Ca^{2+} content and $\Delta\mu_{Ca}/F$ over the course of development, but particularly during peri- and post-metamorphic stages. Thus, it was important to consider interactions between the contents of the egg mass and the surrounding environment that may facilitate the process of embryonic acquisition of shell-forming ions.

The saturation-type kinetics that we observed in the post-metamorphic embryos of *L. stagnalis* were remarkably similar to those reported by Greenaway (1971b) in adults of the species. Greenaway calculated a half-saturation point of 300 µmol Ca^{2+} l^{-1} and determined that the uptake pathway reached the maximum of 0.5 µmol g^{-1} h^{-1} at 1000-1500 µmol Ca^{2+} l^{-1}. That maximum value was comparable to the maximum of 0.4 µmol g^{-1} h^{-1} above 600 µmol Ca^{2+} that we found here. However, the observed half-saturation value (91 µmol Ca^{2+} l^{-1}) was nearly 1/3 of his calculated value. This may be due to the difference in developmental stage (embryonic versus adult), difference in pre-experimental $[Ca^{2+}]$, or other parameters.

Over the course of development, changes in the penetrability of the integument of the *tunica capsulis*, and fluctuations in $[Ca^{2+}]$ in the perivitelline fluid were consistent with the presence and use of maternal stores during pre-metamorphic stages. The earliest

studies on various vertebrate eggs including *Raja*, *Triton*, *Bufo*, and salmonid species in freshwater environments indicated changes in their permeability to water and ions during development from impermeability to semi-permeability (Gray 1920, Krogh and Ussing 1937, Krogh *et al.* 1939). The changes in the degree of permeability to water and/or ions were attributed to changes in the protoplasmic membrane (limiting layer) coupled with embryonic activation of osmoregulatory mechanisms. At the egg and embryonic level of development, Krogh (1965) clearly stated that there was no reason to distinguish between vertebrates and invertebrates in freshwater because the problem of preserving maternal ionic stores against the strong outward gradient is universal particularly until the mechanisms for osmoregulation have developed and become active. In preliminary whole egg mass experiments, net uptake of Ca^{2+} from incubation media was observed with developing *L. stagnalis* egg masses but not when the embryos were dead (data not shown). In later time course experiments we found that the egg masses incubated in nominally Ca^{2+}-free and HCO_3^--free media were affected by lack of Ca^{2+} availability in the incubation media but not by HCO_3^--free conditions, which suggests that there is an alternative HCO_3^-/CO_3^{2-} source for shell formation. The increased Ca^{2+} uptake in HCO_3^--free HEPES-buffered conditions points to a likely connection between Ca^{2+} uptake and apparent HCO_3^-/CO_3^{2-} acquisition under depleted HCO_3^-, yet buffered, conditions.

The presence of internal Ca^{2+} stores may explain why when embryos had essentially no exogenous Ca^{2+} sources available they still developed shell but exhibited retarded growth relative to controls. We measured 2 mmol Ca^{2+} l^{-1} in perivitelline fluid of *in situ* eggs containing pre-metamorphic embryos (fig. 3.4). This is less but on the same order of magnitude as the 6 - 7.5 mmol Ca^{2+} l^{-1} (12 - 15 meq Ca^{2+} l^{-1}) measured by

Taylor (1973). There are procedural and possibly population differences to take into consideration between the two studies. Within his study there were greater differences in [Ca^{2+}] between perivitelline fluids of eggs from different egg masses compared to those taken from the same egg mass. This suggests that [Ca^{2+}] in perivitelline fluids of eggs from different snails may differ and account for part of the difference between observations from this study and those of Taylor (1973). Also around the onset of shell formation, when internal Ca^{2+} stores were depleted, substantial Ca^{2+} uptake from the water occurred as evident from both net flux measurements on whole egg masses and microscale measurements whereas there was no significant net movement of either shell-forming ion in pre-metamorphic stages (fig. 3.5). Nonetheless, Taylor (1973) calculated that Ca^{2+} activity in the perivitelline fluid was 4.8 mequiv l^{-1} (*i.e.* 2.4 mmol l^{-1}), in good agreement with our value of 2 mmol l^{-1} in pre-metamorphic embryos. The difference between activity and concentration in the perivitelline fluid may reflect interactions of Ca^{2+} with polyvalent anions and binding of Ca^{2+} by macromolecules. As a result, the Ca reserves in the *tunica interna* and PVF are probably considerably larger than indicated by measurements of Ca^{2+} based on microelectrodes, which measure Ca^{2+} activity.

Measurements of perivitelline fluid using a Ca^{2+}-selective microelectrode revealed that there were significant Ca^{2+} stores in the perivitelline fluid (five to seven times that of the incubation media, fig. 3.4) and gelatinous matrix (three to four times incubation media, fig. 3.3) surrounding the eggs of the egg masses during early developmental stages but that these stores apparently become depleted around the time of shell formation. During metamorphosis or at least by day seven, an inside negative $\Delta\mu_{Ca}/F$ exists across the membranes separating the embryo from the aquatic environment.

This potential was more strongly negative with emergence of the embryos from the egg capsules on day ten. This change in $\Delta\mu_{Ca}/F$ was attributed to decreased [Ca^{2+}] in the perivitelline fluid and *tunica interna*. After metamorphosis, but prior to emergence of embryos from the egg mass, mean $\Delta\mu_{Ca}/F$ across the *tunica capsulis* became more negative (day seven: -19.7 mV, day ten: -51.0 mV) despite a lack of significant change in transmembrane voltage difference (day seven: -9.2 ± 0.60 mV, day ten: -8.7 ± 1.11 mV). However, the strengthening in $\Delta\mu_{Ca}/F$ from day seven to day ten was accompanied by decreased [Ca^{2+}] in the *tunica interna* to 20% of day 7 values (fig. 3.3). For excised eggs, mean $\Delta\mu_{Ca}/F$ across the *membrana interna* and *externa* was more negative on day nine (-26.4 mV) relative to peri-metamorphic values (day five, -3.7 mV), but voltage difference across these membranes became less negative over the same time period (day five: -21.4 ± 0.92 mV, day nine: -9.1 ± 0.77 mV). Thus, the increase in $\Delta\mu_{Ca}/F$ was likely due to the decrease in [Ca^{2+}] to 13% of day five values (fig. 3.4). The depletion of maternal stores available for calcification to concentrations below aquatic levels (figs. 3.3, 3.4) thus favors diffusive Ca^{2+} influx in these later stages (i.e. movement of Ca^{2+} down the concentration gradient from the ambient media to the Ca^{2+}-depleted perivitelline fluid).

Considering the aforementioned findings and observations of changes in *tunica capsulis* integrity over the development of the embryos and findings by Beadle (1969a) that *Biomphalaria sudanica* embryos have osmoregulatory capabilities, we propose that around the time of embryonic metamorphosis there is also a concurrent change in the membranes of the egg mass. The altered state may allow for Ca^{2+} diffusion and/or uptake as influenced by Ca^{2+} removal from the perivitelline fluid by the embryo for calcification.

Thus the *tunica interna* and *tunica capsulis* may serve to resist ion efflux during early developmental phases but allow Ca^{2+} uptake during shell formation. Our techniques did not allow for determining what role, if any, the limiting membrane, which is located between the *tunica interna* and *tunica capsulis*, plays in this development of permeability.

High calcium accretion of nearly five-fold over the course of development (Taylor 1977) apparently leads to a reduction in $[Ca^{2+}]$ in the *tunica interna* by day seven (fig. 3.3) and perivitelline fluid by at least day nine (fig. 3.4) to concentrations below ambient media. This provides a reasonable explanation for the observed increase in the inside negative $\Delta\mu_{Ca}/F$ over the post-metamorphic stages. One point for further consideration is that reduced $[Ca^{2+}]_{PVF}$ to below water concentrations may allow for less energy consumptive Ca^{2+} uptake. Similar measurements were made by Taylor (1973) on pre-gastrula (pre-metamorphic) stage embryos. Taylor excised pre-gastrula stage (< 24 h old) egg capsules from the *tunica interna* and allowed them to equilibrate with experimental media for at least 24 h at 22 - 25 °C. In contrast, the microelectrode measurements reported as part of the present study for post-metamorphic embryos were taken immediately after eggs were excised and completed within one to two hours.

The concomitant occurrence of several events led to the consideration that it may not be just the embryo that metamorphoses but that the embryo-egg mass complex transforms over the course of development. Maternal Ca^{2+} reserves provided in the perivitelline fluid apparently decrease over development. This reduction is concurrent with strengthening of inward negative $\Delta\mu_{Ca}/F$ across the membranes between the developing embryo and the aquatic environment. Around this same time, active Ca^{2+}

uptake from the surrounding medium also begins. In the SIET measurements, day seven egg masses exhibited a net Ca^{2+} flux of 0.04 µmol cm^{-2} h^{-1}, which translates to 0.48 µmol g^{-1} h^{-1} for an egg mass 2 cm long and 0.43 cm diameter. This was of the same order of magnitude as the 0.29 µmol g^{-1} h^{-1} that was measured in whole egg mass net Ca^{2+} fluxes. Furthermore, documented accumulation of 0.13 µmol Ca^{2+}/embryo in isolated eggs over the period from the blastula stage through hatching (Taylor 1977) equates to 7.7 µmol Ca^{2+} over the time period for an average egg mass with 59 eggs. The blastula stage occurs during the latter half of day one for *L. palustris* embryos maintained at 25 °C (Morrill 1982). In whole egg mass fluxes, embryos, which were maintained at 20 - 22 °C, removed 16.9 µmol Ca^{2+} from flux media over the period of day 2 - 11. Thus flux measurements using microscale and whole egg mass methods produced similar results and were in reasonable agreement with literature values.

Similar trends were expected in titratable alkalinity kinetics as those observed for Ca^{2+} kinetics over a range of ambient bicarbonate and/or [Ca^{2+}]. However considering 1) that embryos developed in HCO_3^-/CO_3^{2-}-free media, 2) the lack of a significant relationship between HCO_3^-/CO_3^{2-} transport and either Ca^{2+} or HCO_3^- availability, and 3) a significant apparent titratable alkalinity flux under HCO_3^--free, HEPES-buffered conditions there is apparently another source of HCO_3^-/CO_3^{2-} for these post-metamorphic embryos. The likely HCO_3^-/CO_3^{2-} source in *L. stagnalis* is hydration of endogenous, metabolic CO_2. The notion of retaining and using endogenously produced HCO_3^-/CO_3^{2-} for calcification was suggested by Baldwin (1935) following measurements of oxygen consumption and bound CO_2 in *L. stagnalis* embryos. He reported significantly greater O_2 uptake rates with developmental progress. Furthermore, the onset of the formation of

true shell, which was labeled as stage II in the study, was concurrent with a spiked increase in CO_2 content and O_2 consumption. In a study on the adults of this species, Greenaway (1971a) proposed a model in which Ca^{2+} was exchanged between the external medium, blood, fresh tissues, and shell compartments. Additionally, H^+ and HCO_3^- that were produced through the hydration of metabolic CO_2 were exchanged for Ca^{2+} from the external medium and used for $CaCO_3$ deposition, respectively. To maintain HCO_3^-/CO_3^{2-} production from CO_2 hydration ($CO_2 + H_2O \rightarrow HCO_3^- + H^+ \rightarrow CO_3^{2-} + H^+$) and allow for continued shell formation, H^+ extrusion is necessary. Indeed, such H^+ extrusion likely accounts for the apparent titratable alkalinity uptake in HCO_3^--free media because net acid excretion would be expressed as apparent base uptake when measuring changes in concentrations of absolute alkalinity equivalents. This suggestion is supported by Taylor (1973), who reported that lowering the pH in the bathing medium from 8.5 to 4.0 reduced the concentration of Ca^{2+} in the perivitelline fluid by up to 85%. It is possible that the increase in water $[H^+]$ in the Taylor (1973) study would drastically reduce the capacity to excrete H^+. Cation uptake in freshwater fish (Bury and Wood 1999, Fenwick *et al.* 1999, Grosell and Wood 2002, Lin and Randall 1991) and in *L. stagnalis* (Ebanks and Grosell 2008) has been linked to an electrochemical gradient that is in part established by excretion of the H^+ from carbonic anhydrase-mediated hydration of respiratory CO_2. Calcium uptake in *Lymnaea* exposed to low ambient pH would likely be impaired, explaining the earlier observations by Taylor (1973) of reduced $[Ca^{2+}]$ in the perivitelline fluid.

Lastly, the observed increase in ammonia excretion and Ca^{2+} uptake under HCO_3^-/CO_3^{2-}-free HEPES-buffered conditions was another indicator of the use of endogenously

produced HCO_3^-/CO_3^{2-} in post-metamorphic embryos. Under these conditions the embryos would be forced to rely exclusively on the hydration of CO_2 to produce the necessary HCO_3^-/CO_3^{2-} for shell-formation thus producing greater amounts of H^+ to be excreted to the surrounding media in order to maintain acid-base balance and favorable internal conditions for calcification. Increased ammonia excretion, as a result of further acidification of boundary layers and consequent diffusion trapping of NH_3 as NH_4^+, may thereby explain the observations of elevated ammonia excretion in absence of ambient HCO_3^-/CO_3^{2-}. The increased H^+ excretion under HCO_3^-/CO_3^{2-}-free HEPES buffered conditions would possibly also enhance hyperpolarization of the apical membrane, which would provide a stronger electrochemical gradient leading to the observed increased Ca^{2+} uptake.

Implications of findings

Utilizing whole egg mass and micro-scale analytical techniques, the need for aquatic Ca^{2+} for proper development and timely hatching of embryos has been confirmed for the freshwater common pond snail *Lymnaea stagnalis*. The embryos apparently utilize an endogenous source of HCO_3^-/CO_3^{2-} because they can develop in the absence of ambient HCO_3^-/CO_3^{2-}. Furthermore, increased Ca^{2+} uptake under HCO_3^-/CO_3^{2-}-depleted conditions indicates a connection between Ca^{2+} transport pathways and endogenous HCO_3^-/CO_3^{2-} production and thus H^+ extrusion. Therefore, while Ca^{2+} requirements for complete embryonic shell formation and development are met via uptake, the necessary HCO_3^-/CO_3^{2-} is acquired in part from endogenous sources, likely via carbonic anhydrase-catalyzed hydration of CO_2 coupled with H^+ extrusion with no significant correlation to

ambient HCO_3^-/CO_3^{2-} availability. Lastly, excretion of H^+ from hydration of CO_2 seems to facilitate uptake of Ca^{2+}, a subject of ongoing studies.

Chapter 4:

Characterization of Mechanisms for Ca^{2+} and HCO_3^-/CO_3^{2-} Acquisition for Shell Formation in Embryos of the Freshwater Common Pond Snail *Lymnaea stagnalis*

4.1. Background

Embryos of the freshwater common pond snail *Lymnaea stagnalis* complete direct development, emerging as shell-bearing hatchlings in approximately ten days post-oviposition in a low-ionic strength, minimally buffered environment. In the absence of ambient Ca^{2+}, they tend to develop at a retarded rate relative to controls but grow and hatch at least as well as controls when reared in carbonate-free water (Ebanks *et al.* 2010a). While they are provided with maternal stores of Ca^{2+} and carbonate in the perivitelline fluid and within the gelatinous matrix (*tunica interna*) of the egg mass, they begin to rely on Ca^{2+} from the surrounding media as maternal stores in the perivitelline fluid and *tunica capsulis* become depleted, at approximately day 5 post-oviposition (Ebanks *et al.* 2010a). At this point in embryonic development, embryos increase oxygen consumption and total CO_2 retention (Baldwin 1935). Metamorphosis and shell-formation are also observed for *Lymnaea palustris* (Morrill 1982), *L. stagnalis* (Ebanks *et al.* 2010a), and another freshwater pulmonate snail *Biomphalaria glabrata* (Bielefeld and Becker 1991, Marxen *et al.* 2003). While the post-metamorphic Ca^{2+} requirements seem to be met entirely via active uptake, the carbonate requirements can apparently be accommodated through both uptake and endogenous sources or by endogenous sources exclusively (Ebanks *et al.* 2010a).

The idea of Ca^{2+} uptake in freshwater being via active uptake through Ca^{2+} channels has been presented, studied, and reviewed from many angles and by many

researchers but mostly in freshwater trout (Flik *et al.* 1995, Marshall *et al.* 1992, Perry and Flik 1988, Shahsavarani and Perry 2006). An electrochemical gradient for Ca^{2+} established by basolateral Ca^{2+}-ATPase and Na^{+}/K^{+} ATPase activity and further facilitated and maintained by an apical, outwardly directed H^{+} pump collectively provide the necessary gradient to allow for Ca^{2+} uptake under these conditions (Perry *et al.* 2003b). Hydrogen ions supplied to this pump are mostly from hydration of CO_2. In addition to acid excretion by the H^{+} pump, protons can be extruded in exchange for monovalent as well as divalent cations via Na^{+}/H^{+} exchangers (NHE) by electroneutral or electrogenic exchange (see Ahearn *et al.* 2001 for review). Also, more recent work by Okech *et al.* (2008) indicated cation exchange for hydrogen ions coupled with V-H^{+} ATPase activity on electrogenic Na^{+}/H^{+} antiporters. A further point of consideration important to this study is that $2Na^{+}/1H^{+}$ electrogenic exchange that appears to be unique to invertebrates can also accommodate divalent cations, including Ca^{2+} (Ahearn *et al.* 1994).

Previous observations of unimpeded growth under HCO_3^{-}-free conditions (Ebanks *et al*. 2010a) led to subsequent experiments of the transport of acid and base units under calcifying, post-metamorphic conditions. The onset of apparent net titratable alkalinity uptake was concurrent with metamorphosis, the onset of Ca^{2+} uptake, and shell formation. Also, Ca^{2+} uptake was significantly greater and apparent net titratable alkalinity uptake was significantly reduced, but not inhibited, under HCO_3^{-}-free conditions (Ebanks *et al.* 2010a). These findings motivated the series of experiments that are described in this paper to determine the possible sources of carbonate for shell formation.

Considering that carbonic anhydrase-mediated CO_2 hydration produces HCO_3^-, this was a logical starting point. The possibility of endogenous bicarbonate contributing to calcification in the embryos (Baldwin 1935) and adults (Greenaway 1971b) of this species has been suggested previously in the literature. However, the point of development at which this pathway is activated has not been studied until recently (Ebanks *et al.* 2010a). Also, the possible role of the proton, resulting from CO_2 hydration and $CaCO_3$ formation, in the acquisition of the essential shell forming ions by these embryos remains to be evaluated. Therefore, the objectives of this study were to use a pharmacological approach in whole egg mass fluxes and microscale fluxes to determine the acquisition pathways for shell-forming ions in post-metamorphic embryos of the freshwater common pond snail *Lymnaea stagnalis*. Additionally, the evaluation of the possible relationship between protons produced via carbonic anhydrase activity and Ca^{2+} uptake were targeted. Each of the proposed pathways was evaluated on whole egg mass and microscale levels where possible.

4.2. Materials and methods

Test animals

Egg masses of the common pond snail *Lymnaea stagnalis* were collected from laboratory snail culture in 24-hour intervals with the day of collection considered day zero post-oviposition, for age determination. Embryos were incubated at room temperature (20-22°C) in aerated, dechlorinated Miami-Dade County tap water (Grosell *et al.* 2007). Egg masses were selected and scored for viability in accordance with criteria outlined in Ebanks *et al.* (2010a).

Whole egg mass flux experiments

Three Ca^{2+} channel blockers were used independently to assess the role and subsequently the type of Ca^{2+} channels that may be involved. Nifedipine, which is a voltage-dependent L-type Ca^{2+} channel blocker, was applied as was verapamil, another voltage-dependent L-type Ca^{2+} channel blocker and α1-adrenoceptor antagonist. Lanthanum, an indiscriminate Ca^{2+} channel blocker was also tested. Day seven egg masses were scored for normal development and placed in Miami Dade County tap water that was either drug-free control (0.1% DMSO), treated with 10 µmol l^{-1} nifedipine (Sigma-Aldrich), with 10 µmol l^{-1} verapamil hydrochloride (Sigma-Aldrich), 10 µmol l^{-1} La^{3+}, or 100 µmol l^{-1} La^{3+} as $LaCl_3$ and incubated for 24 h. Initial and final water samples were collected for Ca^{2+} and titratable alkalinity net flux determinations, which were completed following the protocol for double-endpoint titration from Ebanks *et al.* (2010a) and reported in µmol g^{-1} h^{-1}. Considering that carbonate necessary for calcification could be from aquatic sources or endogenous processes (Ebanks *et al.* 2010a), a multi-pronged experimental approach was required. The role of carbonic anhydrase (CA) in the production of endogenous bicarbonate via CO_2 hydration was evaluated using a lipophilic carbonic anhydrase inhibitor, ethoxzolamide (ETOX; Sigma-Aldrich), dissolved in DMSO. Controls (0.1% DMSO) and 100 µmol l^{-1} ETOX-exposed egg masses were incubated for 24 h with water samples taken before and after for Ca^{2+} and TA net flux determinations. In addition to HCO_3^-, CA-catalyzed hydration of CO_2 also produces equal quantities of H^+, which are counterproductive to shell formation and must be excreted to make CO_2 hydration a viable source of CO_3^{2-} for shell formation.

Thus the role of V-H^+ ATPase (H^+-pump) in the removal of protons and possibly Ca^{2+} uptake was evaluated with the considering that apical Ca^{2+} channels may be driven by an inward-directed electrochemical gradient fueled in part by electrogenic H^+ excretion via the H^+-pump. Bafilomycin (Sigma-Aldrich), a proton pump inhibitor, was dissolved in DMSO for a final concentration of 1 μmol l^{-1} bafilomycin and 0.1% DMSO in each flux chamber. Day seven egg masses were scored for viability and placed in individual flux chambers for a 24-h incubation after which net Ca^{2+} and titratable alkalinity flux was determined as described below. Also, because of the potential for direct exchange of Ca^{2+} for H^+ on an apical invertebrate-specific cation/1H^+ exchanger, a 24-h flux experiment was completed in which day seven egg masses were treated with 100 μmol l^{-1} of the NHE-specific amiloride analogue, ethylisopropylamiloride (EIPA; Sigma-Aldrich) dissolved in a final concentration of 0.1% DMSO.

Analytical procedures for whole egg mass experiments

The procedures for determination of flux rates were in accordance with those outlined in Ebanks *et al.* (2010a). In brief, samples of pre- and post-flux media were collected for each treatment and Ca^{2+} net flux was determined by using the difference in [Ca^{2+}] in initial and final flux media following the 24-h flux. Samples were measured by flame atomic absorption spectrophotometry (Varian SpectrAA220, Mulgrave, Victoria, Australia) and flux rates were calculated from the change in [Ca^{2+}], mass of egg mass (g), and elapsed time (h). Net titratable alkalinity flux was calculated from the change in titratable alkalinity as determined via double endpoint titration (Ebanks *et al.* 2010a),

mass of egg mass (g), and elapsed time (h). Final values for both Ca^{2+} and titratable alkalinity net flux parameters are presented as µmol g^{-1} h^{-1}.

Ca^{2+}-selective and H^{+}-selective microelectrodes

Microelectrodes used to measure $Ca^{2+}$and H^{+} gradients in the unstirred layer next to the surface of egg masses and isolated eggs were pulled from unfilamented 1.5 mm borosilicate capillary glass (A-M systems, Carlsborg, WA). They were then silanized by exposure to the vapors of dimethyldichlorosilane at 200 °C for 60 minutes and stored over silica gel until use. Ca^{2+}-selective microelectrodes were backfilled with 100 mmol l^{-1} $CaCl_2$ and tip-filled with a 300 - 500 µm column of Ca^{2+} ionophore I, cocktail A (Fluka, Buchs, Switzerland). H^{+}-selective microelectrodes were backfilled with a solution of 100 mmol l^{-1} NaCl and 100 mmol l^{-1} Na citrate at pH 6, then front-filled with a 300 - 500 µm column of H^{+} Ionophore I, cocktail B (Fluka).

Ca^{2+} and H^{+} fluxes: Microscale measurements using the scanning ion electrode technique

Transport of calcium ions or protons into or out of egg masses or isolated eggs produces gradients in Ca^{2+} or H^{+} concentration in the unstirred layer adjacent to the surface of the preparation. These gradients can be calculated from the voltages recorded by an ion-selective microelectrode moved between two points within the unstirred layer. Calcium flux can then be calculated from the Ca^{2+} concentration gradients using Fick's law. Measurement of fluxes in this way is the basis of the scanning ion electrode

technique (SIET), which allows fluxes to be repeatedly measured in near real-time at sites along the length of an egg mass or isolated egg (Ebanks *et al.* 2010a).

SIET measurements were made using hardware from Applicable Electronics (Forestdale, MA, USA) and automated scanning electrode technique (ASET) software (version 2.0) from Science Wares Inc. (East Falmouth, MA, USA). Egg masses or isolated eggs were placed in a 35 mm diameter petri dish filled with 5 ml of artificial Miami-Dade County tap water. Reference electrodes were made from 10 cm lengths of 1.5 mm borosilicate glass capillaries that were bent at a 45° angle, 1 - 2 cm from the end, to facilitate placement in the sample dish. Capillaries were filled with boiling 3 mol l^{-1} KCl in 3% agar and connected to the ground input of the Applicable Electronics amplifier headstage through a Ag/AgCl half cell.

Ca^{2+}-selective microelectrodes for use with SIET were calibrated in 0.1, 1, and 10 mmol l^{-1} Ca^{2+}. All scans were performed in artificial Miami-Dade water with a Ca^{2+} concentration of 400 µmol l^{-1}. The Ca^{2+}-selective microelectrode was initially placed 5-10 µm from the surface of the egg mass or isolated egg. The microelectrode was then moved a further 50 µm away, perpendicular to the egg mass surface. The "wait" and "sample" periods at each limit of the 50 µm excursion distance were 4.5 and 0.5 s, respectively. Voltage differences across this excursion distance were measured three times at each of the four to six sites along the surface of each egg mass or isolated egg. Voltage differences were corrected for electrode drift measured at a reference site 10 - 20 mm away from the egg mass. Voltage differences at measurement sites and at reference sites were typically >300 µV and <10 µV, respectively. Voltage differences (ΔV) were

converted to the corresponding Ca^{2+} concentration difference by the following equation (Donini and O'Donnell 2005):

$$\Delta C = C_B \times 10^{(\Delta V/S)} - C_B$$

where ΔC is the Ca^{2+} concentration difference between the two limits of the excursion distance ($\mu mol\ cm^{-3}$), C_B is the background Ca^{2+} concentration in the bathing medium , ΔV is the voltage gradient (mV), and S is the slope of the electrode between 0.1 and 1 $mmol\ l^{-1}$ Ca^{2+}. Although ion-selective microelectrodes measure ion activity and not concentration, data can be expressed in terms of concentrations if it is assumed that the ion activity coefficient is the same in calibration and experimental solutions. Expression of data in units of concentrations aids comparison of Ca^{2+} microelectrode data with techniques such as atomic absorption spectrophotometry, which measures Ca^{2+} concentration. Concentrations can be converted to activities by multiplying by the activity coefficient (0.81 for Miami-Dade County tap water).

Concentration differences were used to determine the Ca^{2+} flux using Fick's law of diffusion:

$$J_{Ca} = D_{Ca}(\Delta C/\Delta X)$$

where J_{Ca} is the net flux in $\mu mol\ cm^{-2}\ s^{-1}$, D_{Ca} is the diffusion coefficient of Ca^{2+} ($1.19x10^{-5}\ cm^2\ s^{-1}$), ΔC is the Ca^{2+} concentration gradient, and ΔX is the excursion distance between the two points (cm).

Calculation of H^+ fluxes requires knowledge of the buffers that are present (e.g. Donini and O'Donnell 2005). Ideally, a non-volatile buffer such as HEPES is used. However, because we wished to use the same Miami-Dade tap water as used for the

whole egg mass flux experiments, water composition was not modified and therefore H^+ gradients are presented as microelectrode voltage rather than proton flux in the Results.

Statistical analyses

Comparisons were completed using either t-test or an ANOVA with contingent significant results evaluated as pairwise comparisons following the Holm-Sidak method after an analysis for whether the datasets were normally distributed. Statements of significance were reserved for those comparisons for which $P < 0.05$.

4.3. Results

Results from the multi-pronged pharmacological approach indicated that voltage-dependent Ca^{2+} channels, H^+-pump activity, and Na^+/H^+ antiport function in conjunction with CA activity allow the post-metamorphic embryonic snail to complete calcification and shell formation in freshwater. The two voltage-dependent Ca^{2+} channel blockers exhibited differential effectiveness against net Ca^{2+} uptake with nifedipine being the more effective blocker when examined by net Ca^{2+} flux measurements and SIET techniques (figs. 4.1, 4.2). Verapamil did not significantly block net Ca^{2+} transport at 10 $\mu mol\ l^{-1}$ but 10 $\mu mol\ l^{-1}$ nifedipine did in whole egg mass experiments (fig. 4.1). Scanning Ca^{2+}-selective microelectrode results showed that both voltage-dependent Ca^{2+} channel blockers reduced Ca^{2+} transport at 10 $\mu mol\ l^{-1}$ but that 100 $\mu mol\ l^{-1}$ verapamil completely blocked net Ca^{2+} uptake (fig. 4.2). Neither drug influenced net titratable alkalinity flux (data not shown). Lanthanum blocked net Ca^{2+} uptake at 100 $\mu mol\ l^{-1}$ but not at 10 $\mu mol\ l^{-1}$ in whole egg mass experiments (fig. 4.3). There was also a significant

Figure 4.1. Net Ca^{2+} flux rate (µmol g^{-1} h^{-1}) under control conditions (0.1 % DMSO) and during pharmacological manipulations (10 µmol l^{-1} verapamil or 10 µmol l^{-1} nifedipine). Values are presented as mean ± S.E.M. Number in parentheses is the number of egg masses for indicated condition. Ambient [Ca^{2+}] = 648 ± 7 µmol l^{-1}. * = significantly different from control ($P < 0.05$).

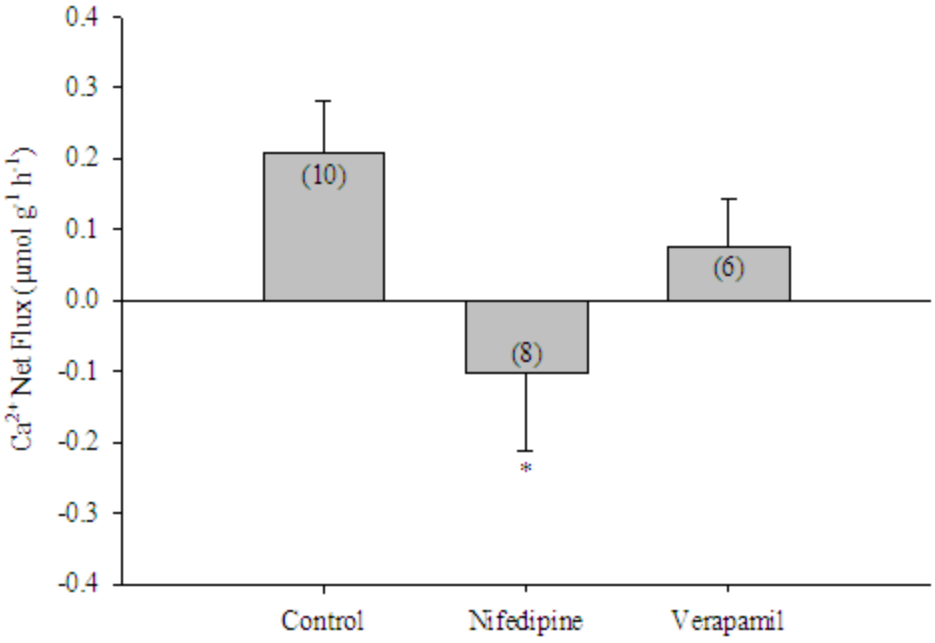

Figure 4.2. Scanning Ca^{2+}-selective microelectrode results for day nine isolated eggs in control or treatment with a voltage-dependent Ca^{2+} channel blocker (nifedipine or verapamil). Values are presented as mean ± S.E.M. Number in parentheses is the number of eggs scanned each with five to seven measurements. * = significant reduction from control values. Ambient $[Ca^{2+}]$ = 400 µmol l^{-1}.

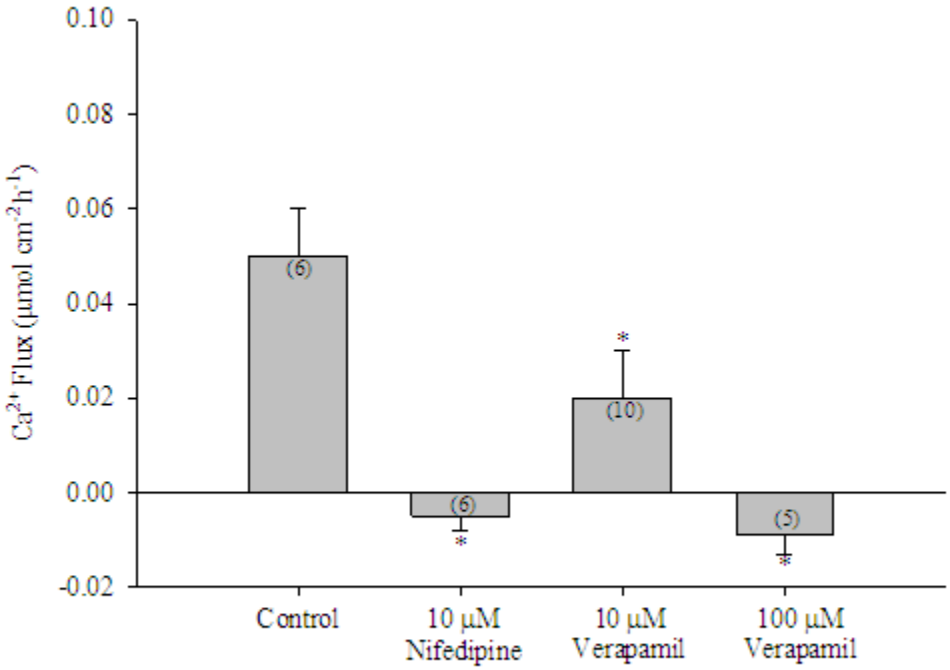

Figure 4.3. Net Ca^{2+} flux rates (µmol g^{-1} h^{-1}) under control conditions and during treatment with 10 µmol l^{-1} or 100 µmol l^{-1} La^{3+} as $LaCl_3$. Values are mean ± S.E.M. Number in parentheses is the number of egg masses for indicated condition. Ambient [Ca^{2+}] = 762 ± 0.3 µmol l^{-1}. * = significantly different from control ($P < 0.05$).

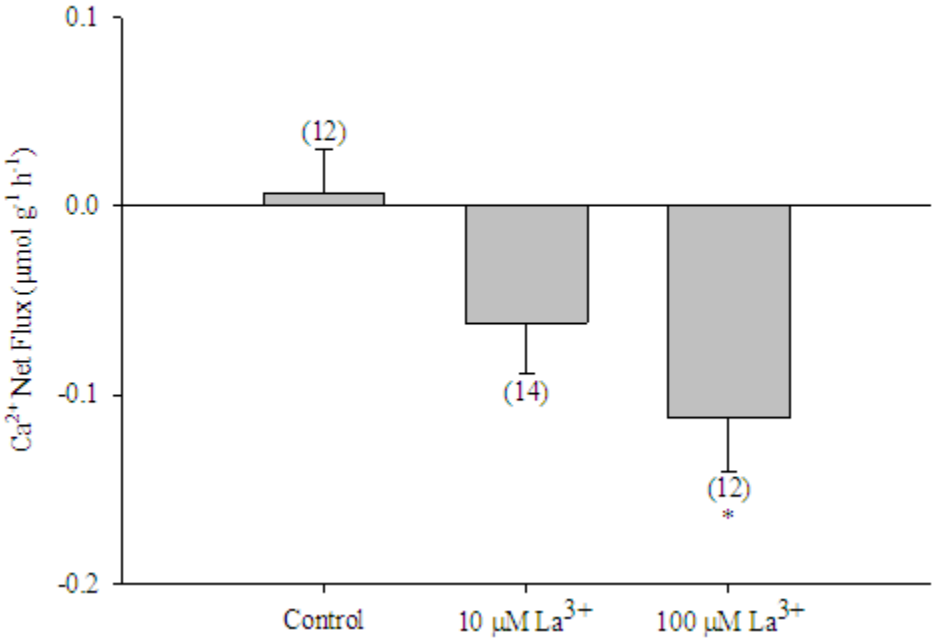

increase in apparent net titratable alkalinity uptake in the presence of 100 µmol La^{3+} l^{-1} (data not shown). Microelectrode experiments revealed a tendency for reduced Ca^{2+} uptake with 100 µmol l^{-1} La^{3+} but just below statistical significance (fig. 4.4).

Using 100 µmol l^{-1} ETOX to evaluate the role of CA-catalyzed hydration of CO_2 on whole egg mass flux rates, we observed a significant reduction in both net Ca^{2+} uptake and apparent titratable alkalinity uptake (fig. 4.5). The link between CO_2 hydration and Ca^{2+} uptake led to the testing of the possible role of the apical H^+ pump and Na^+/H^+ exchange by evaluating the inhibitory effects of bafilomycin and EIPA at concentrations of 1 µmol l^{-1} and 100 µmol l^{-1}, respectively, on Ca^{2+} and titratable alkalinity transport. Proton-pump inhibition resulted in inhibition of net Ca^{2+} uptake (fig. 4.6A) and apparent net titratable alkalinity uptake (equivalent to reduced acid secretion; fig. 4.6B). Scanning Ca^{2+}-selective microelectrode measurements revealed that bafilomycin had a significant inhibitory effect of up to 80% on Ca^{2+} transport for post-metamorphic egg masses (data not shown).

Furthermore, and in agreement with whole egg mass fluxes, isolated eggs containing later-stage day 11 - 13 embryos, treated with 1 µmol l^{-1} bafilomycin displayed inhibited Ca^{2+} uptake (fig. 4.7A) and effectively reversed H^+ gradients (fig. 4.7B) as measured with ion-selective microelectrodes in the unstirred boundary layer. Similar to the bafilomycin treatment, both Ca^{2+} (fig. 4.8A) and titratable alkalinity (fig. 4.8B) net flux were reversed in whole egg mass fluxes where flux media was treated with 100 µmol l^{-1} EIPA.

Figure 4.4. Scanning Ca^{2+}-sensitive microelectrode results for intact day nine to ten egg masses in control conditions or during treatment with a voltage-independent Ca^{2+} channel blocker (100 µmol l^{-1} La^{3+} as $LaCl_3$). Values are presented as mean ± S.E.M. Number in parentheses is the number of egg masses for indicated condition each with five to ten measurements. Ambient [Ca^{2+}] = 400 µmol l^{-1}.

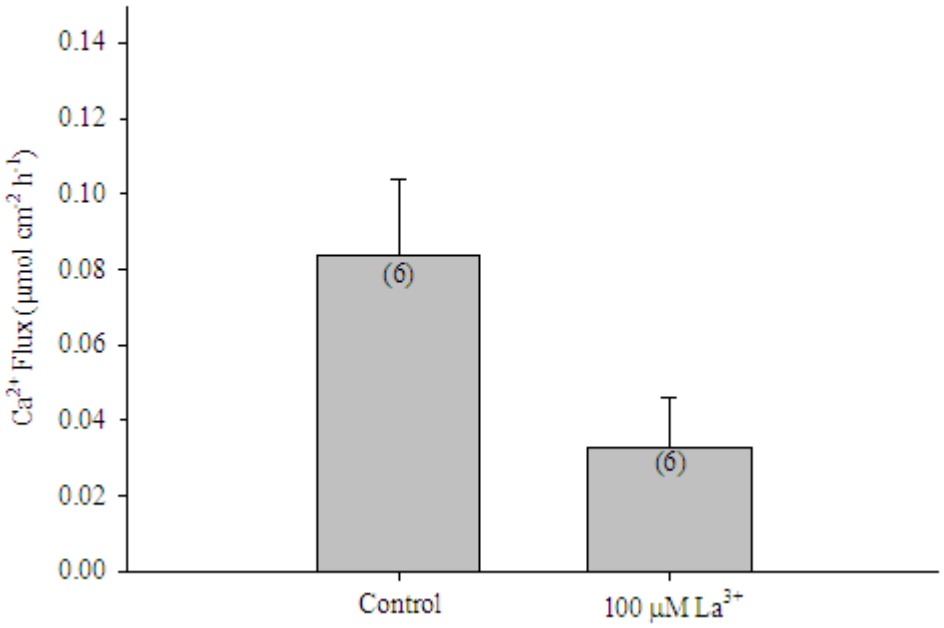

Figure 4.5. Comparison of net Ca^{2+} (A) and titratable alkalinity (B) flux rates (μmol g^{-1} h^{-1}) under control conditions (0.1% DMSO) and during pharmacological manipulation with 100 μmol l^{-1} ethoxzolamide (ETOX). Values presented as mean ± S.E.M. Number in parentheses is the number of egg masses for indicated condition. Ambient [Ca^{2+}] = 1388 ± 79 μmol l^{-1}. * = significantly different from control ($P < 0.05$).

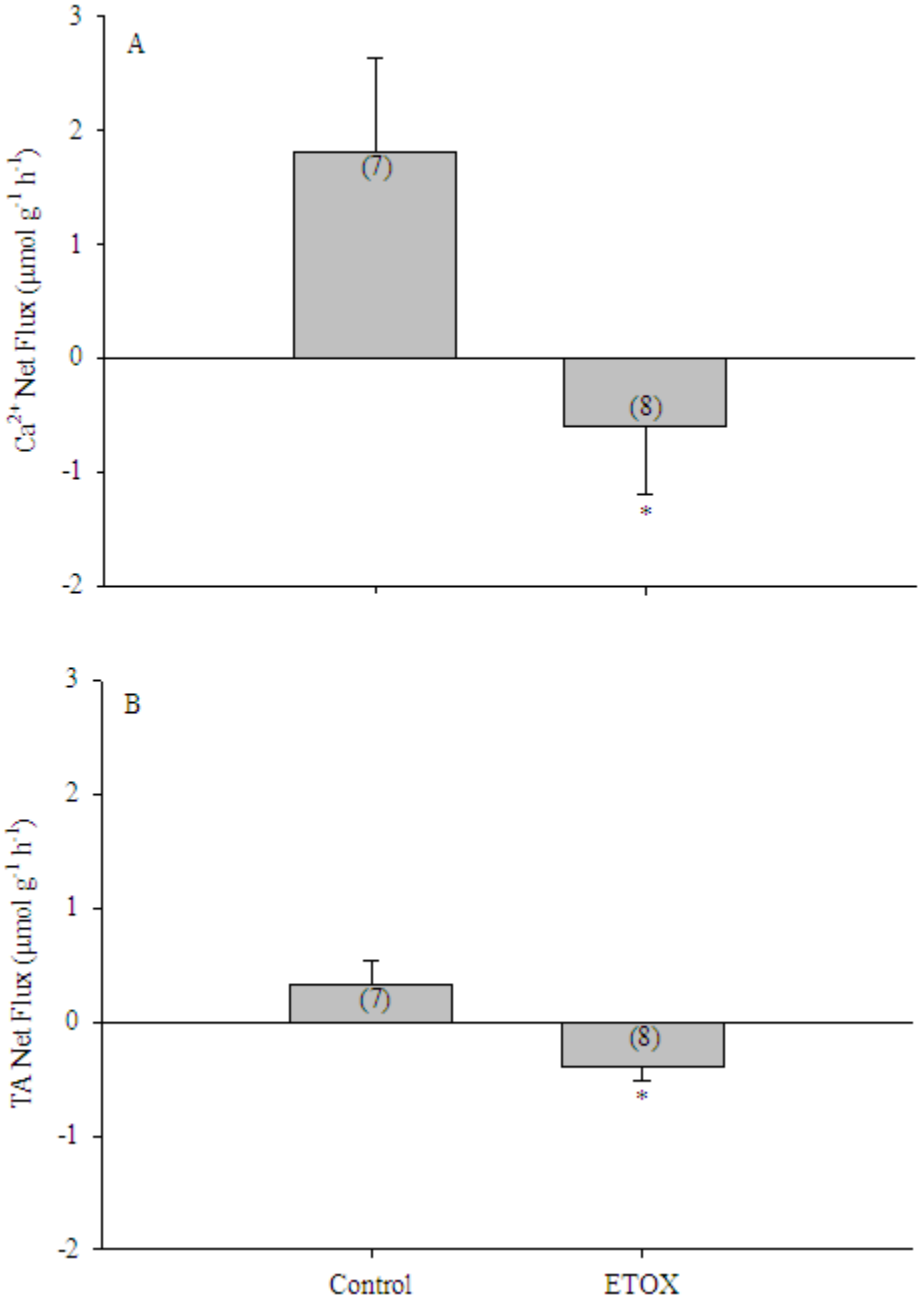

Figure 4.6. Comparison of net Ca^{2+} (A) and titratable alkalinity (B) flux rates (μmol g^{-1} h^{-1}) under control conditions (0.1% DMSO) and during treatment with 1 μmol l^{-1} bafilomycin. Values are presented as mean ± S.E.M. Number in parentheses is the number of egg masses for indicated condition. Ambient [Ca^{2+}] = 407 ± 1 μmol l^{-1}. * = significantly different from control ($P < 0.05$).

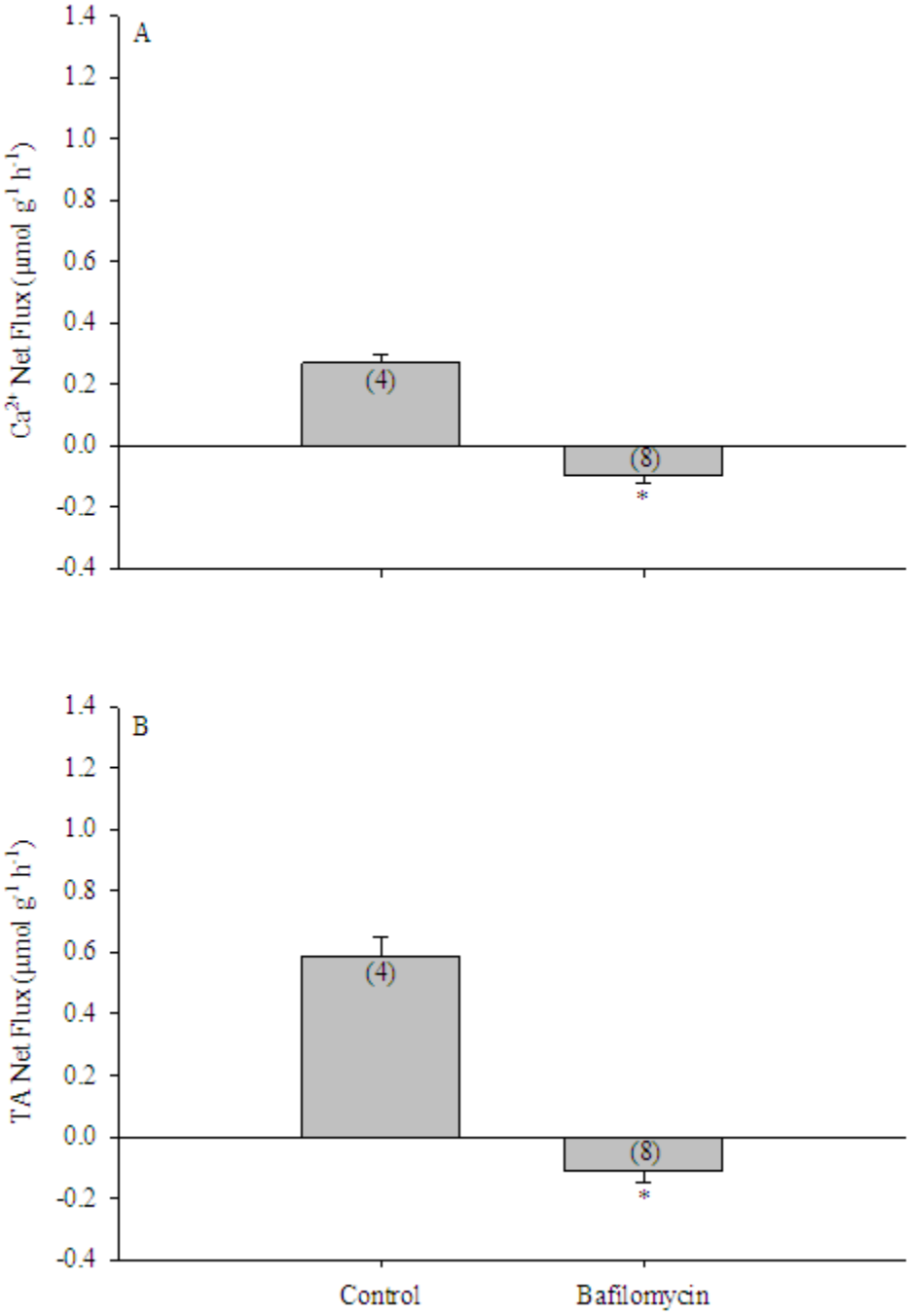

Figure 4.7. Comparison of Ca^{2+} flux (A) and H^{+} gradients (B) within the unstirred boundary layer of post-metamorphic isolated eggs at days seven and eight under control and treatment with 1 µmol l^{-1} bafilomycin. Eggs were scanned using an Ca^{2+}- or H^{+}-selective microelectrode under control conditions, exposed to drug for 30 - 60 min, then scanned in drug-treated media (paired design). Values are mean ± S.E.M. Number in parentheses is the number of eggs for indicated condition. Ambient [Ca^{2+}] = 400 µmol l^{-1}. * = significantly different from control ($P < 0.05$).

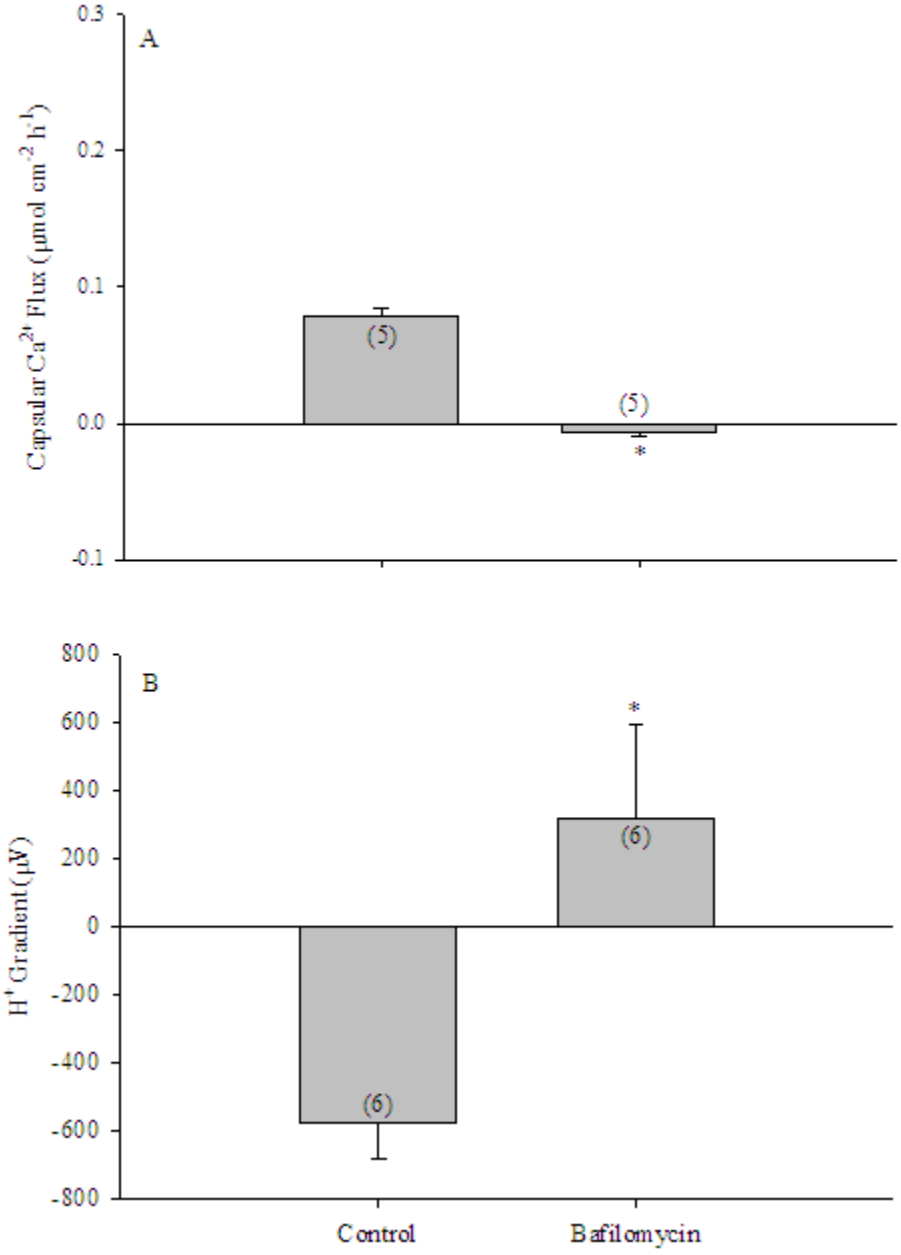

Figure 4.8. Comparison of net Ca^{2+} (A) and titratable alkalinity (B) flux rates (μmol g^{-1} h^{-1}) under control (0.1% DMSO) and treatment with 100 μmol l^{-1} EIPA. Values are presented as mean ± S.E.M. Number in parentheses is the number of egg masses for indicated condition. Ambient [Ca^{2+}] = 838 ± 16 μmol l^{-1}. * = significantly different from control ($P < 0.05$).

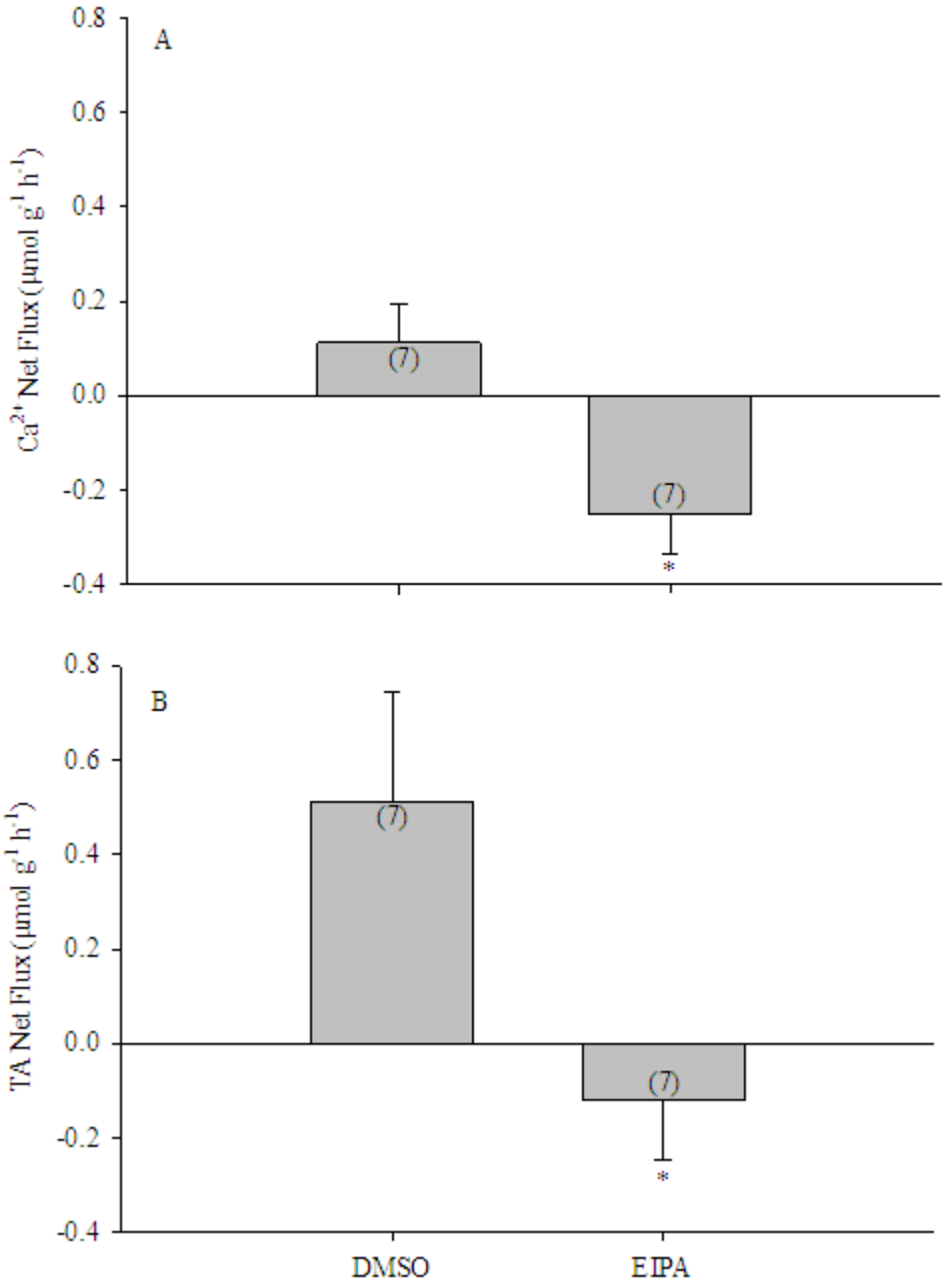

4.4. Conclusions and implications

The system for Ca^{2+} and carbonate acquisition in the freshwater common pond snail *Lymnaea stagnalis* exhibited sensitivity to several pharmacological agents, which indicate that both Ca^{2+} uptake from the environment as well as endogenous HCO_3^-/CO_3^{2-} production work together directly and indirectly for the post-metamorphic embryo to acquire the necessary ions for calcification in freshwater (fig. 4.9). The model proposed here for post-metamorphic embryos compliments findings modeled by Greenaway (1971a) using radioisotopic techniques on adults of the species. Considering that these embryos complete direct development, hatching as fully developed snails, it is not surprising to find that the method for acquisition of shell forming ions in embryos is similar to that modeled by Greenaway (1971a).

When applying pharmacological agents that were developed and tested for use on mammals, it is necessary to consider that there may be a reduced degree of specificity of the drug. Additionally, using these chemicals with ion-sensitive microelectrodes can interfere with the sensitivity and function of the electrode. However, preliminary tests for drug interaction and/or poisoning of the electrode and the general agreement between results obtained by the two techniques used in the present study give confidence in the accuracy of our findings. The voltage-dependent Ca^{2+} channel blockers and bafilomycin gave consistent results between whole egg mass net flux measurements and assessment of flux rates by microelectrodes validating the reported observation. With the exception of EIPA, none of the drugs interfered with microelectrode function at the concentrations used in these experiments. Unfortunately, EIPA interfered with both Ca^{2+}- and H^+-selective microelectrodes preventing verification of whole egg mass flux observations

that suggested the presence of a cation/H^+ exchanger. Nevertheless, the excellent agreement between observations when made with both techniques is reassuring. Also, L-type voltage-dependent Ca^{2+} channels and an EIPA-sensitive cation exchanger appear to be involved in Ca^{2+} uptake in post-metamorphic embryos (fig. 4.9).

In the absence of external HCO_3^-, *Lymnaea stagnalis* embryos grow, form shell, develop normally, and hatch in the same time intervals as controls (Ebanks *et al.* 2010a). These observations point to an internal source of HCO_3^-/CO_3^{2-} for shell formation via the hydration of endogenous CO_2. For this hydration reaction to allow for CO_3^{2-} accumulation within the organism and for shell formation, hydrogen ions resulting from the hydration reaction must be eliminated (fig. 4.9). The results of this study indicate that the enzyme carbonic anhydrase (CA), which facilitates the hydration of endogenous CO_2 is involved in the acquisition of ions for calcification. Also, though developing snails show an apparent net uptake of Ca^{2+} and HCO_3^- equivalents, the movement of acid-base equivalents is in reality a combination of acid secretion and base uptake because it persists, although at reduced rates, in absence of ambient HCO_3^- (Ebanks *et al.* 2010a). SIET measurements of H^+ gradients further confirm the role of H^+ excretion.

The effects of CA inhibition indicated a direct role for CA in carbonate production in post-metamorphic embryos but also points to an indirect role in Ca^{2+} acquisition that is revealed when considered in conjunction with the bafilomycin A_1 results. Bafilomycin inhibits V-type H^+ ATPase activity, which has been found to be ubiquitous among eukaryotes (Harvey 1992, Finbow and Harrison 1997, Harvey *et al.* 1998). This includes invertebrates and more directly related to the model species used for these experiments, calcifying organisms such as blue crabs (Cameron and Wood

1985). The CA enzyme has also been characterized in tissues of freshwater bivalves *Anodonta cygnea* (Machado *et al.* 1990, da Costa *et al.* 1999, Oliveira *et al.* 2004), *Unio complanatus* (Hudson 1993), and *Nucella lamellosa* (Clelland and Saleuddin 2000). The connection between H^+-pump activity and cation uptake has been demonstrated in epithelia of a variety of species (Harvey *et al.* 1998), including Ca^{2+} uptake by post-moult blue crabs *Callinectes sapidus* (Cameron and Wood 1985, Neufeld and Cameron 1992). There have also been reviews on the presence of this pathway in crustaceans (Neufeld and Cameron 1993). Furthermore, H^+-pump-driven active cation uptake has been documented in adults of this species (Ebanks and Grosell 2008) as well as in several other freshwater species including carp (Fenwick *et al.* 1999), tilapia (Fenwick *et al.* 1999), and trout (Bury and Wood 1999, Grosell and Wood 2002, Lin and Randall 1991). Thus it appears consistent to find inhibition of Ca^{2+} uptake in the presence of the V-H^+ ATPase inhibitor, bafilomycin, in developing snail embryos and that this is persistent across later time points (up to 80% reduction in post-metamorphic Ca^{2+} uptake). Thus, the H^+ pump plays a significant role in Ca^{2+} flux in post-metamorphic stages. By electrogenic excretion of H^+s, the electrical potential across the apical membrane, and thereby the electrochemical gradient for Ca^{2+} uptake is maintained. In addition, the observations of reduced acid excretion and Ca^{2+} uptake in the presence of the specific Na^+/H^+ exchange inhibitor, EIPA, points to an even more direct coupling of H^+ extrusion to Ca^{2+} uptake. However, Hudson (1993) found no effect of 1 mmol l^{-1} amiloride or Na^+-depleted solutions on acid secretion in Ussing-type chamber experiments on mantle epithelia of *U. complanatus*. EIPA was not included in the study but there was no detectable coupling between a proxy for acid secretion, cAMP-dependent short-circuit

current (I_{SC}; Machado *et al.* 1990), and unidirectional Na^+, K^+, Ca^{2+}, or Cl^- fluxes in the same species (Hudson 1993). Nevertheless, the data suggest the presence and involvement of a Ca^{2+}/H^+ exchanger in *L. stagnalis*. It is interesting to note that electrogenic Ca^{2+}/H^+ exchange would be facilitated by parallel electrogenic H^+ extrusion by the H^+-pump.

Taken together, the results of this study suggest that through the use of the ionic products of CO_2 hydration, H^+ and HCO_3^-, the high Ca^{2+} and carbonate demands for shell formation in freshwater are met and maintained with notable efficiency. The higher the rate of CO_2 hydration the higher the rate of HCO_3^- formation and the higher the amount of H^+ excretion via the proton pumps and/or cation exchange, which in turn provides for Ca^{2+} uptake. Inhibition of CA activity leads to inhibition of transport of both shell-forming ions. Admittedly, inhibition of the ability to hydrate respiratory CO_2 can have broader impacts on the physiological level. However, when the results of CA inhibition are taken in conjunction with the response to H^+ pump and NHE inhibition as well as the ability of the embryos to develop in HCO_3^--free conditions (Ebanks *et al.* 2010a), there is substantial evidence that endogenously produced carbonate can be an exclusive carbonate source for these post-metamorphic embryos.

Figure 4.9. A schematic diagram of proposed mechanisms for Ca^{2+} and HCO_3^- acquisition by post-metamorphic embryos of the freshwater common pond snail *L. stagnalis*. Through CA-catalyzed hydration of CO_2, H^+ and HCO_3^- are produced. The H^+s are excreted via the H^+-pump (apical closed circle with ~), which contributes to maintenance of an inside negative electrical gradient, driving Ca^{2+} uptake through voltage-dependent Ca^{2+} channels (VDCC). In addition, H^+ excretion facilitates exchange of Ca^{2+} for H^+ on an electrogenic $Ca^{2+}/1H^+$ exchanger that appears to be unique to invertebrates (solid circle with ?, Greenaway 1971b, Okech *et al.* 2008, Ahearn *et al.* 1994, Ahearn *et al.* 2001). There is also evidence that HCO_3^- uptake when available in the water, occurs via an undefined pathway (Ebanks *et al.* 2010a). It is assumed that a basolateral Ca^{2+}-ATPase is responsible for excretion of Ca^{2+} across the basolateral membrane and that HCO_3^- ions are passed across the basolateral membrane to the extracellular fluid/hemolymph. See text for further details.

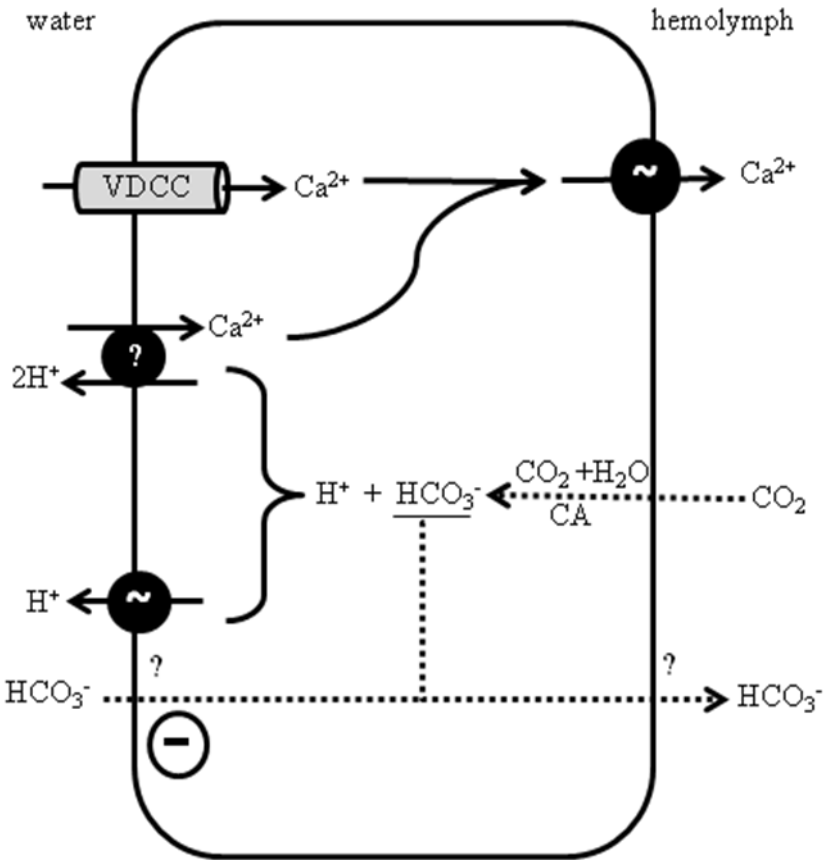

A further point to consider is that in addition to protons produced from hydration of metabolic CO_2, H^+s are liberated by the calcification process ($HCO_3^- + Ca^{2+} \rightarrow CaCO_3 + H^+$) adding to the need for acid secretion by these animals. By coupling Ca^{2+} uptake and HCO_3^- production with the generation of inside alkaline conditions via H^+ extrusion, the conditions for calcification within the egg and egg mass are enhanced. Furthermore, the depletion of Ca^{2+} within the perivitelline fluid and gelatinous matrix (*tunica interna*) between the eggs to levels below water concentrations during later embryonic stages (Ebanks *et al.* 2010a) creates an inward Ca^{2+} gradient and thus can enhance the influx of Ca^{2+} from the surrounding water while decreasing the energy required for ion uptake.

Implications of findings

Acquisition of the necessary Ca^{2+} and carbonate for calcification by embryos of the freshwater common pond snail *Lymnaea stagnalis* are intricately intertwined. These embryos take up Ca^{2+} from ambient media after maternal stores in the perivitelline fluid have been depleted; but they also directly utilize endogenously produced bicarbonate from the CA-catalyzed hydration of CO_2. Protons generated from CO_2 hydration are excreted, which fuels continued Ca^{2+} uptake and allows for accumulation of bicarbonate and maintenance of alkaline internal conditions that are favorable for calcification. With endogenous production of HCO_3^- for calcification perpetuating continued Ca^{2+} uptake, these embryos are capable of efficient calcification under low ionic strength conditions. Considering global climate change, studies are necessary to determine how ambient pH and bicarbonate buffering affect the ability of these freshwater snails to calcify. Furthermore, evaluating the extent to which acid secretion rather than base uptake is the

basis for calcification in other freshwater as well as marine calcifiers offers an exciting area for comparative studies.

Chapter 5:

The Impact of Water Chemistry and Pb Exposure on Ca^{2+} Acquisition and Embryonic Development in the Freshwater Common Pond Snail *Lymnaea stagnalis*

5.1. Background

The calcium antagonist, lead (Pb), is a potent inhibitor of voltage-sensitive Ca^{2+} channels in both invertebrates and vertebrates (Audesirk 1993) and has been found to compete with Ca^{2+} for voltage-independent Ca^{2+} channels in branchial tissues of the freshwater rainbow trout *Oncorhynchus mykiss* (Rogers and Wood 2004). Invertebrates have the potential for electrogenic $2Na^{+}/1H^{+}$ exchange and divalent cations such as Ca^{2+} can potentially be transported on this protein (Ahearn *et al.* 1994). Thus, the electrogenic $2Na^{+}/1H^{+}$ exchanger may be an access point for Pb as well. Previous studies on the freshwater pond snail *Lymnaea stagnalis* have indicated the apparent activity of the electrogenic $2Na^{+}/1H^{+}$ exchanger in embryos of the species (Ebanks *et al.* 2010b).

A pulmonate freshwater snail, the bloodfluke planorb *Biomphalaria glabrata*, exhibited significant Pb uptake accompanied by reduced growth and significant mortality with no significant effect on reproduction when exposed to Pb at 1 - 250 $\mu mol\ l^{-1}$ $PbCl_2$ (Allah *et al.* 2003). Furthermore, Pb uptake from the water has been demonstrated in adults of *Lymnaea palustris* with significant mortality at 19 $\mu g\ Pb\ l^{-1}$ (Borgmann *et al.* 1978). Grosell *et al.* (2006) demonstrated that Pb uptake from aqueous exposure in new hatchlings of *Lymnaea stagnalis* with a 20% effective concentration (EC20) on growth at $<4\ \mu g\ Pb\ l^{-1}$, the lowest EC20 measured for any organism and possibly below then current water quality standards (ca. 3.3 $\mu g\ Pb\ l^{-1}$). Grosell *et al.* (2006) documented reduced growth that may be due to interference of Pb with Ca^{2+} uptake in these

organisms, which have significant Ca^{2+} requirements for shell formation (Grosell and Brix 2009).

Voltage-dependent Ca^{2+} channels are important to Ca^{2+} transport in later-stage *L. stagnalis* embryos (Ebanks *et al.* 2010b). Considering the apparent negative effect of Pb on voltage-dependent Ca^{2+} channels (Audesirk 1993), Pb is an interesting contaminant to test for effects on Ca^{2+} uptake. Furthermore, in metal contamination, early life stages are generally most sensitive (Wang 1987), especially when exposed during the earliest, least developed stages (Reish *et al.* 1976, Harrison *et al.* 1984, Nebeker *et al.* 1985). Thus, the first objective of this study was to examine Pb-effects on the embryonic stages of *L. stagnalis* to determine relative sensitivity compared to juveniles of the same species. Also, *L. stagnalis* makes use of the H^+ and HCO_3^- produced in carbonic anhydrase (CA)-catalyzed hydration of CO_2 to acquire aquatic Ca^{2+} for calcification (Ebanks *et al.* 2010a, Ebanks *et al.* 2010b). The utilization of the CA-catalyzed hydration of CO_2 for the purpose of ion acquisition has been studied in freshwater fish (Bury and Wood 1999, Fenwick *et al.* 1999, Grosell and Wood 2002, Lin and Randall 1991) and in *L. stagnalis* (Ebanks and Grosell 2008). However, only recently has there been data to indicate that the process is active during embryonic stages of development in *L. stagnalis* (Ebanks *et al.* 2010a, Ebanks *et al.* 2010b). Interaction between Ca^{2+} and Pb occurs on voltage-dependent Ca^{2+} channels (Audesirk 1993) and Ca^{2+} transport via these channels is mediated in part by excretion of H^+ supplied by CA-catalyzed hydration of CO_2. The use of this pathway for cation uptake commences around the time of metamorphosis in *L. stagnalis* and apparently plays a role throughout the later stages of embryonic development (Ebanks *et al.* 2010b); however, it is unclear whether Pb toxicity is on the

activation of the pathway or is limited to its functionality. Additionally, chronic Pb exposure reduces Ca^{2+} uptake in young adult (Grosell and Brix 2009) and juvenile (Grosell *et al.* 2006) *Lymnaea* so negative effects on Ca^{2+} uptake in embryos are likely to be significant. Therefore, the second objective of this study was to determine whether Ca^{2+} acquisition and embryonic development are Pb-sensitive on an acute or chronic level.

Another factor that must be considered is the role that water chemistry plays in Pb toxicity. In general, there appears to be an inverse relationship between ambient water hardness, specifically [Ca^{2+}] and the toxicity of Pb at least for some species ([USEPA] 2009, Grosell *et al.* 2006). Young adult *Lymnaea* growth and net Ca^{2+} uptake are hypersensitive to Pb, which is apparently due to high Ca^{2+} requirements (Grosell and Brix 2009). Calcium has served as the primary water quality parameter for consideration in the USEPA Pb water quality criteria. However, research in the last few years provides evidence that points to significant protection from chronic Pb toxicity by dissolved organic carbon (Grosell *et al.* 2006, Mager *et al.* 2008, Mager *et al.* 2010a) and bicarbonate in the fathead minnow *Pimephales promelas* (Mager *et al.* 2010a). Furthermore, calcium may not be protective against chronic Pb toxicity to all organisms (Mager *et al.* 2008, Mager *et al.* 2010b, Mager *et al.* in prep). Thus, the final objective of this study was to determine the role of water chemistry, by the measurement of natural variability in DOC, bicarbonate, and calcium concentrations, on Pb toxicity in the later stages of embryonic development for *L. stagnalis*.

5.2. Materials and methods

Animals

Egg masses of the common pond snail *Lymnaea stagnalis* were collected in 24-hour intervals from mass cultures with the day of collection considered day zero post-oviposition, for age determination. Embryos were incubated at room temperature (20-22°C) in aerated, dechlorinated Miami-Dade County tap water (Grosell *et al.* 2007) or natural water, as indicated. Prior to flux experiments, the egg masses were weighed (g), measured (mm), and viability was determined. Egg masses with less than 80% development were excluded from all experiments and analyses. Additionally, all morphological descriptors used in this study have been thoroughly described previously by Plesch *et al.* (1971) and Morrill (1982).

Toxicity in laboratory water: *Chronic and acute exposures*

To determine whether Pb affected Ca^{2+} uptake as a result of long-term or acute exposures, an experiment was completed with acute (24-h) and chronic (day zero to hatch) exposures of the same nominal [Pb] of 3 $\mu g\ l^{-1}$ in dechlorinated Miami-Dade County tap water (MDTW, Grosell *et al.* 2007). Egg masses were exposed to Pb as $Pb(NO_3)_2$ (Sigma-Aldrich) from the time of collection and through the duration of the experiments for the chronic exposure. The acute exposure was for the 24 hours starting at day seven after collection. Water was replaced daily for both acute and chronic Pb exposures of egg masses.

Toxicity in natural waters: Chronic exposures

In addition to MDTW, three natural waters that varied widely in water chemistries were used in this study. Waters were collected from French Lake, which is located within the south central section of the Canadian Shield (Ontario, Canada). Additional waters were collected from Green Cove, located in northeast Florida, U.S.A. and from Sweetwater, FL, U.S.A., which is located within the Everglades, in the southwest region of the state. Water chemistry parameters for the three site waters are listed in table 5.1.

For the natural waters, individual egg masses were exposed to Pb from day zero and for the course of development. The range of [Pb] was 0 – 3.2 $\mu g\ l^{-1}$ in Canadian Shield water, 0 – 1.3 $\mu g\ l^{-1}$ in Green Cove water, and 0 – 26.4 $\mu g\ l^{-1}$ in Sweetwater experiments. These different concentrations were chosen based on expectations of protection by water chemistry against Pb in the respective waters and comparisons to observations in MDTW experiments. However, the differences in [Pb] between Canadian Shield and Green Cove waters were due to differences in Pb adsorption and solubility but the nominal [Pb] was the same for these two waters.

In exposing the egg masses from day zero there is no opportunity to recognize that the egg masses lack the sufficient number of viable embryos (80%) until after substantial water resources have been used. Thus, over the course of the exposure periods for these experiments, there were cases in which egg masses were determined to be sub-standard on or around day four or five but by that point, one or two pre-metamorphic fluxes had been completed. Such egg masses were excluded from the present report and analyses.

Table 5.1
Water chemistry of site waters used in embryonic studies on *Lymnaea stagnalis*. All ion concentrations are in µmol l^{-1}.

Site	Collection Date	pH	Na^+	Ca^{2+}	K^+	Mg^{2+}	Cl^-	NO_3^-	SO_4^{2-}	HCO_3^-	DOC
Canadian Shield, French Lake, Canada (CS)	Summer 2009	7.58	98.2	74.4	5.7	49.1	83.5	4.87	20.6	326.7	579.7
Green Cove, Jacksonville, Florida, U.S.A. (GC)	Summer 2009	8.27	173.3	828.4	47.8	758.5	141.9	0	477.9	1448.8	92.1
Sweetwater, Florida, U.S.A. (SW)	Fall 2009	8.71	231.2	1539.6	0	71.9	207.4	0	0	2796.9	813.0

Net Ca^{2+} flux

In MDTW, an initial flux was completed on pre-metamorphic day two embryos that either had not been exposed to Pb (controls and acute group prior to exposure) or that had been exposed from day zero post-oviposition (chronic). A second flux was then completed on all of the egg masses on day eight. The acutely exposed egg masses were exposed for 24 h prior to these day eight fluxes. The procedures for determination of flux rates were in accordance with those outlined in Ebanks *et al.* (2010a). In brief, samples of pre- and post-flux media were collected from fluxes that were done on pre-metamorphic and post-metamorphic embryos. Net calcium flux was then calculated from the change in $[Ca^{2+}]$, mass of the egg mass (g), and elapsed time (h) and was presented as $\mu mol\ g^{-1}\ h^{-1}$. The chronic exposure experimental procedure was repeated with a range of [Pb] in each of the three natural waters.

Developmental observations

Egg masses were observed using a dissecting microscope fitted with a Nikon Coolpix digital camera with Q-Capture software. Images were taken for at least one pre-metamorphic and one post-metamorphic time point to record any morphological or developmental differences across site waters and Pb concentrations. Additionally, growth comparisons were completed using ovum diameter in pre-metamorphic embryos, which are those stages prior to the onset of shell formation and shell length was measured for post-metamorphic embryos (hippo stage and later, Morrill 1982). Another parameter used to assess developmental effects was time to first emergence and time to first hatch. The term "first emergence" is used here to describe the time at which the first embryo

exits the membrane of its egg capsule but before the first embryo exits the *tunica capsulis*. Thus, during the period between "first emergence" and "first hatch," embryos are roving within the *tunica interna*. The term "first hatch" indicates the time when the first embryo exits the *tunica interna* and *tunica capsulis* of the egg mass and has entered the external environment.

Water chemistry analyses

Water samples were analyzed for major cations and anions as well as pH and dissolved organic carbon (DOC) and the results are listed in table 1. DOC was measured by high-temperature catalytic oxidation using a Shimadzu total organic carbon-VCSH analyzer (Kyoto, Japan; Hansell and Carlson 2001). pH was measured using a Radiometer Analytical MeterLab meter (PHM201, Copenhagen, Denmark). Cation concentrations were determined via flame atomic absorption spectrophotometry (Varian SpectrAA220, Mulgrave, Victoria, Australia) and anion concentrations, except for bicarbonate, were determined by anion chromatography (DIONEX DX 120, Sunnyvale, California, USA). Bicarbonate concentrations were determined by double endpoint titration (Hills 1973, Wilson *et al.* 1996, Grosell *et al.* 1999, Ebanks *et al.* 2010a). All Pb measurements were by graphite furnace atomic absorption (Varian 220Z; Mulgrave, Victoria, Australia). The standard protocol used for the [Pb] measurements on the graphite tube furnace is two measurements, each a single injection of 30 µl. The minimum detection limit (MDL) for the single injection analysis was approximately 5 µg Pb l^{-1}. This protocol was modified to a two measurement, triple injection format for a total volume of 90 µl per sample. This modified, higher-volume injection procedure

lowered the MDL to encompass the lower range of [Pb] used in the laboratory and natural water studies (nominal sample [Pb] as low as 0.3 μg Pb l^{-1}). The triple injection protocol was used for any samples for which the expected [Pb] was below 5 μg Pb l^{-1}.

Statistical analyses

All statistical analyses were completed using SigmaPlot for Windows version 11.00. Comparisons among experimental groups were completed using the Student's t-test or an ANOVA with post-hoc pairwise comparisons where appropriate following the Holm-Sidak method. These parametric analyses were performed after an evaluation with the Shapiro-Wilk test to determine whether the data sets were normally distributed. All values are means ± S.E.M. and statements of statistical significance indicate comparisons for which $P < 0.05$.

5.3. Results

Acute-chronic exposure comparison in Miami-Dade County tap water

There was no Pb-related mortality in either the acute or chronic Pb exposures. Pre-metamorphic embryos chronically exposed to Pb exhibited the same growth patterns and net Ca^{2+} flux rates as those that had not been exposed (controls and pre-acute exposure groups). However, post-metamorphic embryos exposed to Pb for chronic and acute periods in Miami-Dade County tap water exhibited differential emergence and hatch times. Net Ca^{2+} flux values were not significantly different between controls and treatment groups prior to day seven but after that point, the chronic exposure group showed reduced net Ca^{2+} uptake, at least at some time points (fig. 5.1). There were no

significant differences in net Ca^{2+} transport between the acute exposure and control groups. Also, there were no significant differences between controls and acute or chronic treatment groups for ovum diameter or shell length over the course of development (fig. 5.2). However, chronically exposed egg masses spent longer roving within the egg mass after emerging from the individual egg capsule compared to controls and those that were acutely exposed (fig. 5.3).

Site water experiments

There was no Pb-related mortality over the course of these experiments. In the experiments with natural waters, net Ca^{2+} flux rates for Pb-exposed embryos were not significantly different from controls during pre-metamorphic (day two) fluxes (fig. 5.4). For post-metamorphic fluxes (days seven and eight), trends varied across the different site waters (fig. 5.4). In the Canadian Shield water (CS), post-metamorphic Ca^{2+} uptake rates were significantly reduced for egg masses exposed to 0.1 and 0.6 µg Pb l^{-1} and post-metamorphic Pb-exposed egg masses generally tended to have lower Ca^{2+} uptake rates at all Pb concentrations relative to controls (fig. 5.4A). In Green Cove water (GC), there was generally Ca^{2+} uptake by post-metamorphic embryos and higher rates than in CS with some disruption at the lower Pb concentrations (fig. 5.4B). For the embryos that were raised in Sweetwater (SW) media, post-metamorphic flux measurements were performed on day eight rather than on day seven as for CS and GC due to delayed metamorphosis in this group. There was net Ca^{2+} efflux at nearly all Pb concentrations for embryos that were incubated in SW media (fig. 5.4C).

Figure 5.1. Net Ca^{2+} flux over the course of development for embryos of the freshwater pond snail *Lymnaea stagnalis* in Miami-Dade County tap water. Fluxes were for 24 h and were repeated as indicated in either no Pb for the duration of the experiment (control), 24-h exposure of 0.7 µg Pb l^{-1} as $Pb(NO_3)_2$ at day seven post-oviposition (acute), or 1.3 µg Pb l^{-1} as $Pb(NO_3)_2$ from day zero through the duration of the experiment (chronic). *significant difference from control and acute at time point indicated. ID = insufficient sample size to complete statistical analysis by day 13 due to hatching, which began at day 11.

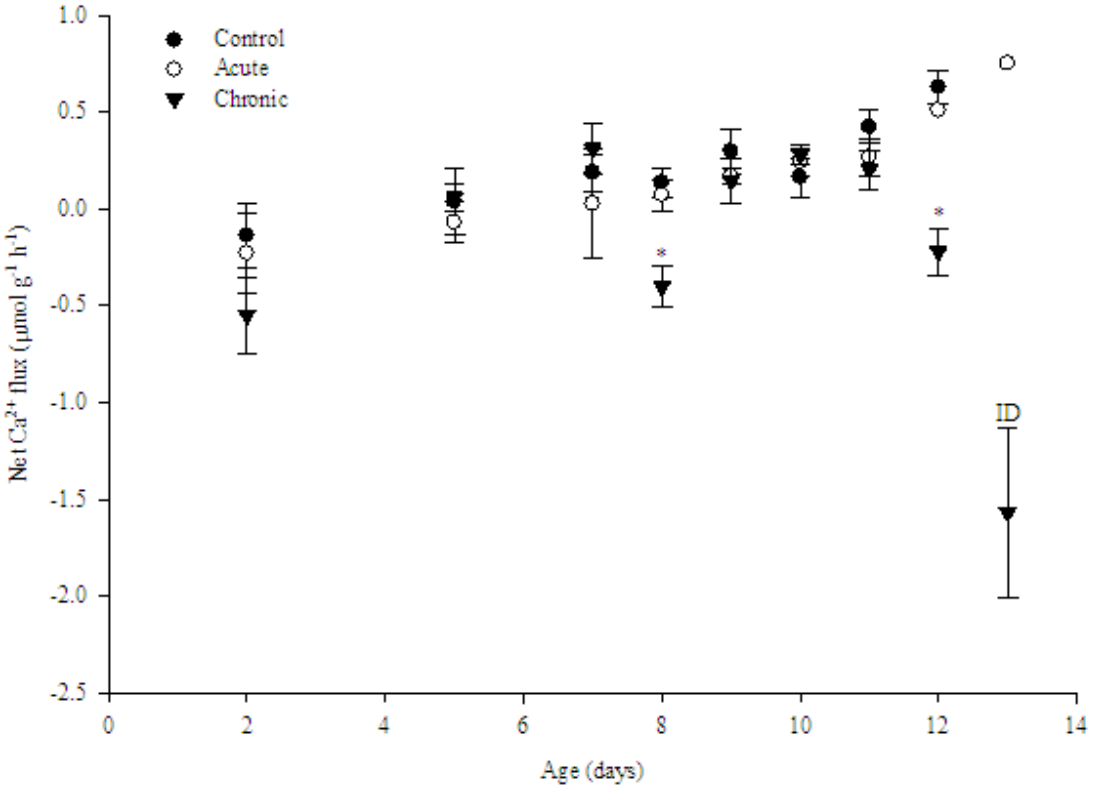

Figure 5.2. Ovum diameter (before day five) and embryonic shell length (on and after day five) over the course of development for the freshwater pond snail *Lymnaea stagnalis* in Miami-Dade County tap water. Embryos were incubated in either no Pb for the duration of the experiment (control), 24-h exposure of 0.7 µg Pb l^{-1} as $Pb(NO_3)_2$ at day seven post-oviposition (acute), or 1.3 µg Pb l^{-1} as $Pb(NO_3)_2$ from day zero through the duration of the experiment (chronic).

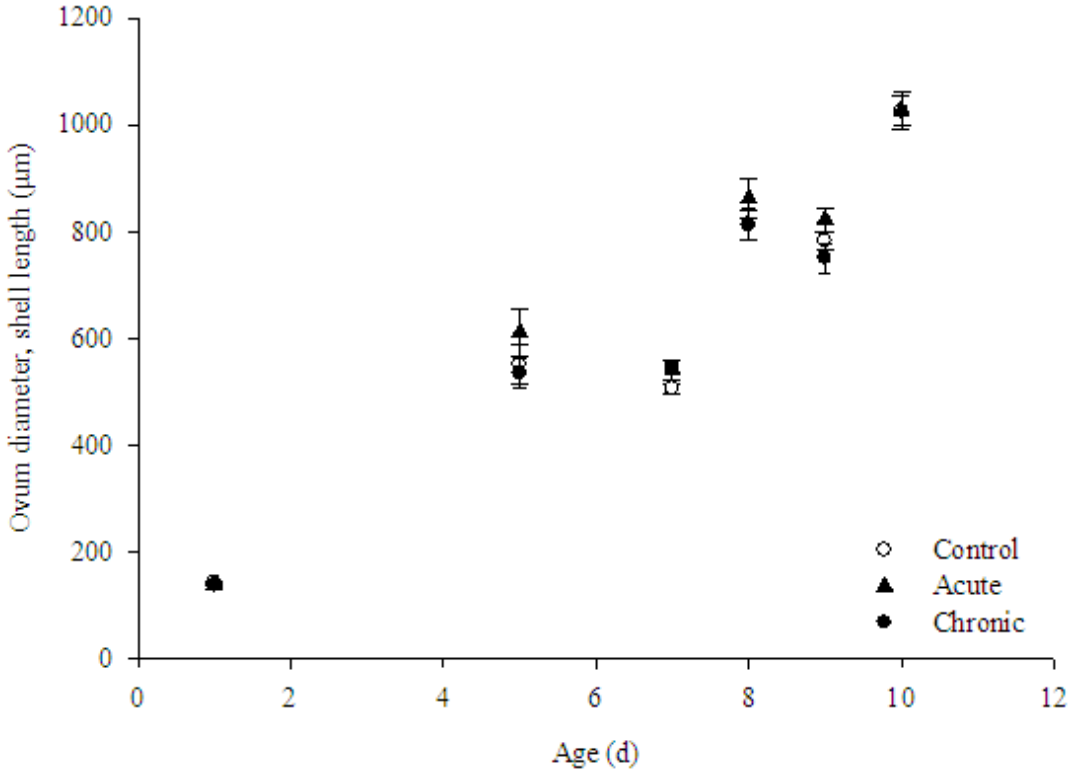

Figure 5.3. Time to emergence from egg capsule (black bars) and time to hatch from egg mass (gray bars) for embryos of the freshwater pond snail *Lymnaea stagnalis* in Miami-Dade County tap water. Embryos were incubated in either no Pb for the duration of the experiment (control), 24-h exposure of 0.7 µg Pb l^{-1} as $Pb(NO_3)_2$ at day seven post-oviposition (acute), or 1.3 µg Pb l^{-1} as $Pb(NO_3)_2$ from day 0 through the duration of the experiment (chronic). *significantly longer time between emergence and hatch in chronic exposure.

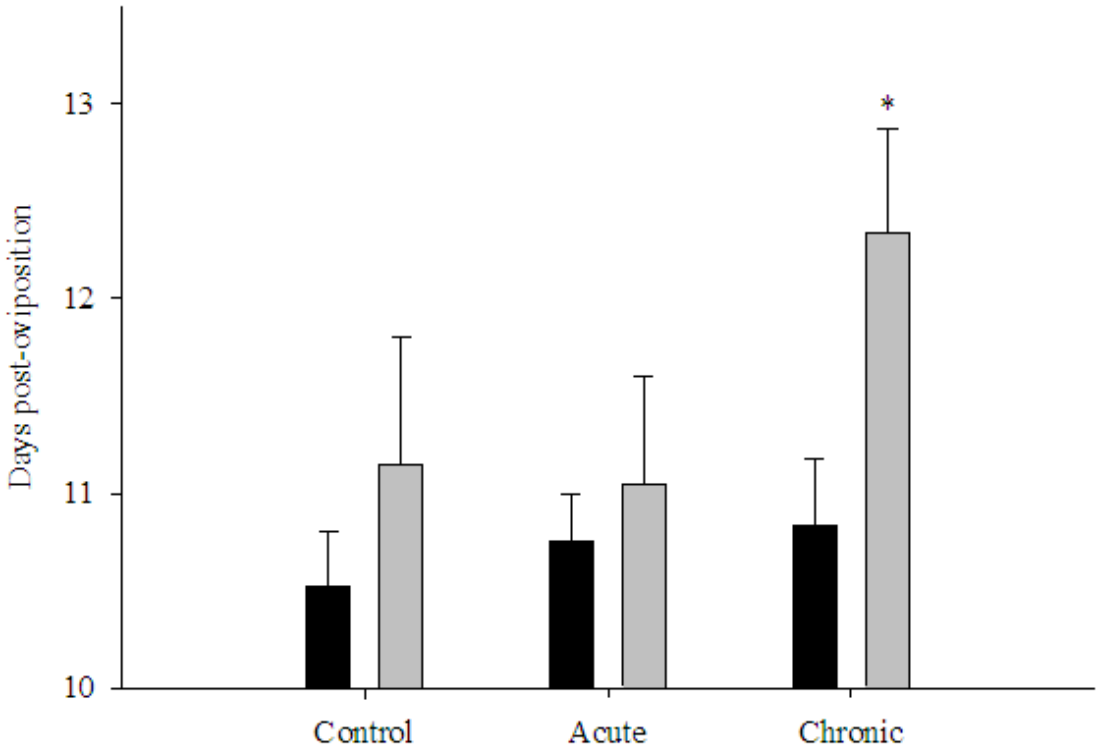

All viable embryos exhibited growth and morphological development over the observation period with growth indicated by ovum diameter and shell length for embryos raised in the different site water-[Pb] combinations. Ovum diameter was approximately 100 µm at the time of collection from the cultures. In the CS water, pre-metamorphic Pb-exposed embryos were smaller than controls at day two (fig. 5.5A). The degree of growth inhibition between controls and the lowest [Pb] in CS water (0.13 µg Pb l^{-1}) was consistent over the course of development, though not always with statistical significance. In GC water, there was nearly a ten-fold increase in size over the period from day zero to day nine post-oviposition but no apparent effect of Pb on growth over the embryonic period (fig. 5.5B). Embryos raised in Sweetwater (SW) media, exhibited the least growth with a mean shell length of only 725 µm at day ten, with a large degree of variability (fig. 5.5C). There were no consistent statistically significant differences in size among Pb treatments; and embryos raised in SW generally grew more slowly and were smaller than those incubated in CS or GC waters.

With respect to time to emergence and time to hatch, there was no significant difference between the time to emergence and the time to hatch under control conditions and acute exposure in MDTW; but there was a significant difference with chronic Pb exposure (fig. 5.3). However, in nearly all cases for the natural waters (except 0.3 µg Pb l^{-1} in CS and 13.44 µg Pb l^{-1} in SW), embryos took significantly longer to hatch from egg masses than they took to emerge from their egg capsules (table 5.2). Thus, their excursion time within the internal environment of the *tunica capsulis* was significant. In CS water, hatch time was less than 15 days and there were no significant differences across [Pb], but mean time to emerge and mean time to hatch tended to be slightly longer

for Pb-exposed embryos relative to controls (table 5.2). For the embryos raised in GC water, emergence time was approximately the same as for those in CS water (≤ 12 days) but they took longer to leave the egg mass (table 5.2). Embryos incubated in SW media began to emerge from their egg capsules to rove inside the *tunica capsulis* approximately one to two days later than those in CS or GC waters and did not begin to hatch from the *tunica capsulis* and enter the surrounding environment until days 16 – 17 post-oviposition (table 5.2).

5.4. Conclusions and implications

Considering the negative responses in egg masses exposed to Pb for the duration of their embryonic development in contrast to the lack of response to the acute exposure, sensitivity to Pb in this early life stage of *Lymnaea* seems to be most pronounced during chronic exposure. Embryos exposed to Pb in laboratory waters (MDTW) showed significant effects of Pb on net Ca^{2+} flux and hatch times with chronic exposure to 1.25 µg Pb l^{-1} but not acute exposure. This concentration is likely lower than the 20% effect concentration (EC20) calculated for the juveniles of this species in similar waters (< 4 µg Pb l^{-1}; Grosell *et al.* 2006).

Figure 5.4. Net Ca^{2+} flux as determined in 24-h fluxes on pre-metamorphic (○) and post-metamorphic (●) egg masses of the freshwater pond snail *Lymnaea stagnalis* in Canadian Shield (panel A, days two and seven), Green Cove (panel B, days two and seven), and Sweetwater (panel C, days two and eight) waters over a range of [Pb] as $Pb(NO_3)_2$. Fluxes were for 24 h on egg masses that were exposed to Pb from day zero through the duration of the embryonic development. *significant difference from control (no Pb) for post-metamorphic embryos at the [Pb] indicated.

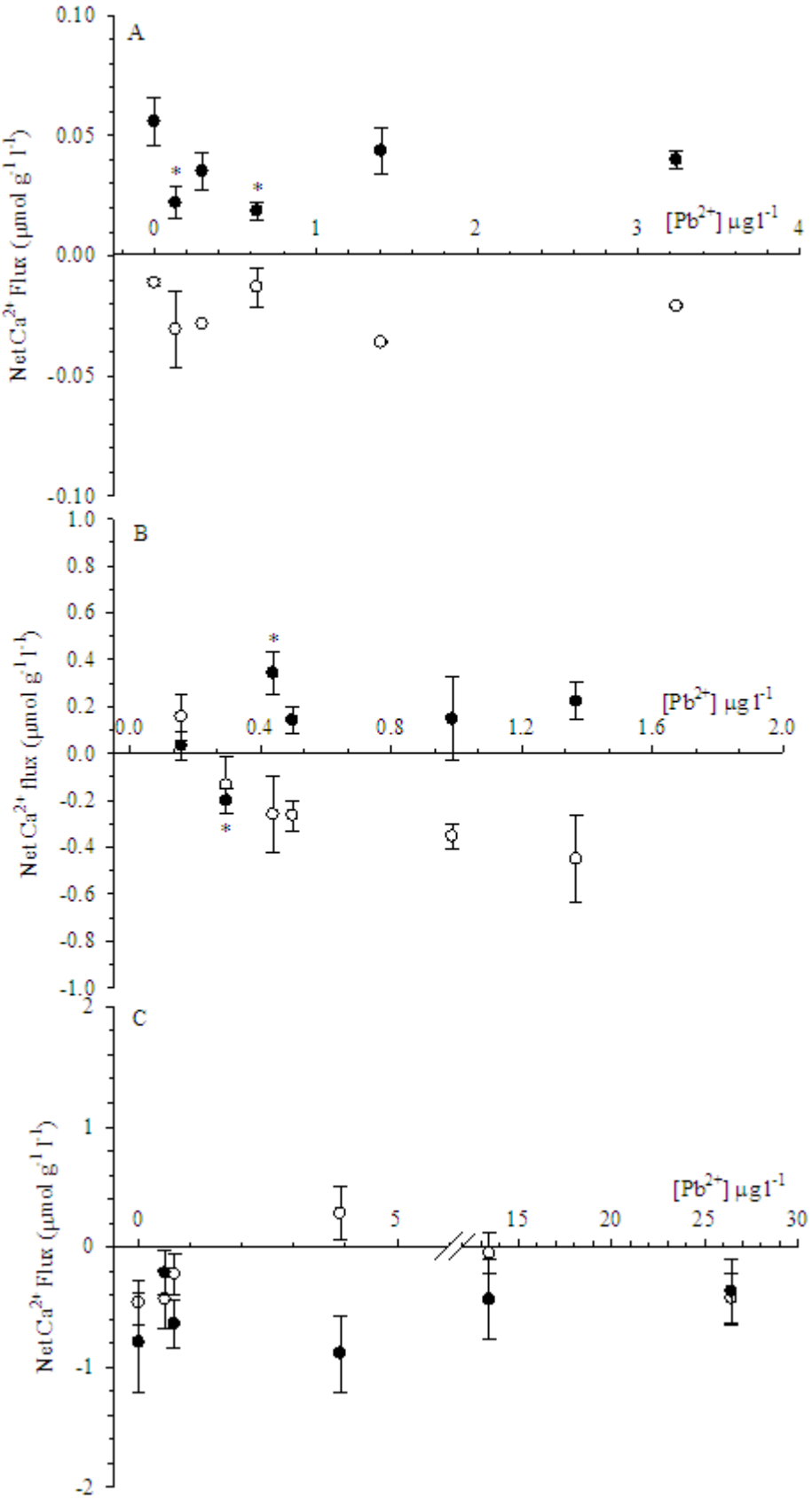
A
B
C
Net Ca2+ Flux (µmol g-1 l-1)
[Pb2+] µg l-1
0.10
0.05
0.00
-0.05
-0.10
1.0
0.8
0.6
0.4
0.2
0.0
-0.2
-0.4
-0.6
-0.8
-1.0
2
1
0
-1
-2
0
1
2
3
4
0.0
0.4
0.8
1.2
1.6
2.0
5
15
20
25
30
*

Figure 5.5. Ovum diameter (days zero to four) and shell length (days seven to ten) for embryos of the freshwater pond snail *Lymnaea stagnalis* in Canadian Shield (A), Green Cove (B), and Sweetwater (C) waters over a range of [Pb] as $Pb(NO_3)_2$. a, b = Pb-treated embryos at these Pb concentrations were significantly smaller than control (no Pb) group for time point indicated.

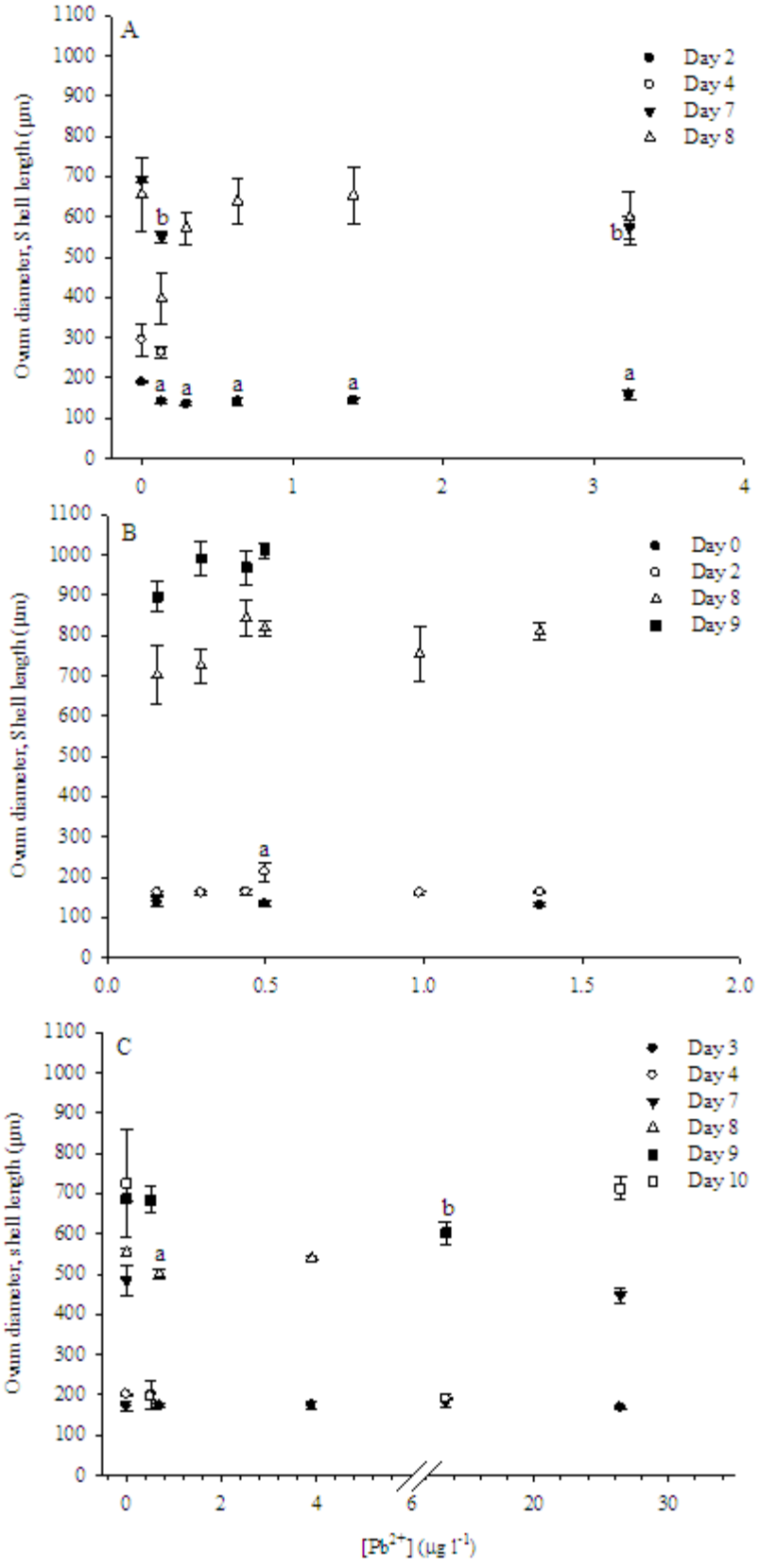
A
Day 2
Day 4
Day 7
Day 8
Ovum diameter, Shell length (µm)
B
Day 0
Day 2
Day 8
Day 9
Ovum diameter, Shell length (µm)
C
Day 3
Day 4
Day 7
Day 8
Day 9
Day 10
Ovum diameter, shell length (µm)
[Pb2+] (µg l-1)

Table 5.2. Time to emergence from egg capsule and time to hatch from egg mass for embryos of the freshwater pond snail *Lymnaea stagnalis* in natural waters. Times are days post-oviposition. Embryos were incubated in a range of [Pb] as indicated from day zero and through the duration of development.

Source of water	[Pb] $\mu g\ Pb\ l^{-1}$	Time to emergence (days ± S.E.M.)	Time to hatch (days ± S.E.M.)	N (no. egg masses)
Canadian Shield (CS)	0	11 ± 0.4	12.5 ± 0.6	6
	0.13	12 ± 0.4	13.8 ± 0.5	6
	0.30	12 ± 0.6	13.7 ± 1.4	4
	0.64	11.8 ± 0.2	13.6 ± 0.7	5
	1.41	11.7 ± 0.2	13.7 ± 0.7	4
	3.24	11.7 ± 0.2	13.8 ± 0.4	6
Green Cove (GC)	0.16	11.3 ± 0.3	13.9 ± 0.5	14
	0.30	12 ± 0.3	14.8 ± 0.6	9
	0.44	10.6 ± 0.3	13.5 ± 0.4	6
	0.50	10.3 ± 0.2	13 ± 0.4	6
	0.99	10.6 ± 0.3	14.3 ± 1.2	3
	1.37	11 ± 0	15 ± 0.6	4
Sweetwater (SW)	0	13.3 ± 0.2	16.1 ± 0.6	13
	0.51	13 ± 0.7	16 ± 0.7	4
	0.69	14 ± 0	17.4 ± 0.5	5
	3.90	13.3 ± 0.3	16.7 ± 0.3	4
	13.44	14.3 ± 0.5	16.3 ± 0.9	4
	26.42	13.8 ± 0.5	16.4 ± 0.4	5

Transport pathways are apparently activated around the time of metamorphosis; and ambient ion availability for calcification during and after metamorphosis is critical to embryonic growth and development in *Lymnaea* (Ebanks *et al.* 2010a). Results of the acute verses chronic Pb exposure experiments suggest that Pb may be impacting the pre- or peri-metamorphic activation of Ca^{2+} uptake (fig. 5.1) and possibly other biological systems. However, general water chemistry seemed to have a greater influence than any of the tested Pb concentrations.

Lead toxicity and water chemistry, specifically cation concentrations, are intricately intertwined as indicated by the water-hardness-dependent water quality criteria for Pb as issued by the USEPA. Furthermore, recent studies provide evidence that

additional water quality parameters, namely bicarbonate and DOC concentrations, should be considered in modeling potential Pb toxicity (Grosell *et al.* 2006, Mager *et al.* 2008, Mager *et al.* 2010a, Mager *et al.* 2010b). The waters used in this study can be characterized as low ion-high DOC water (Canadian Shield), middle to high ion-low DOC water (Green Cove), and high ion-high DOC water (Sweetwater). Clearly the covariance of water quality parameters makes it difficult to ascertain the effects of the individual characters on Pb toxicity. However, a comparison between responses in laboratory water and natural waters indicates greater Pb sensitivity of Ca^{2+} uptake and growth in the low ion, high DOC Canadian Shield (CS) water in which the lowest effect concentration was 0.13 µg Pb l^{-1} (figs. 5.4A and 5.5A). This is nearly an order of magnitude less than the 1.25 µg Pb l^{-1} in MDTW at which there was a significant reduction in Ca^{2+} uptake and delayed hatching (figs. 5.1 – 5.3). Surprisingly, the effects of Pb on net Ca^{2+} flux in the natural waters were limited to the lower and intermediate Pb concentrations, which suggested a possible capacity for compensatory response at the higher Pb concentrations. In Green Cove (GC) water (intermediate [Ca^{2+}] and [HCO_3^-] with low DOC), the lowest concentration showing an effect of Pb was 0.30 µg Pb l^{-1} for Ca^{2+} uptake. Considering that the water hardness-corrected Criteria Continuous Concentration as estimated from the United States Environmental Protection Agency National Recommended Water Quality Criteria (2009) for CS and GC are 0.24 and 4.15 µg Pb l^{-1}, respectively, post-metamorphic *L. stagnalis* are apparently not adequately protected under current water quality criteria. For the embryos raised in the high Ca^{2+}, HCO_3^-, and DOC conditions of the Sweetwater (SW) media, strong protection against Pb toxicity was expected. Calcium uptake was clearly inhibited in this water compared to

CS, GC, and laboratory waters but showed no apparent relationship to [Pb] over the range of Pb concentrations tested.

Calcium flux observations in the laboratory waters correlated with delayed emergence in the chronic treatment (figs. 5.1 and 5.3). However, there was no significant connection within groups of embryos incubated in natural waters for Pb toxicity on net Ca^{2+} flux, growth (ovum diameter and shell length), emergence, or hatch times. For CS and GC waters there were moderate, non-statistically significant delays in emergence and hatch times at the same Pb concentrations causing reduced Ca^{2+} uptake (≤ 0.30 µg Pb l^{-1}). Emergence and hatch times were recorded daily and there was nearly a one-day delay at these lower Pb concentrations. Possibly by increasing resolution to the hour level, clearer trends might have emerged. Considering findings published elsewhere (Ebanks *et al.* 2010a, Ebanks *et al.* 2010b) on net Ca^{2+} flux in various [Ca^{2+}] and [HCO_3^-], slower growth and delayed hatching were expected in the low Ca^{2+} CS water and indeed that was the case with a mean shell length of approximately 600 µm by day eight compared to 830 µm in MDTW. Embryos that were incubated in SW were expected to have the greatest protection against Pb toxicity because SW had the highest concentrations of Ca^{2+}, HCO_3^-, and DOC. While this group was not impacted by Pb across the range tested, all embryos that were incubated in the SW media had low or no net Ca^{2+} uptake, mediocre growth rates, and significantly delayed hatching compared to CS, GC, and even previous observations in MDTW.

The use of natural waters illustrate how variations in ambient water chemistry can affect the Ca^{2+} transport, growth, and hatching in *L. stagnalis*. With respect to Pb toxicity, both CS and GC waters offered less protection than the laboratory waters

(MDTW). However, unexpectedly poor growth and development for embryos incubated in the high Ca^{2+}, HCO_3^-, and DOC conditions of the Sweetwater media suggests that there may be antagonists to proper Ca^{2+} acquisition, growth, and development in the Sweetwater media that were examined as part of this study. The U.S. Geological Survey has dedicated extensive resources to studying the presence and effects of mercury (Hg) in the Everglades including the Aquatic Cycling of Mercury in the Everglades (ACME, Project # OH 712). In ACME and the National Assessment Study of Mercury Contamination of Aquatic Ecosystems (Project # AK 710), the USGS has found the Everglades region to be one of the three most contaminated sites for Hg (>0.4 ng Hg l^{-1}) and MeHg (>8% methylation efficiency) in the country. Mercury toxicity has been extensively studied but the irreversible binding of inorganic Hg to Ca^{2+} binding sites, specifically voltage-dependent Ca^{2+} channels (VDCCs) in *Aplysia* (Pekel *et al.* 1993), is of direct importance to *L. stagnalis* embryos, which apparently utilize VDCCs, during peri- and post-metamorphic stages (Ebanks *et al.* 2010b). In addition to Hg, Miles and Pfeuffer (1997) reviewed and reported on the wide-ranging variety (200+), large quantity (14,500+ tons), and long history of pesticide prevalence in the Everglades. Some of the compounds within these groups of pesticides such as molluscicides, DDT, and PCBs have been found to interact with calcium with respect to muscle action (Brezdan and Gardner 1983), calcium binding in neurons (Ghiasuddin and Matsumura 1979), and calcium metabolism (Wong *et al.* 1974), respectively. Thus SW media, used in the present study, is possibly contaminated with a variety of substances that can negatively impact the endpoints presented in this study.

Results from these experiments have shown the need for inclusion of more diversity in the natural waters selected. By adding a natural water low in ions and DOC the lower Ca^{2+}, HCO_3^-, and DOC concentrations would be covered. Also, considering the potential additional anthropogenic sources of calcium antagonists in SW, the inclusion of a source with similar ion and DOC concentrations to SW (high Ca^{2+}, HCO_3^-, and DOC concentrations) but with minimal anthropogenic factors would be useful.

Implications of findings

Embryos of the common pond *Lymnaea stagnalis* were shown to be more sensitive to chronic Pb exposure for calcium uptake and development compared to documented values for juveniles of the same species. This sensitivity was below current US EPA water quality criteria values for Pb. Additionally, natural variations in water chemistry, specifically DOC, bicarbonate, and calcium concentrations, collectively impacted post-metamorphic embryonic calcium uptake and growth as well as hatching rates. The collective protective nature of DOC, bicarbonate, and calcium against chronic Pb toxicity were less resolved but presents a fruitful area for further study.

Chapter 6:

Discussion

Lessons learned in culturing Lymnaea

The culture and care of the common pond snail *Lymnaea stagnalis* is relatively undemanding assuming that certain procedures are followed. For example, though the species is naturally found in relatively lentic environments, flow-through conditions are evidently necessary for the snails to thrive in the laboratory. Without water replacement, all observed life stages of *L. stagnalis* acidify tank water and reduce ambient [Ca^{2+}]. Also, by maintaining a balance of sufficient water flow and removing any food that is no longer being actively consumed by the snails, the water quality (especially pH) is maintained, which promotes a healthy periostracum layer and snail health in general. With respect to egg production, a modification to the feeding cycle starting a few days before the eggs are needed can trigger increased egg production. To encourage egg production, copious amounts of fresh food (Romaine lettuce, carrots, and sweet potatoes) should be provided for two to three days and then the tanks should be cleared of all food for approximately 24 – 48 hours. The snails are likely to consistently produce egg masses during the food-deprivation period without a noticeable reduction in egg quality.

Broader-scale implications of this research

During the course of this dissertation research, I had the opportunity to participate in a new collaboration between our laboratory and the O'Donnell Group at McMaster University. Their research group specializes in the utilization of electrophysiological techniques to quantify and evaluate ion presence, activity, and transport in and around

various tissues and morphological features of a variety of organisms. By combining the microelectrode techniques with the whole egg mass flux, water chemistry manipulations, and pharmacological techniques, another scale of dimension was added to the dissertation. I was able to gain exposure to microscale analyses and the O'Donnell group was able to apply the microelectrode technique to the eggs of a different species.

The initial overall goal of this dissertation was to utilize studies of ion transport in *L. stagnalis* as a starting point for determining suitable endpoints, primarily during post-bleed recovery and embryonic Ca^{2+} acquisition, for characterizing effects of chronic lead (Pb) exposure on *L. stagnalis*. However, during the preliminary studies, there was a clear indication that (1) daily net uptake rates of shell-forming substrates differed over the course of embryonic development and (2) both Na^{+} uptake in adults and Ca^{2+} acquisition in embryos were correlated to apparent titratable alkalinity flux. These findings sparked more extensive exploration on the whole egg mass and microscale levels into the nature of the titratable alkalinity flux under various water chemistry conditions. Thus the dissertation research transitioned into a more physiology-intensive endeavor than initially expected with emphasis on developing embryos. The outcome was notable results with implications that can be applied to both environmental metal contamination and possibly assessment of the impacts of increased atmospheric CO_2 on calcifying freshwater organisms.

The findings from this dissertation research were the result of several multi-pronged experimental approaches to address each objective and regardless of the approach, the conclusion was the same. The common pond snail *L. stagnalis* is apparently well-suited for studying physiological capacity and efficiency for ion

acquisition by a freshwater organism. Young adults recovering solute loss associated with full-body withdrawal displayed increased activity of basal ionoregulatory pathways as well as activation of apparently dormant pathways to facilitate remarkable recovery of up to 30% loss of Na^+ and other major cations within 24 – 48 h (Ebanks and Grosell 2008). Furthermore, embryos of the species showed use of an endogenous carbonate source for development and use of the same pathway (CA-catalyzed hydration of CO_2) to produce H^+ to fuel Ca^{2+} acquisition (Ebanks *et al.* 2010a, Ebanks *et al.* 2010b). Early and effective activation and use of these pathways allow *L. stagnalis* to thrive in relatively low ion conditions (Na ≤ 1000 µmol l^{-1}, Ca ≤ 310 µmol l^{-1}, HCO_3^- ≤ 680 µmol l^{-1}). As such, *L. stagnalis* seems to conform well to the Krogh principle for physiological studies, "for many problems there is an animal on which it can be most conveniently studied" (Krebs 1975). The physiological pathways utilized by this species allow it to meet acute demands for high-capacity recovery of major constituents of extracellular fluids (Ebanks and Grosell 2008) as well as high demand for calcification substrates during embryonic, juvenile, and young adult life stages (Ebanks *et al.* 2010a, Ebanks *et al.* 2010b, Grosell *et al.* 2006, Grosell and Brix 2009). However, this high efficiency ion transport makes the early life stages (embryos to young adults) more susceptible to negative impacts from chronic lead (Pb) exposure and may cause greater interactions with other waterborne elements antagonistic to its physiology and development.

Freshwater systems are generally the first line of defense for the aquatic habitats against most anthropogenic environmental stressors such as Pb. However, with respect to aquatic acidification, certain freshwater organisms, calcifiers in particular, may serve as the "canaries in the cave" for signs of negative consequences of shifts in environmental

pH. While *L. stagnalis* has been repeatedly shown to be the most sensitive organism known thus far to metal contamination (Borgmann *et al.* 1978, Grosell *et al.* 2006, Ebanks and Grosell in prep.), use of this species as a model indicator may extend to freshwater acidification as well. There are several levels of sub-lethal endpoints that may be reliable identifiers for environmental pH stress in *L. stagnalis*. Loss of the periostracum layer is often a readily visible indicator of environmental stress on these animals. Under reduced pH, freshwater snails tend to lose the proteinaceous layer coating the shell and the shell begins to whiten and eventually softens if neutral or alkaline levels are not restored (pers. obs.). Additionally, the parameters observed for Na^+ recovery in adults (Ebanks and Grosell 2008) and acquisition of calcification substrate in the embryos (Ebanks *et al.* 2010a, Ebanks *et al.* 2010b) are both dependent upon H^+ excretion, which may be challenged by environmental acidification. Furthermore, this species has been historically classified as a calciphile and thus is characterized by greater dependence (80+ %) on aquatic than dietary Ca^{2+} sources (van der Borght and Puymbroeck 1966). It preferentially inhabits environments with [Ca^{2+}] greater than 500 µmol Ca^{2+} l^{-1} (Boycott 1936). Acute fluctuations in environmental [Ca^{2+}] from higher levels of 2000 µmol Ca^{2+} l^{-1} down to 500 µmol Ca^{2+} l^{-1} have been recently reported to significantly alter the respiratory physiology and behavior of adult *L. stagnalis* (Dalesman and Lukowiak 2010). However the cultures, test snails, and test embryos utilized in this dissertational research were maintained in dechlorinated Miami-Dade County tap water (MDTW) with approximately 300-700 µmol Ca^{2+} l^{-1} and exposed to waters with as low as 74 µmol Ca^{2+} l^{-1} (Canadian Shield). While the embryos that were incubated in Canadian Shield waters were 20% smaller at day eight than those

incubated in MDTW, they still reached the developmental milestones on approximately the same time scales as those raised in MDTW.

The combination of high Ca^{2+} requirements coupled with the use of voltage-dependent Ca^{2+} channels and possibly Ca^{2+}/H^+ exchange pathways for Ca^{2+} acquisition most likely renders *Lymnaea* susceptible to environmental pH changes. Increased environmental $[H^+]$ would make HCO_3^-/CO_3^{2-} less available for uptake and calcification. Thus, the need for endogenous production of HCO_3^- via CA-catalyzed hydration of metabolic CO_2 would be increased under reduced environmental pH. Endogenous production of HCO_3^- for the use of calcification requires H^+ excretion to maintain the necessary alkaline internal environment for calcification. If environmental $[H^+]$ is increased as a result of climate change-induced aquatic acidification, the ability to excrete H^+ resulting from endogenous production of HCO_3^- against the gradient is impaired. Thus, though the model proposed by Ebanks *et al.*(2010b) was developed through the study of Ca^{2+}, pharmacological data from a Na^+ study on the same species indicate that endogenously produced H^+ are exchanged for aquatic Na^+ as well (Ebanks and Grosell 2008), which would assist in the maintenance of an alkaline internal environment. Retention of HCO_3^-/CO_3^{2-} and excretion of H^+ that are produced through the CA-catalyzed hydration of metabolic CO_2 allows for a net increase in internal pH, which is favorable for calcification. Sodium uptake for recovery following full-body withdrawal is dependent upon V-H^+ ATPase for H^+ excretion as well as a Na^+/H^+ exchanger as indicated by reduction in Na^+ uptake under treatment with bafilomycin 1A and EIPA, respectively (Ebanks and Grosell 2008).

Another point for consideration is that metal hypersensitivity in *Lymnaea* is not limited to Pb. Other metals such as silver (Ag), mercury (Hg), copper (Cu), and aluminum (Al) have demonstrated linkages to mortality or have sub-lethal impacts at levels of 100 µg l^{-1} or less (Evans 1982, Khangarot and Ray 1987, Truscott *et al.* 1995). For example, Al exposure has been associated with behavioral modification and changes in activity level in *Lymnaea* (Truscott *et al.* 1995), which can have implications for predator avoidance (Townsend and McCarthy 1980). Furthermore, Cu and Zn (< 100 µg l^{-1}) interfere with the digestive tract of *Lymnaea* (Evans 1982), which may have implications for the absorption of essential ions, such as Ca^{2+} from the diet for soft-water lymnaeid species that rely heavily on dietary sources of Ca^{2+} (Boycott 1936). Possibly more important is the fact that rarely are aquatic organisms faced with a single xenobiotic (Wang 1987) and thus the synergistic effects of multiple simultaneous metal exposures would be the ultimate, albeit challenging, goal of determining the actual impacts of environmental metal exposure on these highly sensitive organisms.

Clearly the results of this dissertational research point to the need to evaluate the potential impacts of expected environmental changes associated with global climate change on the freshwater environment. *L. stagnalis* would be well-suited for the study of freshwater acidification, as well as metal contamination and the interaction between the two. Its suitability is largely due to its intricate use of multiple transport pathways (i.e. H^+-pump, CA-catalyzed hydration of metabolic CO_2, cation exchangers, and channels) to maintain an alkaline internal environment and acquire the necessary ions for recovery, calcification, and development. The low buffering capacity of the freshwater environment relative to marine habitats is problematic in the face of potential aquatic

acidification associated with increased atmospheric CO_2. The freshwater environment is faced with the same atmospheric inputs but has reduced buffering capacity relative to the oceans. Thus, further study in this area is necessary to understand the impacts of freshwater acidification and furthermore the likely cumulative negative effect of metal contamination and aquatic acidification. The interconnected nature of these physiological and developmental endpoints in *L. stagnalis* provide an unique, highly sensitive tool for aquatic environmental assessment of changes associated with metal contamination and aquatic acidification.

Bibliography

Ahearn GA, Mandal PK, Mandal A (2001) Biology of the $2Na^{1+}/1H^{1+}$ antiporter in invertebrates. J Exp Zool 289:232-244

Ahearn GA, Zhuang Z, Duerr J, Pennington V (1994) Role of invertebrate electrogenic $2Na^{+}/1H^{+}$ antiporter in monovalent and divalent cation transport. J Exp Biol 196:319-335

Alexander JE Jr., Covich AP (1991) Predation risk and avoidance behavior in two freshwater snails. Biol Bull 180:387-393

Allah ATA, Wanas MQA, Thompson SN (2003) Dissolved heavy metals, lead cadmium and mercury accumulate in the body of the schistosome vector, *Biomphalaria glabrata* (Gastropoda: Pulmonata). J Moll Stud 69:35-41

Arshavsky YI, Deliagina TG, Okshtein IL, Orlovsky GN, Panchin YV, Popova LB (1994) Defense reaction in the pond snail *Planorbis corneus*. I. Activity of the shell-moving and respiratory systems. J Neurophysiol 71:882-890

Audesirk G (1993) Electrophysiology of lead intoxication: effects on voltage-sensitive ion channels. NeuroToxicology 14:137-148

Baldwin E (1935) The energy sources in ontogenesis: VII. The respiratory quotent of developing gastropod eggs. J Exp Biol 12:27-35

Bayne CJ (1968) Histochemical studies on the egg capsules of eight gastropod molluscs. Proc Malacological Soc Lond 38:199-212

Beadle LC (1969a) Salt and water regulation in the embryos of freshwater pulmonate molluscs I. The embryonic environment of *Biomphalaria sudanica* and *Lymnaea stagnalis*. J Exp Biol 50:473-479

Beadle LC (1969b) Salt and water regulation in the embryos of freshwater pulmonate molluscs III. Regulation of water during the development of *Biomphalaria sudanica*. J Exp Biol 50:491-499

Bielefeld U, Becker W (1991) Embryonic development of the shell in *Biompharia glabrata* (Say). International Journal for Developmental Biology 35:121-131

Borgmann U, Kramar O, Loveridge C (1978) Rates of mortality, growth, and biomass production of *Lymnaea palustris* during chronic exposure to lead. J Fish Res Board Can 35:1109-1115

Boycott AE (1936) The habitats of fresh-water Mollusca in Britain. J Animal Ecol 5:116-186

Bradford MM (1976) A rapid and sensitive method for the quantitation of microgram quantities of protein utilizing the principle of protein-dye binding. Analytical Biochem 72:248-254

Brezden BL, Gardner DR (1983) Calcium entry blockers inhibit contractures induced by the molluscicide Frescon in *Lymnaea stagnalis* smooth and cross-striated muscles. Pesticide Biochemistry and Physiology 20:269-277

Brönmark C, Malmqvist B (1986) Interactions between the leech *Glossiphonia complanata* and its gastropod prey. Oecologia 69:268-276

Brown KM (1991) Mollusca: Gastropoda. In *Ecology and Classification of North American Freshwater Invertebrates*, eds. J. H. Thorp and A. P. Covich), pp. 911. New York: Academic Press

Burton RF (1968) Ionic balance in the blood of pulmonata. Comparative Biochemistry and Physiology 25:509-516

Bury NR, Wood CM (1999) Mechanism of branchial apical silver uptake by rainbow trout is via the proton-coupled Na^+ channel. Am J Physiol Regul Integr Comp Physiol 277:R1385-1391

Cameron JN, Wood CM (1985) Apparent H^+ excretion and CO_2 dynamics accompanying carapace mineralization in the blue crab (*Callinectes sapadus*) following moulting. J Exp Biol 114:181-196

Clelland ES, Saleuddin ASM (2000) Vacuolar-Type ATPase in the accessory boring organ of *Nucella lamellosa* (Gmelin) (Mollusca: Gastropoda): Role in shell penetration. Biological Bulletin 198:272-283

da Costa AR, Oliveira PF, Barrias C, Ferreira HG (1999) Identification of a V-type proton pump in the outer mantle epithelium of *Anodonta cygnea*. Comp Biochem Physiol A 123:337-342

Dalesman S, Lukowiak K (2010) Effect of acute exposure to low environmental calcium on respiration and locomotion in *Lymnaea stagnalis* (L.). J Exp Biol 213:1471-1476

Dawson DC, Liu X (2008) Osmoregulation: Some principles of water and solute transport. In *Osmotic and Ionic Regulation*, ed. D.H. Evans, pp. 1-36. Boca Raton:CRC Press

de With ND (1980) Water turn-over, ultrafiltration, renal water reabsorption and renal circulation in fed and starved specimens of *Lymnaea stagnalis*, adapted to different external osmolarities. Zoology Proceedings C 83:109-120

de With ND, Kok TP, van der Schors RC (1987) Relationships between apparent net H^+ excretion and Na^+, Ca^{2+} and Cl^- uptake in the pulmonate freshwater snail *Lymnaea stagnalis*. Comp Biochem and Physiol 87A:671-675

de With ND, van der Schors RC (1982) On the interrelations of the Na^+-and Cl^--influxes in the pulmonate freshwater snail *Lymnaea stagnalis*. J Comp Physiol B 148:131-135.

Donini A, O'Donnell MJ (2005) Analysis of Na^+, Cl^-, K^+, H^+ and NH_4^+ concentration gradients adjacent to the surface of anal papillae of the mosquito *Aedes aegypti*: application of self-referencing ion-selective microelectrodes. J Exp Biol 208:603-610

Ebanks SC, Grosell M (2008) Fluid and osmolyte recovery in the common pond snail *Lymnaea stagnalis* following full-body withdrawal. J Exp Biol 211:327-336

Ebanks SC, O'Donnell MJ, Grosell M (2010a) Acquisition of Ca^{2+} and carbonate for shell formation in embryos of the common pond snail *Lymnaea stagnalis.* J Comp Physiol B (published online April 2010)

Ebanks SC, O'Donnell MJ, Grosell M (2010b) Characterization of mechanisms for Ca^{2+} and HCO_3^-/CO_3^{2-} acquisition for shell formation in embryos of the freshwater common pond snail *Lymnaea stagnalis*. J Exp Biol (submitted)

Evans NA (1982) Effects of copper and zinc on the life cycle of *Notocotylus attenuatus* (Digenea:Notocotylidae). International Journal for Parasitology 12:363-369

Fenwick JC, Wendelaar Bonga SE, Flik G (1999) In vivo bafilomycin-sensitive Na($^+$) uptake in young freshwater fish. J Exp Biol 202:3659-3666

Finbow ME, Harrison MA (1997) The vacuolar H^+-ATPase: a universal proton pump of eukaryotes. The Biochemical Journal 324:697-712

Flik G, Verbost PM, Wendelaar Bonga SE (1995) Calcium transport processes in fishes. In *Cellular and molecular approaches to fish ionic regulation*, eds. C. M. Wood and T. J. Shuttleworth, pp. 317-336. New York: Academic

Ghiasuddin SM, Matsumura F (1979) DDT inhibition of Ca-ATPase of the peripheral nerves of the American lobster. Pesticide Biochemistry and Physiology 10:151-161

Gray J (1920) The relation of the animal cell to electrolytes. J Physiol 53:308-319

Greenaway P (1970) Sodium regulation in the freshwater mollusc, *Limnaea stagnalis* (L.) (Gastropoda: Pulmonata). J Exp Biol 53:147-163

Greenaway P (1971a) Calcium regulation in the freshwater mollusc *Limnaea stagnalis* (L.) (Gastropoda: Pulmonata): II. Calcium movements between internal calcium compartments. J Exp Biol 54:609-620

Greenaway P (1971b) Calcium regulation in the freshwater mollusc *Limnaea stagnalis* (L.) (Gastropoda: Pulmonata): I. The effect of internal and external calcium concentration. J Exp Biol 54: 199-214

Grosell M, Blanchard J, Brix KV, Gerdes R (2007) Physiology is pivotal for interactions between salinity and acute copper toxicity to fish and invertebrates. Aquatic Toxicol 84:162-172

Grosell M, Brix KV (2009) High net calcium uptake explains the hypersensitivity of the freshwater pulmonate snail, *Lymnaea stagnalis*, to chronic lead exposure. Aquatic Toxicology 91:302-311

Grosell M, De Boek G, Johannsson O, Wood CM (1999) The effects of silver on intestinal ion and acid-base regulation in the marine teleost fish, *Parophrys vetulus*. Comp Biochem and Physiol C 124:259-270

Grosell M, Gerdes RM, Brix KV (2006) Chronic toxicity of lead to three freshwater invertebrates- *Brachionus calyciflorus*, *Chironomus tentans*, and *Lymnaea stagnalis*. Environmental Toxicology and Chemistry 25:97-104

Grosell M, Hogstrand C, Wood CM, Hansen HJM (2000) A nose-to-nose comparison of the physiological effects of exposure to ionic silver versus silver chloride in the European eel (*Anguilla anguilla*) and the rainbow trout (*Oncorhynchus mykiss*). Aquatic Toxicology 48:327-342

Grosell M, Taylor JR (2007) Intestinal anion exchange in teleost water balance. Comp Biochem and Physiol 148:14-22

Grosell M, Wood CM (2002) Copper uptake across rainbow trout gills: mechanisms of apical entry. J Exp Biol 205:1179-1188

Hansell DA, Carlson CA (2001) Biogeochemistry of total organic carbon and nitrogen in the Sargasso Sea: Control by convective overturn. Deep-Sea Res. Part 2, Top Stud Oceanogr 48:1649-1667

Harrison FL, Knezovich JP, Rice DW (1984) The toxicity of copper to the adult and early life stages of the freshwater clam, *Corbicula manilensis*. Archives of Environmental Contamination and Toxicology 13:85-92

Harvey WR (1992) Physiology of V-ATPases. J Exp Biol 172:1-17

Harvey WR, Maddrell SHP, Telfer WH, Wieczorek H (1998) H^+ V-ATPases energize plasma membranes for secretion and absorption of ions and fluids. Amer Zool 38:426-441

Hills AG (1973) Acid-base balance: Chemistry, physiology, pathophysiology. Baltimore: The Williams and Wilkins Co.

Hudson RL (1993) Bafilomycin-sensitive acid secretion by mantle epithelium of the freshwater clam, *Unio complanatus*. Am J Physiol Regul Integr Comp Physiol 264:R946-951

Khangarot BS, Ray PK (1987) Sensitivity of freshwater pulmonate snails, *Lymnaea luteola* L., to heavy metals. Bull Environ Contam Toxicol 41:208-213

Kirschner LB (2004) The mechanism of sodium chloride uptake in hyperregulating aquatic animals. J Exp Biol 207:1439-1452

Kleyman TR, Cragoe EJJ (1988) Amiloride and its analogs as tools in the study of ion transport. Journal of Membrane Biology 105:1-21

Kniprath E (1972) Formation and structure of the periostracum in *Lymnaea stagnalis.* Calcified Tissue International 9:260-271

Krebs HA (1975) The August Krogh principle: "For many problems there is an animal on which it can be most conveniently studied." J Exp Zool 194:221-226

Krogh A (1938) The active absorption of ions in some freshwater animals J Comp Physiol A 25:335-350

Krogh A (1939) Osmotic regulation in aquatic animals. New York: Dover Publications, Inc.

Krogh A (1946) Croonian lecture: The active and passive exchanges of inorganic ions through the surfaces of living cells and through living membranes generally. Proceedings of the Royal Society of London, Series B 133:140-200

Krogh A (1965) Osmotic regulation in aquatic animals, pp.170-190. New York: Dover Publications, Inc.

Krogh A, Schmidt-Nielsen K, Zeuthen E (1939) The osmotic behaviour of frogs eggs and young tadpoles. J Comp Physiol A 26:230-238

Krogh A, Ussing HH (1937) A note on the permeability of trout eggs to D_2O and H_2O. J Exp Biol 14:35-37

Lin H, Randall D (1991) Evidence for the presence of an electrogenic proton pump on the trout gill epithelium. J Exp Biol 161:119-134

Machado J, Ferreira KG, Ferreira HG, Fernandes PL (1990) The acid-base balance of the outer mantle epithelium of *Anodonta cygnea*. J Exp Biol 150:159-169

Mager EM, Brix KV, Grosell M (2010a) Influence of bicarbonate and humic acid on effects of chronic waterborne lead exposure to the fathead minnow (*Pimephales promelas*). Aquat Toxicol 96:135-144

Mager E, Brix KV, Gerdes R, Ryan A, Grosell M (2010b) Effects of water chemistry on chronic lead toxicity to the cladoceran, *Ceriodaphnia dubia*. Ecotoxicology and Environmental Safety. (submitted)

Mager EM, Wintz H, Vulpe CD, Brix KV, Grosell M (2008) Toxicogenomics of water chemistry influence on chronic lead exposure to the fathead minnow (*Pimephales promelas*). Aquat Toxicol 87:200-209

Marshall W, Bryson S, Wood C (1992) Calcium transport by isolated skin of rainbow trout. J Exp Biol 166:297-316

Marshall WS, Grosell M (2006) Ion Transport, Osmoregulation, and Acid-Base Balance. In *The Physiology of Fishes*, eds. D. H. Evans and J. B. Claiborne, pp. 177-230. Boca Raton: Taylor & Francis Group

Masereel B, Pochet L, Laeckmann D (2003) An overview of inhibitors of Na^+/H^+ exchanger. European Journal of Medicinal Chemistry 38:547-554

Marxen JC, Becker W, Finke D, Hasse B, Epple M (2003) Early mineralization in *Biomphalaria glabrata*: Microscopic and structural results. *J. Mollus. Stud.* 69:113-121

McCarthy TM, Fisher WA (2000) Multiple predator-avoidance behaviours of the freshwater snail *Physella heterostropha pomila*: Responses vary with risk. Freshwater Biology 44:387-397

Miles CJ, Pfeuffer RJ (1997) Pesticides in canals of South Florida. Arch Environ Contam Toxicol 32:337-345

Morrill JB (1982) Development of the pulmonate gastropod, *Lymnaea*. In: Harrison W, Cowdon RF (eds) Developmental Biology of Freshwater Invertebrates. Alan R. Liss, New York, pp 399-483

Nebeker AV, Savonen C, Stevens DG (1985) Sensitivity of rainbow trout early life stages to nickel chloride. Environmental Toxicology and Chemistry 4:233-239

Neufeld DS, Cameron JN (1992) Postmoult uptake of calcium by the blue crab (*Callinectes sapadus*) in water of low salinity. J Exp Biol 171:283-299

Neufeld DS, Cameron JN (1993) Transepithelial movement of calcium in crustaceans. J Exp Biol 184:1-16

Okech BA, Boudko DY, Linser PJ, Harvey WR (2008) Cationic pathway of pH regulation in larvae of *Anopheles gambiae*. J Exp Biol 211:957-968

Oliveira PF, Lopes IA, Barrias C, Rebelo da Costa AM (2004). H^+-ATPase of crude homogenate of the outer mantle epithelium of *Anodonta cygnea*. Comp Biochem Physiol Part A 139:425-432

Pekel M, Platt B, Büsselberg D (1993) Mercury (Hg^{2+}) decreases voltage-gated calcium channel currents in rat DRG and *Aplysia* neurons. Brain Res 632:121-126

Perry SF, Flik G (1988) Characterization of branchial transepithelial calcium fluxes in freshwater trout, *Salmo gairdneri*. Am J Physiol Regul Integr Comp Physiol 254:R491-498

Perry SF, Furimsky M, Bayaa M, Georgalis T, Shahsavarani A, Nickerson JG, Moon TW (2003a) Integrated responses of Na^+/HCO_3^- cotransporters and V-type H^+-ATPases in the fish gill and kidney during respiratory acidosis. Biochimica et Biophysica Acta (BBA) - Biomembranes 1618:175-184

Perry SF, Shahsavarani A, Georgalis T, Bayaa M, Furimsky M, Thomas SLY (2003b) Channels, pumps, and exchangers in the gill and kidney of freshwater fishes: Their role in ionic and acid-base regulation. J Exp Zool A 300:A53-62

Plesch B, de Jong-Brink M, Boer HH (1971) Histological and histochemical observations on the reproductive tract of the hermaphrodite pond snail *Lymnaea stagnalis* (L.). Neth J Zool 21:180-201

Reish DJ, Martin JM, Piltz FM, Word JQ (1976) The effect of heavy metals on laboratory populations of two polychaetes with comparisons to the water quality conditions and standards in Southern California marine waters. Water Research 10:299-302

Rheault M, O'Donnell MJ (2001) Analysis of K^+ transport in Malpighian tubules of *Drosophila melanogaster*: Evidence for spatial and temporal heterogeneity. J Exp Biol 204:2289-2299

Rheault MR, O'Donnell MJ (2004) Organic cation transport by Malpighian tubules of *Drosophila melanogaster*: Application of two novel electrophysiological methods. J Exp Biol 207:2173-2184

Rogers JT, Wood CM (2004) Characterization of branchial lead-calcium interaction in the freshwater rainbow trout *Oncorhynchus mykiss*. J Exp Biol 207:813-825

Rundle SD, Brönmark C (2001) Inter- and intraspecific trait compensation of defense mechanisms in freshwater snails. *Proceedings of the Royal Society of London B* 268:1463-1468

Schlichter LC (1981) Ion relations of haemolymph, pallial fluid, and mucus of *Lymnaea stagnalis*. Canadian Journal of Zoology 59:605-613

Shahsavarani A, Perry SF (2006) Hormonal and environmental regulation of epithelial calcium channel in gill of rainbow trout (*Oncorhynchus mykiss*). Am J Physiol Regul Integr Comp Physiol 291:R1490-1498

Sminia T (1977) Physiology of haemocyanin: Haemocyanin-producing cells in gastropod molluscs. In *Proceedings in Life Sciences: Structure and Function of Haemocyanin*, ed. J. V. Bannister, pp. 279-288. New York: Springer-Verlag

Taylor HH (1973) The ionic properties of the capsular fluid bathing embryos of *Lymnaea stagnalis* and *Biomphalaria sudanica* (Mollusca:Pulmonata). J Exp Biol 59:543-564

Taylor HH (1977) The ionic and water relations of embryos of *Lymnaea stagnalis*, A freshwater pulmonate mollusc. J Exp Biol 69:143-172

Townsend CR, McCarthy TK (1980) On the defence strategy of *Physa fontinalis* (L.), a freshwater pulmonate snail Oecologia 46:75-79

Tresguerres M, Parks SK, Katoh F, Goss GG (2006) Microtubule-dependent relocation of branchial V-H^+-ATPase to the basolateral membrane in the Pacific spiny dogfish (*Squalus acanthias*): A role in base secretion. J Exp Biol 209:599-609

Truchot JP (1976) Carbon dioxide combining properties of the blood of the shore crab *Carcinus maenas* (L): Carbon dioxide solubility coefficient and carbonic acid dissociation constants. J Exp Biol 64:45-57

Truscott R, McCrohan CR, Bailey SER, White KN (1995) Effect of aluminum and lead on activity in the freshwater pond snail *Lymnaea stagnalis*. Can J Fish Aquat Sci 52:1623-1629

USEPA (2007) National Recommended Water Quality Criteria. Office of Water, Washington D.C.

van Aardt WJ (1968) Quantitative aspects of the water balance in *Lymnaea stagnalis* (L.) Netherlands Journal of Zoology 18:253-312

van der Borght O, van Puymbroeck S (1966) Calcium metabolism in a freshwater mollusk: Quantitative importance of water and food as supply for calcium during growth. Nature 210:791-793

Verdouw H, Van Echteld CJA, Dekkers EMJ (1978) Ammonia determination based on indophenol formation with sodium salicylate. Water Res 12:399-402

Wilson R, Gilmour K, Henry R, Wood C (1996) Intestinal base secretion in the seawater-adapted rainbow trout: a role in acid-base balance? J Exp Biol 199:2331-2343

Wang W (1987) Factors affecting metal toxicity to (and accumulation by) aquatic organisms -- Overview. Environment International 13:437-457

Wong RG, Nowicki HG, Norman AW (1974) The effects of polychlorinated biphenyls on calciferol (vitamin D) mediated calcium metabolism. Pesticide Biochemistry and Physiology 4:170-177

Zall DM, Fisher D, Garner MQ (1956) Photometric determination of chlorides in water. Analytical Chemistry 28:1665-1668